VOLUME XII APRIL, 1933 NUMBER 2

THE BELL SYSTEM TECHNICAL JOURNAL

DEVOTED TO THE SCIENTIFIC AND ENGINEERING ASPECTS OF ELECTRICAL COMMUNICATION

AMERICAN TELEPHONE AND TELEGRAPH COMPANY
NEW YORK

50c per Copy *$1.50 per Year*

THE BELL SYSTEM TECHNICAL JOURNAL

Published quarterly by the
American Telephone and Telegraph Company
195 Broadway, New York, N. Y.

SUBSCRIPTIONS

Subscriptions are accepted at $1.50 per year. Single copies are fifty cents each. The foreign postage is 35 cents per year or 9 cents per copy.

PRINTED IN U. S. A.

The Bell System Technical Journal

April, 1933

Ultra-Short Wave Propagation *

By J. C. SCHELLENG, C. R. BURROWS and E. B. FERRELL

Part I of this paper first describes a method of measuring attenuation and field strength in the ultra-short wave range. A résumé of some of the quantitative experiments carried out in the range between 17 mc. (17 meters) and 80 mc. (3.75 m.) and with distances up to 100 km. is then given. Two cases are included: (1) "Optical" paths over sea-water and (2) "Non-optical" paths over level and hilly country. An outstanding result is that the absolute values of the fields measured were always less than the inverse distance value. Over sea-water, the fields decreased as the frequency increased from 34 mc. (8.7 m.) to 80 mc. (3.75 m.) while the opposite trend was found over land. As a rule, the signals received were very steady, but some evidence of slow fading was obtained for certain cases when the attenuation was much greater than that for free space.

Part II gives a discussion of reflection, diffraction and refraction as applied to ultra-short wave transmission. It is shown, (1) that regular reflection is of importance even in the case of fairly rough terrain, (2) that diffraction considerations are of prime importance in the case of non-optical paths, and (3) that refraction by the lower atmosphere can be taken into account by assuming a fictitious radius of the earth. This radius is ordinarily equal to about 4/3 the actual radius.

The experiments over sea-water are found to be consistent with the simple assumption of a direct and a reflected wave except for distances so great that the curvature of the earth requires a more fundamental solution. It is shown that the trend with frequency to be expected in the results for a non-optical path over land is the same as that actually observed, and that in one specific case, which is particularly amenable to calculation, the absolute values also check reasonably well. It is found both from experiment and from theory that non-optical paths do not suffer from so great a disadvantage as has usually been supposed.

Several trends with respect to frequency are pointed out, two of which, the "conductivity" and the "diffraction" trends, give decreased efficiency with increased frequency, and another of which, the "negative reflection" trend, gives increased efficiency with increased frequency under the conditions usually encountered.

The existence of optimum frequencies is pointed out, and it is emphasized that they depend on the topography of the particular paths, and that different paths may therefore have widely different optimum frequencies. Thus, among the particular cases mentioned, the lowest optimum values vary from frequencies which are well below the ultra-high frequency range up to 1200 mc. (25 cm.). For other paths the lowest optimum frequency may be still higher.

Introduction

WITH the extension of the radio frequency spectrum to higher and higher frequencies have come new problems, both of experiment and of theory, which require quantitative study for solution.

* Presented at New York Mtg. of I. R. E., Nov. 2, 1932. Published in Proc. I. R. E., March, 1933.

The fundamental similarity of visual light and radio waves makes it obvious that somewhere between these regions a transition region must occur in which the apparently different phenomena merge into each other. In theoretical studies of this region it is necessary to use concepts borrowed from both the adjacent frequency ranges. A survey of a part of this field has now been in progress for some time and some of the results obtained to date are given in this paper and in a companion paper by Englund, Crawford and Mumford.

Since the Kennelly-Heaviside layers do not reflect ultra-short waves sufficiently to be a factor in the ordinary phenomena of this range, our interest is confined to the "ground" or direct wave. This term refers to any and all signals which arrive at the receiver except those which are affected by the upper atmosphere. It is otherwise noncommittal as to the mechanism of transmission. The physical pictures of this mechanism which have been so useful in the case of long waves are of little help when the length of the wave is of the order of, or smaller than, the dimensions of irregularities of topography which it encounters. The well-known work of Abraham,[1] Zenneck,[2] Sommerfeld [3] and the more recent studies by Weyl,[4] Eckersley,[5] Strutt,[6] and Wise [7] apply to special cases of ultra-short wave propagation, but generally speaking help but little in the more numerous problems where irregularity of topography is the rule. Likewise, the important work of Watson [8] and of Van der Pol [8] may perhaps find application in the diffraction problems of ultra-short waves, but only to a limited extent.

It is obvious that rigorous solutions of problems in transmission over rough surfaces are out of the question, but progress can be made by way of the general concepts of reflection, diffraction and refraction. We shall endeavor to show that many phenomena observed can be

[1] Abraham, M., *Enz. d. math. Wissen.*, 5, Art. 18.

[2] Zenneck, J., "Über die Fortpflanzung ebenen elektromagnetischer Wellen langs einer ebenen Leiterflache und ihre Beziehung zur drahtlosen Telegraphie," *Ann. d. Phys.*, 4, 23, 846 (1907).

[3] Sommerfeld, Arnold, "Über die Ausbreitung der Wellen der Drahtlosen Telegraphie," *Ann. d. Phys.*, 4, 28, 665–736, Mar. 1909, and "Ausbreitung der Wellen in der drahtlosen Telegraphie. Einfluss der Bodenbeschaffenheit auf gerichtete und ungerichtete Wellenzuge," *Jahr. d. drahtlosen, Tel. u. Tel.*, 4, 157 (1911).

[4] Weyl, H., "Ausbreitung elektromagnetischer Wellen über einer ebenen Leiter," *Ann. d. Phys.*, 4, 60, 481–500 (1919).

[5] Eckersley, T. L., "Short-Wave Wireless Telegraphy," *Jour. I. E. E.*, 65, 600–644, June 1927.

[6] Strutt, M. J. O., "Strahlung von Antennen unter dem Einfluss der Erdbodeneigenschaften," *Ann. d. Phys.*, 5, 1, 721–772 (1929); 4, 1–16 (1930); 9, 67–91 (1931).

[7] Wise, W. Howard, "Asymptotic Dipole Radiation Formulas," *Bell Sys. Tech. Jour.*, 8, 662–671, Oct. 1929.

[8] Watson, G. N., "The Diffraction of Electric Waves by the Earth," *Proc. Roy. Soc.* (London), 95, 83–99, Oct. 7, 1918. Van der Pol, Balth., "On the Propagation of Electromagnetic Waves Around the Earth," *Phil. Mag.*, 6, 38, 365–380, Sept. 1919.

explained quantitatively in this way. Reflection, diffraction and refraction all play their parts.

On the experimental side, the longer distance ultra-short wave transmission studies described in the literature have been made almost exclusively with apparatus capable of making only qualitative measurements. In spite of this handicap, many valuable observations have been made.[9] The outstanding result of these has been the demonstration of the advantages of an "optical" path, or rather, one in which a straight line between the transmitting and receiving antennas is unbroken by the intervening terrain. In many cases, however, this advantage has been greatly over-emphasized.

As a basis for studying the relative importance of the various mechanisms that have been suggested, quantitative measurement must replace qualitative observation. Part I of this paper presents some of the results of an experimental study of the propagation of ultra-short waves, made with the objective of obtaining quantitative data of sufficient accuracy to serve as a basis for theoretical work. Part II discusses the theory of ultra-short wave transmission and analyzes some of the experimental results from that point of view.

Part I—Experiment

Equipment and Procedure

A considerable portion of the transmitting in connection with this survey was done with a 1000-watt transmitter located at Deal, N. J. In this transmitter the last stage employed four 1000-watt radiation-cooled tubes as an oscillator at 69 mc. The frequency was controlled by a 3833-kc. crystal oscillator acting through a chain of amplifiers and harmonic generators. A simple vertical half-wave antenna was used for most of the tests. It was located about 60 meters above ground and was driven through a long two-wire transmission line. The stability of this transmitter was a definite advantage and facilitated the taking of reliable data. Another transmitter of slightly higher power was employed for the lower frequency tests from Deal. Similar antennas were used.

For most of the over-water tests use was made of a mobile transmitter of some 100 watts output, while for some of the very short distance work, a simple portable oscillator using receiving tubes was employed. The radiator, a simple vertical antenna, was located on a wooden tripod on a bluff at Cliffwood Beach, N. J. This bluff over-

[9] On account of the extensiveness of these qualitative studies, no attempt is made to give a complete bibliography. A few articles giving results of especial interest in connection with the present paper are cited in the text.

looks lower New York Bay, and provided antenna heights up to 28 meters above sea level.

The receivers were, for the most part, triple detection sets with calibrated attenuators in the second intermediate frequency amplifier. To this extent they were similar to familiar types of sets used to measure field strengths on short waves [10] and were capable of making accurate comparisons of voltages induced in the receiving antenna.

None of the usual means for introducing a calibrating voltage in the set was provided. Instead, a method due to R. C. Shaw was used, in which calibrations were made by producing *at the antenna itself* a known field from a local source to which the name "standard field generator" [11] has been given. The standard field generator is a small compact self-contained oscillator which is very carefully shielded except for a small balanced loop extending in a vertical plane above the shield (Fig. 1). A thermomilliammeter is located in the loop at

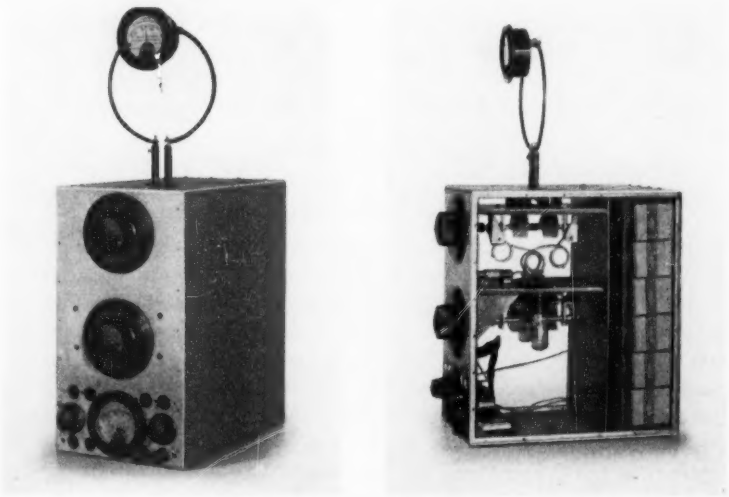

Fig. 1—Standard field generator.

[10] In fact, one included a set similar to that described by Friis and Bruce (*Proc. I. R. E.*, 14, 507–519, Aug. 1926). An extra ultra-high frequency combination (input circuits, beating oscillator, detector and amplifier) provided input at 6 mc. to the standard short wave receiver. The latter was tuned to operate at 6 mc.

[11] Since the writing of this paper, our attention has been called to the method described by K. Sohnemann, *E. N. T.*, 8, 462, Oct. 1931. The Sohnemann method also uses a standard field generator but otherwise the technique is entirely different from that of the Shaw method.

the point of low potential with respect to the shield. From the reading of the meter and the dimensions of the loop, the field at nearby points may be computed.[12] This, therefore, provides a field strength standard by comparison with which the unknown field can readily be obtained.

Signals were received by means of a simple half-wave antenna supported on a portable mast at heights up to 12 meters above the ground. For calibrating, however, the center of the antenna was located about 4 meters above the ground and the standard field generator was placed in operation at the same height one half wave-length away. It has been determined experimentally that this avoided serious complications due to the proximity of the ground. There are certain other refinements which may or may not be important depending upon the accuracy required. Such, for example, is the effect of the finite length of the receiving antenna. It is beyond the scope of the present paper to enter into this matter. It is sufficient to say that the error so produced is less than one decibel. Field strengths of the order of two or three microvolts per meter could be measured in this way. This might be improved by increasing the sensitivity of the set or by using directional receiving antennas.

The meter in the transmitting antenna was calibrated by means of this same standard field generator. The signal from the transmitting antenna was measured at some nearby receiving point. The antenna was then lowered to the ground, the standard field generator was hoisted into the same position and the signal from it measured at the same receiving point. Thus the field radiated from the transmitting antenna was known in terms of the field from the standard field generator. The meter-amperes in the transmitting antenna could then be calculated in terms of the standard field generator.

It is important that both transmitting and receiving equipments were calibrated in terms of the same standards, namely, the dimensions of the loop of the standard field generator and the current in it as

[12] The field from a radiating loop in free space is given by

$$E = \frac{120\pi^2 NAI}{\lambda^2 D}\left(1 - j\frac{\lambda}{2\pi D}\right)$$

where E = electric field strength in volts per meter
N = number of turns in loop
A = area of loop in square meters
I = current in loop in amperes
D = distance between loop and antenna in meters
λ = wave-length in meters

When the distance between the loop and the receiving antenna is a half wave-length the terms in the parentheses become $(1 - j0.318)$ which has an amplitude of 1.05 (0.4 db above unity). Hence the second term increases the total field to 0.4 db above the "radiation" field at this distance.

indicated by the thermomilliammeter. So long as these were duplicated at both ends of the path, it was possible to determine the relative values of fields at the two ends, regardless of absolute errors. Investigation of the behavior of the meter and of the method in general, indicate that the absolute error itself is not large.

The map of Fig. 2 shows the locations of the transmitting and receiving sites used. The tests may be divided into two groups. Propagation over water was studied mainly with the transmitter

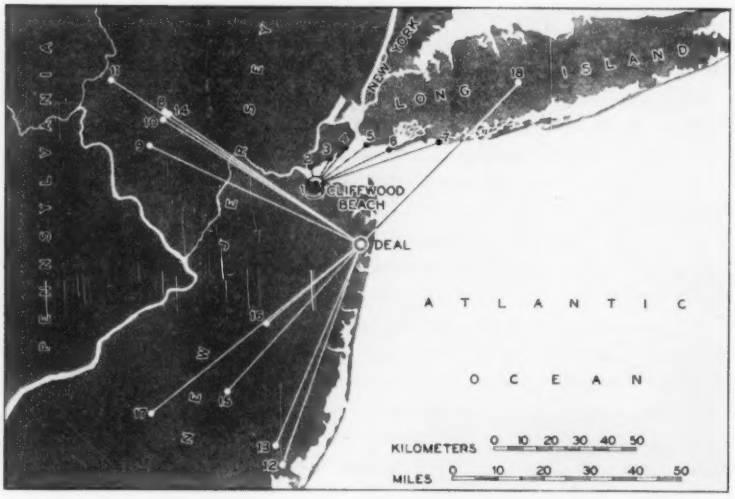

Fig. 2—Transmitting and receiving locations.

located on the bluff at Cliffwood Beach. Measurements on transmission over land were made from the transmitter at Deal. Lines radiating from these two points indicate the various transmission paths studied.

Transmission Over Sea Water

For the measurements on propagation over water at 34, 51 and 80 mc., the receiving antenna was located at the water's edge, except for a few special tests. The height of its midpoint was varied up to a maximum of about twelve meters above sea level. The data presented in Fig. 3 show the results with the maximum elevations and vertical polarization (vertical electric field).

This figure shows that the received field was below the inverse

distance field that would result from radiation in free space.[13] The field strength is more nearly inversely proportional to the second than to the first power of the distance as may be seen by comparison with the light dashed line in Fig. 3.

In addition to the measurements taken on the ground, measurements on the highest frequency, 80 mc., were made with the receiver in an airplane.[14] The results are discussed later in connection with Fig. 11.

The effect of altitude was determined at two distances, 77 and 142 kilometers, using the Deal transmitter at 69 and 17 mc. The results

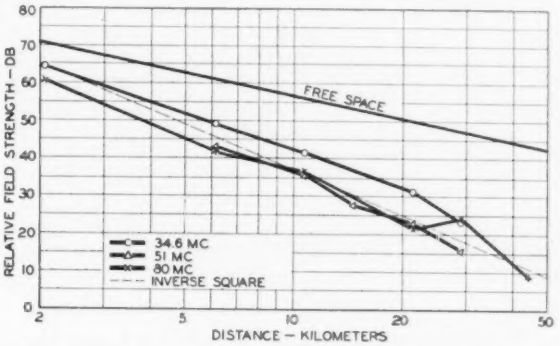

Fig. 3—Field strength as a function of distance for transmission over salt water from Cliffwood Beach.

are shown in Figs. 4 and 5. The increase of signal with elevation was much greater on the higher frequency than on the lower frequency. It is interesting to note, however, that if the field were plotted against altitude in *wave-lengths* the slopes would be approximately the same for the two frequencies. Significance should not be attached to the ratio of the field obtained on one frequency to that obtained on the other.

Transmission Over Land

The transmitters located at Deal were employed for studying the propagation of waves of 17, 34 and 69 mc. over various types of terrain. The transmission paths are shown by the lines radiating from Deal on the map of Fig. 2. Three types of paths are represented. The best for ultra-short wave work was found to be that with the other terminal on high ground, such as is found to the northwest. Another type, not so favorable to the transmission of ultra-short waves, but typical of flat country, could be studied by locating the receiving

[13] In free space, the field produced by a given current in a doublet is one half as great as that produced by the same current and doublet when located at and perpendicular to the surface of a perfect conductor.

[14] These measurements were possible through the cooperation of Mr. F. M. Ryan.

terminal to the south or southwest. Here the intervening ground is fairly level, and there are no high hills that can be used for the receiving terminal. The third type of path is mostly over water to points on

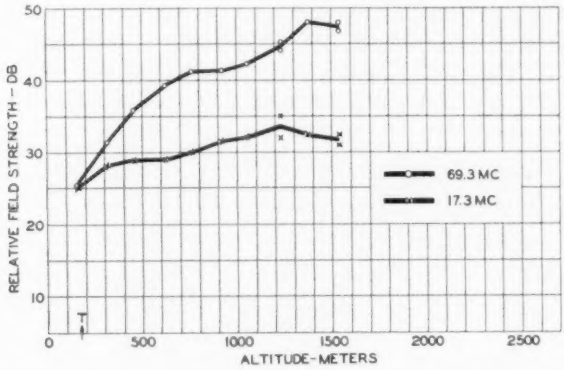

Fig. 4—Field strength as a function of receiver altitude at a distance of 77 km. The path was mostly over water. The arrow T shows the altitude at which the line of sight, neglecting refraction, becomes tangent to the earth's surface.

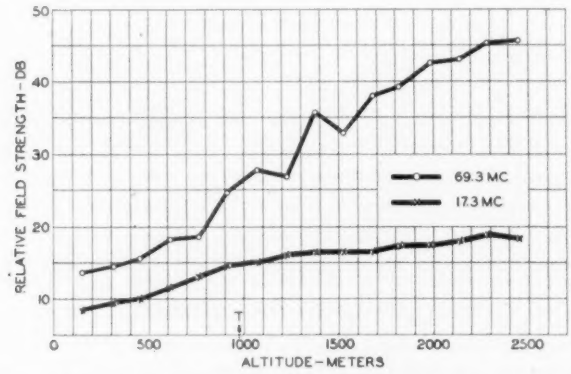

Fig. 5—Field strength as a function of receiver altitude at a distance of 141 km. The path was mostly over water. The arrow T shows the altitude at which the line of sight, neglecting refraction, becomes tangent to the earth's surface.

Long Island. Typical profiles of over-land paths are shown in Fig. 6.

The experimental results of transmission over these paths, together with some of their characteristics, are given in the table of Fig. 7. In the last three columns is given the received field in decibels below

the free space value. At 69 mc. the best paths, 8 and 9, gave values which were 15 and 13 db below the inverse distance amplitude. The former gave 32 db at 17 mc. and the latter gave 28 db at 34 mc. In general, the highest frequency showed the smallest attenuation over land.

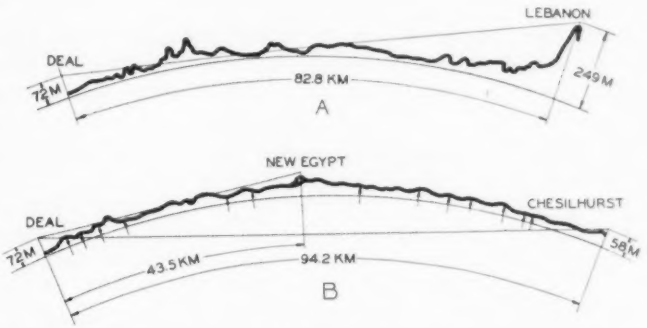

Fig. 6—Profiles of typical overland paths: *A*, path No. 8, over hilly country, with receiving location not masked by nearby hills; *B*, paths Nos. 16 and 17, over level country.

NO.	RECEIVING LOCATION	LAT W	LONG. N	ELEV-ATION m.	DIS-TANCE Km.	RECEIVED FIELD DB BELOW FREE SPACE VALUE		
						17.3mc	34.6md	69.3mc
	HILLY COUNTRY OPEN SITE							
8	LEBANON 1	74°-51'-0	40°-39'-9	238	82.8	32.5		15.1
9	CHERRYVILLE	74°-53'-3	40°-33'-4	165	96.6		28.5	13.2
	HILLY COUNTRY MASKED SITE							
10	LEBANON 2	74°-51'-0	40°-38'-5	119	81.3	45.0	35.5	40.0
11	MONTANA	75°-4'-2	40°-45'-3	342	104.5	43.5	34.5	32.5
	LEVEL COUNTRY							
12	TUCKERTON 1	74°-22'-5	39°-35'-2	24	80.6	50.0	35.5	24.5
13	TUCKERTON 2	74°-23'-5	39°-38'-5	27	77.3	47.5	41.0	36.0
14	LEBANON 3	74°-49'-8	40°-39'-2	110	81.3	40.5	37.5	30.5
15	APPLE PIE HILL	74°-35'-5	39°-48'-5	63	69.2	40.0	35.0	27.7
16	NEW EGYPT	74°-25'-7	40°-0'-9	61	43.5			27.1
17	CHESILHURST	75°-5.3'-9	39°-44'-2	46	94.2			48.3
	OVER WATER							
18	HALF HOLLOW HILLS	73°-23'-3	40°-47'-1	73	81.3			31.5
6	ROCKAWAY BEACH	73°-54'-0	40°-34'-0	0	34.8		29.3	30.5
5	NORTONS POINT	74°-1'-0	40°-34'-5	0	35.1			28.4

Fig. 7—Table of data taken with transmitter at Deal.

It should be pointed out that these measurements are not independent of the local receiving conditions. The proximity of the ground has the effect of making the vertical directive characteristic far different from that of the same antenna in free space. In all cases the field increased as the receiving antenna was raised up to the maximum

height available (12 m.). This effect of the ground was therefore more detrimental when the longer waves were used, since the antenna could not then be raised to corresponding heights. Even taking this into account, the over-land transmission paths of these tests favor the shorter wave-lengths. A theoretical reason for this will be given later.

In one direction from Deal, S. 50° 46′ W., measurements were made on 69 mc. at numerous places along the beam of a directive antenna, up to a distance of about 95 km. The profile of this path along the straight line to the most distant point, Chesilhurst, is shown in Fig. 6-*B*. Displacements of intermediate points from this line are negligible

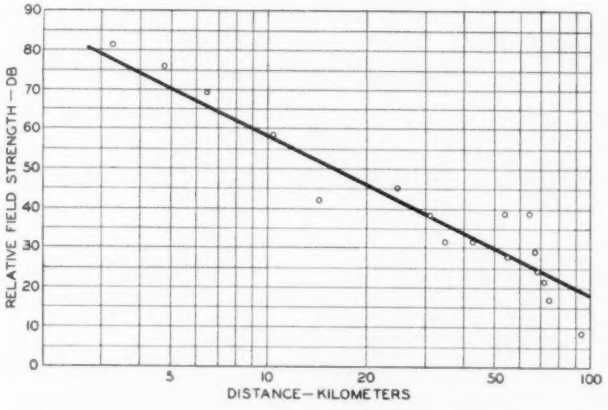

Fig. 8—Field strength as a function of distance for transmission over level country, along the profile of Fig. 6-*B*.

except in the case of New Egypt. Here a slight displacement was made in order to use a favorable receiving site for more extensive measurements. The profile in this neighborhood is superposed on the main profile. The various receiving points are shown by small arrows.

The received field is plotted as a function of distance in Fig. 8. For comparison purposes a straight line representing the inverse square law is drawn. This represents the general trend very well.

Transmission along this path is of particular interest since it represents conditions to be expected over flat land. The profile in Fig. 6-*B* shows that if the immediate neighborhood of terminal points be left out of consideration, the maximum difference in elevation along the path is only 45 meters. This path probably represents a spherical

earth as well as any of similar length that exists in this part of the country.

Stability of Signals

Speaking generally, the signals received in ultra-short wave transmission vary little, if at all. In this respect they are in marked contrast with signals of lower frequencies in the transmission of which the Kennelly-Heaviside layer is involved. In this work, definite indications of fading have been found only in the case of paths in which the attenuation in excess of that represented by the inverse distance formula has been in the order of 30 to 40 db. The variations were in the order of one or two decibels, and the period was a few seconds. This may have been due to variable atmospheric refraction. On the other hand, it is not inconceivable that it may have been due to reflection from clouds. It is, of course, easy to show that there is so little moisture in clouds that reflections must be extremely weak. But we have to explain coefficients of reflection in the order of only 0.01. This is plausible since we are concerned with reflection from the cloud at near-grazing incidence for which the coefficient tends to be unity regardless of the difference in dielectric constant. Further investigation is needed along these lines.

Part II—Theory

Before entering into a quantitative explanation of some of the results which have been presented, it may be well to direct attention to certain ways in which the present problem is related to the familiar concepts of optical reflection, diffraction and refraction.

Reflection

Reflection constants are readily calculated in the case of smooth surfaces such as still water. Having obtained these, the resultant amplitude at the receiver can be calculated for different ground constants. (See Appendix I.)

Even if the surface is rough, it is to be expected that an ultra-short radio wave may be reflected regularly from a body of water. The existence of regular reflection is less obvious when transmission occurs over rolling land. In the first case we have the most simple conditions since the surface waves on the water are irregularities of a single general type and range of dimensions. They are merely deviations from a plane, or rather from a sphere. But in the second case, the irregularities of the land are of all forms and dimensions and the existence of regular reflection cannot be granted without consideration.

In most of the cases of radio propagation now being considered, we are concerned with near-grazing incidence since both transmitter and receiver are located near the ground and are separated horizontally by a comparatively large distance. That regular reflection may occur under such circumstances, even over irregular ground, can be shown by a simple optical experiment. A moderately rough piece of paper, such as a sheet of bond or any other paper without gloss is employed. The paper on which this is printed is rather too smooth to give a striking result, but it may be used. If the reader will focus his eye on some distant object which shows up with contrast against the sky, and if he will then hold the paper about a foot from the eye so that the line of sight is parallel and very close to the plane of the paper, it will be seen that the rough sheet has become a surface with a high gloss. It is helpful to bend the paper slightly so as to produce a cylindrical surface having elements parallel to the line of sight. Images of

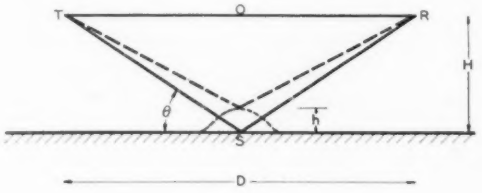

Fig. 9

distant objects can be seen clearly in such a paper mirror and considerable detail can be obtained provided that the angle of incidence differs from 90° by something less than one degree. It is to be remembered that in most of the optical paths encountered in ultra-short wave propagation, we are concerned with angles which are as near to grazing as this is.

The reason for this reflection from a rough surface is readily explained on the basis of Huyghens' principle. The situation is represented in Fig. 9. Let us suppose that the general level of the rough surface is below the line of sight *TOR* by a distance *H*. *H* is assumed small compared with *D*, the length of the path. As a result of variations in *H* due to the ruggedness of the terrain there will be corresponding variations in the total length of the optical path *TSR*. Reflections will be approximately regular, however, if these variations in *TSR* are small enough in comparison with half a wave-length. In Fig. 9, a change in level, *h*, is represented at *S*, the dotted line representing an irregularity which has been added. These assumptions lead readily

to the requirement for regular reflections: h, the height of the hill, should be small compared with $\lambda D/8H$, which equals $\lambda/4\theta$, where $\pi/2 - \theta$ is the angle of incidence. This relation expresses the fact that the regularity of reflection from a given rough surface can be improved either by increasing the wave-length or by decreasing the angle θ.

While these considerations show the reasonableness of regularity of reflection, they do not enable us to calculate the value of the coefficient. In the over-land tests which we have described, the amplitude of the coefficient of reflection would have been very near to unity and its phase angle would have been very near to 180° if the ground had been smooth. In the absence of data on the reflection from rough surfaces, we have used these same values although it is apparent that the coefficient will be less than unity due to scattering and increased penetration. The fact that a fairly good quantitative check has been obtained experimentally indicates that this assumption is reasonable. The check is somewhat better when the magnitude of the reflection coefficient is somewhat reduced (Fig. 16).

Diffraction

In ultra-short wave propagation, the effect of an obstacle, such as a hill, can be visualized best by considering it from the point of view of this same principle of Huyghens. Fig. 10-*A* represents this. A wave

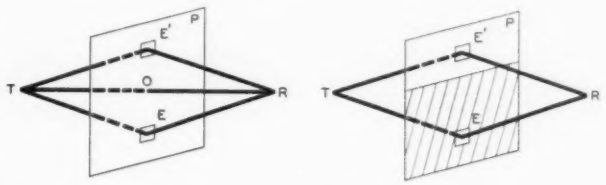

A Fig. 10 *B*

originates at T and travels unobstructed to R, passing through the plane P. It is, of course, incorrect to say that the effect travels exclusively along the line TOR. Consideration must be given to other paths such as TER, and the effect of the latter can be neglected only in case the path length TER exceeds TOR by many wave-lengths; or more properly, a region about E can be neglected only in case the phases of the components transmitted through the elements within it (*e.g.*, along TER) are such as to cause destructive interference among themselves.

When a hill is interposed as shown in Fig. 10-*B*, elements such as *E*, below the profile of the hill, are prevented from contributing to the signal at *R*, while elements such as *E'*, above the profile, contribute as before. This is the simple concept as used in optics and will be used without essential modification in the explanation of non-rectilinear radio transmission.

Refraction

Besides reflection and diffraction, a third optical concept, atmospheric refraction, must be considered in this study.[15] It is a well-known fact that a star, appearing to be exactly on the horizon, is really 35 minutes below it. It is obvious that the "image" of an ultra-short wave transmitting antenna will be elevated above its true direction by this same means. The only question is whether the effect is appreciable or not. The answer, obtained theoretically, is that refraction must be taken into account. Unfortunately, we so far do not have quantitative measurements which show the effect of refraction of ultra-short waves in an unmistakable way. Those that we do have, however, appear to be consistent with expectations based on the theory which will now be presented.

The physical picture to be assumed is one in which the dielectric constant of the atmosphere decreases with height above sea level and is not a function of horizontal dimensions. In other words, the phase velocity of a wave in this medium becomes greater as the distance from the center of the earth increases. In the case of ultra-short waves, we are almost always interested in waves traveling in a substantially horizontal direction. The wave-front, therefore, lies in a plane which is nearly vertical and since the upper portions travel faster than the lower, there is a tendency for the ray to bend slowly back toward the earth.

This phenomenon, in its general aspects, is the same as that which is commonly assumed to explain the bending of longer waves about the earth. There is an important difference, however, in regard to the part of the atmosphere which is important. In the case of these longer waves (for example, one having a wave-length of 15 meters or a frequency of 20 mc.), the ionization in the atmosphere 100 to 400 km. above the earth is the cause of the refraction which makes long distance signaling possible. In the case of ultra-short waves, however (for example, one having a wave-length of 1.5 meters or a frequency of 200 mc.), this upper region is of no importance but it is the region

[15] Jouaust (*L'Onde Electrique*, 9, 5–17, Jan. 1930) has pointed out the importance of refraction in the propagation of ultra-short waves. The authors believe, however, that he has overemphasized its importance.

below one kilometer or so, where the ionization is negligible, that is essential.

The radius of curvature of a ray traveling horizontally in the lower atmosphere can readily be calculated if it is known how the refractive index, n, varies from point to point. If H is the altitude above sea-level, the radius of curvature of the ray is simply

$$\rho = -\frac{n}{dn/dH}.$$

But since $n = \sqrt{\epsilon}$, where ϵ is the dielectric constant, the radius of curvature is

$$\rho = -\frac{2}{d\epsilon/dH},$$

provided n is not very different from unity.

In Appendix II the estimation of this radius of curvature is discussed in some detail. While some of the data upon which such a calculation can be based are rather uncertain, it appears that a good first approximation is obtained by assuming the radius of curvature, ρ, of the refracted ray to be four times the radius of the earth, r_0. As pointed out in the appendix, this varies to some extent with weather, and even as an average value, it may have to be changed when more reliable data on dielectric constants become available.

On first consideration of the ways in which refraction can be taken into account, it appears that the attempt must complicate an already involved situation. Fortunately, however, refraction is much simpler to calculate than diffraction or reflection. The method is presented rigorously in Appendix III. At this point we shall merely state the result and show its plausibility.

In ultra-short wave work we are almost always concerned with propagation in a nearly horizontal direction. The curvature of the ray is $1/\rho$, while that of the earth is $1/r_0$. We are interested, however, in the relative curvature, which we shall call $1/r_e$. If, instead of using simple rectangular coordinates, we transform to a coordinate system in which the ray is a straight line, the curvature of the earth will become $1/r_e$, which is $1/r_0 - 1/\rho$. The equivalent radius of the earth would be

$$r_e = r_0\left(\frac{1}{1 - r_0/\rho}\right),$$

and is therefore greater than the actual radius of the earth by the factor $\frac{1}{1 - 1/4}$ which is 1.33. This fictitious radius is therefore

8500 km. instead of 6370 km. Since in the new system of coordinates, the ray is straight, the new equivalent dielectric is to be assumed constant and equal substantially to unity.

Refraction can therefore be taken into account as follows: In making calculations, we start with the topographical features of the path and construct an equivalent profile [16] of some sort plotted from known elevations of points along the path. If refraction were to be neglected, the actual radius of the earth would be used. To take refraction into account, the process is exactly the same except that the fictitious radius $r_e (= 1.33 r_0)$ is now used. Reflection and diffraction calculations are then based on this equivalent profile, in which account has already been taken of refraction by means of the fictitious radius.

It follows from the discussion given in Appendix III, that this transformation is not limited to optical paths. The discussion applies to the amplitude of the disturbance set up at one point due to a radiating source at any other point, whether that source be an actual antenna or one of the elementary reradiating oscillators of Huyghens. Under all circumstances where Huyghens' principle applies, the signal is passed on from one intermediate plane to another by the repeated application of the principle. Since this transformation is justified for determining the effect that any elementary oscillator at one point produces at a second nearby point it is justified for the process as a whole provided only that the line connecting the two points is inclined to the horizontal by only a small angle.

Optical Path Transmission

Let us now consider the application of these concepts to the case of transmission along an optical path. It has been pointed out that in many cases we would expect to find a well-defined reflected wave superposed on the direct wave. The two will, therefore, interfere constructively or destructively depending on phase relations. In other words, a set of Lloyd's fringes will be set up.

The airplane measurements over New York Bay gave direct evidence of the existence of these fringes. In order to check this quantitatively, the data are presented in Fig. 11-*A*. Vertical polarization was used.

[16] The elevations above sea-level involved are so small compared with the distances along the surface of the earth that they cannot be plotted on the same scale. This difficulty can be overcome within limits by increasing the scale used in plotting elevations, and at the same time decreasing the scale used in plotting the radius of the earth by the same ratio. When this is done, a line which in the actual case is straight remains approximately so even with these distorted scales. This gives a general picture of the profile but due to the slight curvature introduced, all distances involved in the calculations of this paper have been determined analytically. The scales of the profiles shown have thus been altered by a factor of about 50.

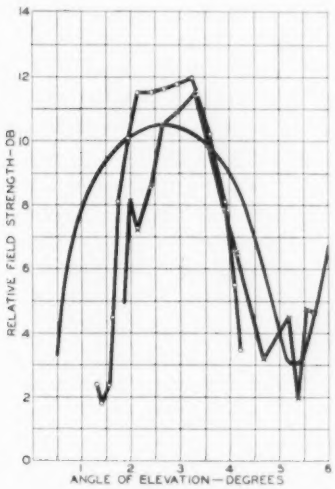

Fig. 11-*A*—Field strength as a function of the angle of elevation of the receiver, for transmission over salt water at 80 mc. The two experimental curves are from data taken with the receiver in an airplane flying at two constant altitudes. The smooth curve is theoretical.

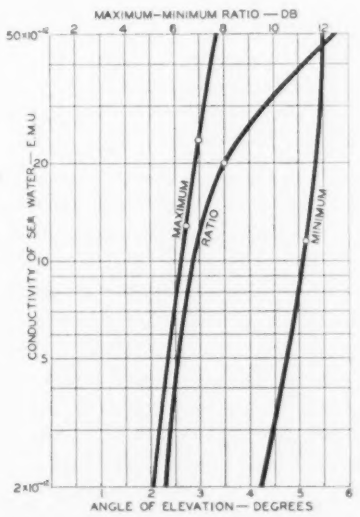

Fig. 11-*B*—Theoretical angles of elevation of maximum and minimum, and magnitude of their ratio, as functions of the conductivity of the water for a dielectric constant of 80, and a frequency of 80 mc. The experimental points shown (from Fig. 11-*A*) indicate a conductivity of about 17×10^{-12} e.m.u.

Since the altitude of the transmitting antenna was small compared with that of the airplane, we would expect, on the basis of the optical picture, that the field received would depend on the distance and the angle of elevation of the plane as seen at the transmitter. In the figure, the distance has been eliminated by recourse to the inverse distance law, which applies to the separate component waves. The result has been plotted for two elevations with varying distance. The peaks and troughs of the Lloyd's fringes are fairly well indicated.[17]

While little weight can be given to the absolute values as measured in the airplane,[18] it is of interest to estimate the conductivity of the

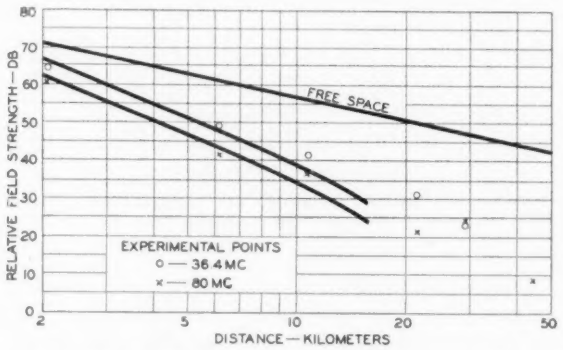

Fig. 12—Theoretical characteristics for transmission over salt water ($\sigma = 1.5 \times 10^{-11}$ e.m.u., $\epsilon = 80$ e.s.u.) on the basis of simple optical reflection. Upper curve: 36.4 mc. Lower curve: 80 mc.

water from the relative values. Fig. 11-*B* shows the theoretical location of maxima, minima and their ratio as functions of the conductivity of sea water. Four experimental values have been plotted. Their average indicates a conductivity of 1.7×10^{-11}. This, at least, has the correct order of magnitude, but the experimental data are too inaccurate to justify much faith in the numerical value otherwise. The important point is that the field pattern is qualitatively what would be expected. The theoretical characteristic for this value is also plotted in Fig. 11-*A*.

Turning now to the more accurate data taken on the ground (already presented in connection with Fig. 3), theoretical curves have been fitted to the data in Fig. 12. In the experiment, the antennas were

[17] Similar fringes were obtained over land by Englund, Crawford and Mumford.

[18] Because of the irregular shape of the airplane, the orientation with respect to the line of sight affects the gain of the receiving antenna. Each of the two curves has been plotted from data taken with approximately constant orientation of the airplane.

some 25 and 6 meters above sea level and under this condition the effect of earth curvature cannot be neglected in the calculation except for paths less than a kilometer in length. This curvature has been taken into account here to the extent of replacing the curved surface by a plane which is tangent to the earth at the point where the reflected ray of geometric optics touches the earth. This is justified for short optical paths but cannot be used at the longer distances when the receiver nearly disappears from the view of the transmitter.

Fig. 12 shows the theoretical curve for vertical polarization based on a conductivity of 1.5×10^{-11} e.m.u. and a dielectric constant of 80 e.s.u. Other values of conductivity give the same type of curve but the best fit to the experimental data is obtained by this curve. The dielectric constant was chosen equal to that which has been found to hold for fresh water throughout this frequency range.[19]

The agreement between the experimental and theoretical curves is reasonably satisfactory. By varying one constant, the conductivity, it has been possible to check approximately the absolute attenuation at two distances and two frequencies.

The conductivity (1.5×10^{-11}) is lower than that measured for sea water at low frequencies. For this reason, it was considered desirable to check the low frequency conductivity in this part of the bay since it may have been reduced by the fresh water emptied into the bay by numerous nearby streams. A number of samples were taken from different points between the transmitting and the receiving locations at both low and high tide. The values varied between 2.9×10^{-11} and 3.7×10^{-11} e.m.u., with an average of about 3.3×10^{-11}. This is more than twice the value of 1.5×10^{-11} indicated by the optical calculations. A sample of undiluted ocean water taken at the same time had a conductivity of 4.3×10^{-11}.

This agreement of experiment with simple optical theory does not prove that the assumed picture of a direct and a reflected wave is complete. It is to be pointed out that a rigorous solution (as opposed to the simple reflection picture), might require an appreciably different conductivity. Mr. C. B. Feldman of these Laboratories has made some short distance experiments over smooth land.[20] Using fre-

[19] Since the writing of this paper, an article by R. T. Lattey and W. G. Davies on "The Influence of Electrolytes on the Dielectric Constant of Water" has appeared (*Phil. Mag.*, 12, 1111–1136, Dec. 1931). Their results indicate that the dielectric constant is materially increased by salt in the water. Their experiments were made for solutions that were very much more dilute than sea water. This, together with the fact that the effect of a combination of solutions was not determined, makes it impossible to estimate the dielectric constant of sea water from their results with a reasonable degree of certainty.

[20] A paper covering this work will appear later: "The Optical Behavior of the Ground for Short Radio Waves," C. B. Feldman.

quencies in the short wave range he found that the simple optical picture cannot always explain the results obtained with vertical polarization. With horizontal polarization, however, satisfactory agreement was obtained. The propriety of the simple optical picture is therefore much clearer for horizontal than for vertical polarization.

Reasons have been given in an earlier section for expecting regularity of reflection even in the case of rugged land, if the incidence is near enough to grazing. It was also shown that there probably exists an effective coefficient of reflection which is actually near to -1 for both polarizations. At the receiver the phase relation between the direct and reflected waves, and hence the field, thus depend only on the path

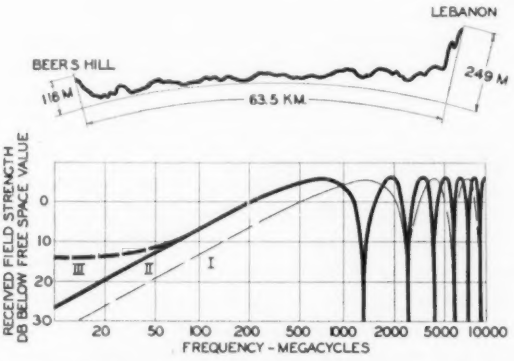

Fig. 13—Above: Profile of "optical" path between Beer's Hill and Lebanon. Below: Calculated frequency characteristics for this path.

Curve I, reflection only (coefficient, -1).
Curve II, refraction and reflection (coefficient, -1).
Curve III, refraction and reflection (coefficient -0.8).

difference measured in wave-lengths. A set of interference fringes will therefore be set up, and the received signal at any given point will be a function of the frequency.

Making these assumptions as to reflection and taking refraction into account, it is interesting to calculate the frequency characteristic of a typical path. For this purpose, we may choose the path from Beer's Hill to Lebanon, which is discussed by Englund, Crawford and Mumford. The characteristic which would be obtained from the foregoing considerations of reflection and refraction is shown in Fig. 13. The light curve shows the frequency characteristic that results by neglecting refraction. It can be seen that below about 500 mc. the expected gain due to refraction is about five db., a gain which is by

no means inconsiderable. For 70 mc. the field strength indicated by the curve is in fair agreement with measurements made over this path by Englund, Crawford and Mumford.

The effect of reducing the reflection coefficient to -0.8 is to raise the low frequency end of the curve, to reduce the maxima to 5.1 db. and to raise the minima to -14 db. This is shown by the dashed curve of Fig. 13.

Another point in connection with the solid curve in Fig. 13 is of interest. At 715 mc. (42 cm.) the path difference is half of a wavelength and the two components now add in phase. This is the optimum phase relation since it gives the largest possible resultant. Hence 715 mc. is an optimum frequency for this particular path on these assumptions and a field 6 db above the inverse distance value would be expected. Even at one third this frequency, 240 mc. (126 cm.), fields equal to the inverse distance value might be expected. For higher frequencies many maxima and minima are indicated.

Since the lowest optimum frequency depends on the difference between the path lengths of the direct and reflected components, it should be possible to obtain much lower optimum frequencies by picking paths in which the terminals are located very much higher than the valley between them. Thus, optical paths more than one hundred miles long may be found in California for which the lowest optimum frequencies may be considerably less than 30 mc. (10 m.).

Error in the assumption of a phase shift of 180° would change the frequency at which maximum and minimum fields occur, and failure to obtain a reflection coefficient of unity might materially reduce the difference between the received field and the free space value.

The profile shown in Fig. 14 is used to illustrate the effects of change in polarization and ground constants as indicated by calculations based on simple optical theory. In the computations indicated by the various frequency characteristics of this figure, the same profile has always been used, but two different sets of ground constants, and both horizontal and vertical polarizations, have been employed. The curves are self-explanatory. It is especially to be noted that for horizontal polarization the field decreases with decrease in frequency and is nearly the same for land as for sea-water, *i.e.*, it is nearly independent of conductivity and dielectric constant. For vertical polarization this trend is reversed for frequencies such that the conduction currents are large compared with the displacement currents. In this example, this occurs in the neighborhood of 60 mc. in the case of sea-water and 5 mc. in the case of "average" land. Thus for vertical polarization there exists a "poorest" frequency separating the

excellent transmission at very low frequencies, where there is no phase shift due either to reflection or to path difference, from the excellent transmission at very high frequencies (*e.g.*, 2000 mc.) where large phase shifts due to these two causes nullify each other.

In those cases in which calculations of this sort indicate a very weak resultant field, these estimates may be considerably in error due to neglect of terms which are usually unimportant.

It may be of interest to note that two of the experiments described have given an inverse square of distance variation. In both cases the antennas were near the surface of the earth. It can easily be shown that this should be expected when total reflection occurs with reversal

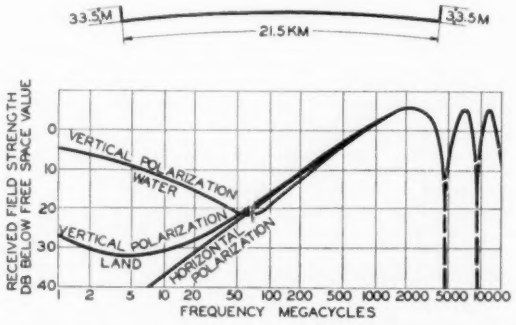

Fig. 14—Above: Profile of a hypothetical path. Below: Calculated frequency characteristics for various conditions. Curves are shown for vertical polarization over sea water ($\sigma = 20 \times 10^{-12}$ e.m.u., $\epsilon = 80$ e.s.u.), for vertical polarization over land ($\sigma = 5 \times 10^{-14}$ e.m.u., $\epsilon = 15$ e.s.u.), and for horizontal polarization over either (ground constants not important in this case).

of phase provided that the difference in path length is smaller than one sixth of a wave-length. Thus, in Fig. 9 the signal received at R will tend to be zero or very small, except as the phase relation is altered by the difference in the path lengths TOR and TSR. The corresponding phase difference in radians is $4\pi H^2/D\lambda$, if H is small. Since the differences of two vectors of equal magnitude are equal to the product of their phase difference, if small, and their magnitude, the resultant field is equal to $4\pi KH^2/\lambda D^2$. One of the inverse distance factors is due to the phase angle and the other is due to the fact that the amplitude, K/D, of the direct wave itself varies inversely with the distance. Under these conditions, therefore, the signal would vary inversely as the square of the distance, D, directly as the square of elevation, H, and inversely as the wave-length. Qualitatively, at least, all of these tendencies have been observed experimentally.

Even with vertical polarization, the reflection coefficient is also approximately -1 for transmission over smooth land with near-grazing incidence. The same inverse square tendency is therefore to be expected with vertical polarization under these conditions.

Non-Optical Paths

We shall now discuss one type of non-optical path which is of interest both because it occurs frequently and because on the basis of the assumptions made it is amenable to approximate calculation. It is represented in simplified form in Fig. 15.

T and R are located on opposite sides of a hill, M, and the distances TM and TR are great compared with the altitudes involved. The low land on both sides of the hill is comparatively flat, though not

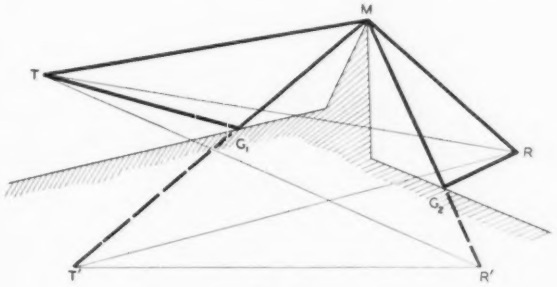

Fig. 15

necessarily coplanar. As previously discussed, the magnitude of the coefficient of reflection to be expected will be close to unity [21] for many conditions likely to be met and the phase change will be not much different from 180°. In other words, the wave reflected from the ground between T and M will appear to have come from a negative virtual image, T'. The disturbance above the mountain, M, will be made up of two components corresponding to the antenna and its negative image. In passing from the region above M to the receiver, R, each of these components is broken down into two new components due to reflection between M and R. One of these proceeds directly to the receiving antenna. The other proceeds indirectly, being reflected by the intervening ground; it may be thought of as traveling

[21] An exception of this occurs in the case of vertical polarization over surfaces having appreciable conductivity, such as sea-water. Recent experimental work not described in this paper indicates that the assumption is incorrect over land at frequencies considerably higher than those of the present experiment. In such cases the theory is still tenable if appropriate constants are used.

to the virtual image of the receiving antenna, R', with a phase change of 180° due to reflection between M and R.

The received field is therefore propagated in four ways: (1) directly from T to R by diffraction at M represented by TMR, (2) by reflection at G_1 and diffraction at M represented by TG_1MR, (3) by diffraction at M and reflection at G_2 represented by TMG_2R, and (4) by reflection at G_1, diffraction at M and a second reflection at G_2 represented by TG_1MG_2R. The amplitudes and phases of these four components can be calculated by usual methods of diffraction (see Appendix IV) by assuming the components to travel from the real transmitting antenna or its virtual image, to the real receiving antenna or its virtual image. The ratio of the received field to the free space field may then be calculated by combining the four components as follows:

$$\begin{aligned} E/E_0 = {} & C_1 \exp\left[-j(\eta_1 + \zeta_1)\right] \\ & + C_2K_1 \exp\left[-j(\eta_2 + \zeta_2 - \varphi_1)\right] \\ & + C_3K_2 \exp\left[-j(\eta_3 + \zeta_3 - \varphi_2)\right] \\ & + C_4K_1K_2 \exp\left[-j(\eta_4 + \zeta_4 - \varphi_1 - \varphi_2)\right], \end{aligned}$$

where the C's are the ratios of the field strengths with and without diffraction, the η's are the phase lags introduced by diffraction and the ζ's are the phase lags due to path lengths TR, $T'R$, TR' and $T'R'$, while the K's are magnitudes of the reflection coefficients and the φ's are the phase advances at reflection.

It is true that actual conditions will seldom be as simple as these. The valleys will not be flat. There will often be more than one hill and it may be impossible to represent the obstructions accurately by the single straight edge, M, which we shall assume. It will often be possible, however, to choose equivalent planes and straight edges in such a way as to justify some confidence in the results.

On these assumptions the frequency characteristic of the transmission path from Deal to Lebanon has been calculated (Fig. 16). By actual measurement it has been found that the attenuation over this path at 17 mc. (17 meters) was more than that at 69 mc. (4 meters). This characteristic of poorer transmission on the longer wave-lengths is the opposite of what would have been expected either on the basis of diffraction alone or by analogy with the trend observed on lower frequencies. The calculations show, however, that this is the characteristic that we should expect on the theory outlined. In view of uncertainties in the reflection coefficients and errors of measurement, the agreement of the absolute values calculated and measured is as good as should be expected. An improvement in this agreement

is obtained by assuming a reflection coefficient of − 0.8. The resulting curve is shown by the broken line in Fig. 16. In the case of the optical path of Fig. 13 reflection coefficients of − 1 and − 0.8 agree equally well with the experimental point. (In Fig. 16 a correction has been applied to the experimental data eliminating the effect of local reflections at the receiver.)

This curve brings out the important fact that even for non-optical paths, one may expect to find optimum frequencies. On this particular

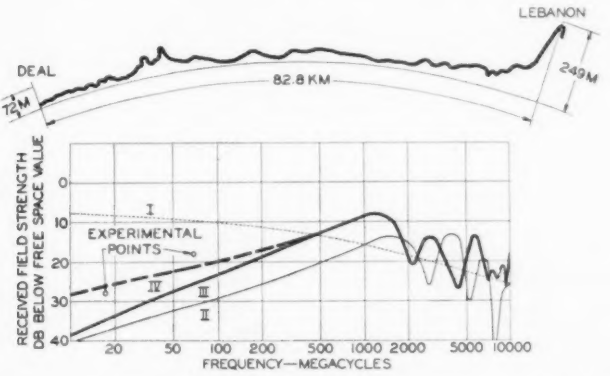

Fig. 16—Above: Profile of "non-optical" path between Deal and Lebanon. Below: Frequency characteristics for this path calculated on various assumptions.

Curve I takes only the shadow effect (diffraction) into account. Note that the experimental points fall far below it.

Curve II is calculated on the basis of diffraction and reflection (coefficient − 1.0). Note that this gives a better check with experiment, but values are too low.

Curve III adds to II a correction for refraction.

Curve IV assumes diffraction, refraction and a reflection coefficient of − 0.8. It checks the experimental points to within experimental error.

The original experimental data have been corrected to eliminate the effect of ground reflection near the receiver. The transmitter, being above level ground, needed no such correction.

path the simple assumptions give 1200 mc. (25 cm.) for the lowest of these. On other paths which have been calculated, optimum frequencies would be expected in the range between 1 and 10 meters.

It is fully realized that the details of these curves will probably not be found experimentally. We do not as yet have sufficient experience to pick the simple picture that will in effect represent a complicated topography and transmission mechanism, and it is obvious that this may never be possible. It is encouraging, however, that the limited number of measurements which have already been made experimentally, agree reasonably well with the theory proposed.

Discussion of Certain Trends with Respect to Frequency

It may be helpful, in recapitulating, to consider the different trends which ultra-short wave transmission shows with respect to frequency, and to mention their relationships to the phenomena of the ground wave at lower frequencies.

The simplest trend is that to be found in free space, that is, in cases for which the effect of the ground is negligible. Changes, if any, in transmission efficiency with frequency are then due to the air itself. Such evidence as there is on this point indicates that the assumption of absorption by the air is unnecessary within the range of our experiments, and in fact this is to be expected on theoretical grounds. The "free space" trend therefore gives merely a horizontal line. In Figs. 13 and 14 the high frequency portion of the curve oscillates about this line and would approach it if reflections from the earth were decreased in strength.

In general, however, the effect of the earth will alter this trend in such a way as to give a variation with respect to frequency. Perhaps the most familiar variation is the loss of efficiency in going to high frequencies when vertical polarization is used. The decrease is due to conduction losses in the ground. This "conductivity trend" appears, for example, in the work of Sommerfeld and of Zenneck. Many experimental observations have been made of it at broadcast frequencies for distances up to a few hundred miles over paths which are obviously "non-optical." We have seen it here in the optical path tests made over sea-water, Fig. 3. It appears also in the low frequency end of the "vertical polarization over water" curve in Fig. 14.

In several cases we have noted that 69 megacycles was more efficiently transmitted over land than 17 megacycles. This is opposite to the conductivity trend and appears to have a very different cause. For both optical and non-optical paths it is believed to be associated with a phase change at reflection of 180°, and the effect is most pronounced when reflection occurs without appreciable loss of amplitude. This "negative reflection" trend is exemplified on the one hand by the very poor transmission with very low frequencies when horizontal polarization is used, and, on the other, by the excellent transmission at 75 mc. (4 meters) between Beer's Hill and Lebanon (Fig. 13). In the latter case the difference in path lengths of direct and reflected waves was not negligible compared with a half wave-length, and it is a phase shift due to this cause which apparently prevents destructive interference. This negative reflection trend also appeared in the non-optical paths over level land (Fig. 8). It is affected not only by the negative reflection in the neighborhood of the antennas (negative

image), but also by negative reflection all along the path. (The term "negative reflection" is used here even in the non-optical case, since when we visualize the process in terms of Huyghen's principle, it is apparent that this case is merely a succession of optical paths.) At higher frequencies this characteristic will cease to rise steadily and at least in the case of simple optical paths will oscillate up and down instead. The rising trend at lower frequencies, however, is found so often that it deserves special mention. It is illustrated by the rising curve and the experimental points shown in Fig. 16.

A fourth trend is due to diffraction and it is in the same direction as the conductivity trend. Long waves bend more easily about obstacles than do the short; the obstacle may be a mountain or it may be the ever-present bulge of the earth. This type of characteristic is indicated in Fig. 16 in the high frequency part of the calculated curve, but in our experiments we have so far not had conditions in which its effect could with certainty be separated from the opposite "negative reflection" trend. The reason for this is that the diffraction trend does not predominate except with frequencies which are sufficiently high. In tests from Deal to Lebanon (Fig. 16) it appears that frequencies greater than 1200 megacycles might have to be used in order to separate these effects clearly. This is a point of great importance in view of the wide-spread belief that ultra-short waves suffer most in transmission because of the failure of the waves to bend around obstacles. Except when high mountains or very short waves are involved, the loss in transmission is more likely to be due to reflection.

When reflection of vertically polarized waves takes place from a very good conductor, there is no change of phase at reflection, the "negative reflection" mechanism is therefore absent, and the tendency is toward reinforcement rather than cancellation. Physically these conditions can be found in the case of transmission over sea water for frequencies less than 5 mc. In this case, as shown in an as yet unpublished study, the diffraction trend has definitely been found experimentally and checked quantitatively with theory.

Optimum Frequencies

In the preceding pages calculations have been made for various types of path. Both for optical paths and for non-optical paths these have pointed to certain frequencies which, from the transmission standpoint, give most efficient results. The value of this optimum frequency depends almost entirely upon the topography of the path

and therefore changes from path to path.[22] At the same time there are certain frequencies which give results which are poorer than those obtained with higher or lower frequencies. It is obviously desirable to avoid these in practice. In general, it seems important that in making a choice of frequency, the particular path should be considered by itself in order to insure that maximum transmission efficiency, or at least the best compromise with apparatus difficulties, will be obtained.

Acknowledgment

The experiments described in this paper have been possible only through the assistance of many members of the Bell Telephone Laboratories and we wish to make acknowledgment of this cooperation. We also wish to express our appreciation of the support and encouragement given in the course of this work by Dr. W. Wilson.

Appendix I—Reflection Calculations

The ratio of the resultant of the direct and reflected waves to the direct wave is

$$\sqrt{1 + K^2 - 2K \cos \gamma} = \sqrt{(1 - K)^2 + 4K \sin^2 (\gamma/2)},$$

where K is the ratio of the amplitude of the reflected wave to that of the direct wave and $\gamma \pm \pi$ is their phase difference.

$$\gamma = \psi - \Delta,$$

where Δ is 2π times the path difference in wave-lengths and

$$\varphi = \psi \pm \pi$$

is the phase advance at reflection. The convention here used for phase change at reflection is the change in phase of the vertical component in the case of vertical polarization, and the change in phase of the horizontal component in the case of horizontal polarization. In the case of vertical polarization this is different from the convention

[22] Beverage, Peterson and Hansell ("Application of Frequencies above 30,000 kc. to Communication Problems," *Proc. I. R. E.*, 19, 1313–1333, August 1931) found that a maximum range was obtained with a frequency of 35 mc. in some tests made over sea water. This maximum, if not due to peculiarities of the apparatus, it would seem, must be a function of the heights of transmitting and receiving antennas above sea level and above local ground.

used in optics.

$$K = \sqrt{\frac{1-\alpha}{1+\alpha}}, \quad 1 - K = \alpha\left[1 - \frac{\alpha}{2} + \frac{\alpha^2}{2} - \frac{3}{8}\alpha^3 + \cdots\right],$$

$$\psi = \tan^{-1}\beta = \beta\left[1 - \frac{\beta^2}{3} + \frac{\beta^4}{5} - \frac{\beta^6}{7} + \cdots\right],$$

$$\alpha = \frac{a \sin \xi}{1 + c \sin^2 \xi},$$

$$\beta = \frac{b \sin \xi}{1 - c \sin^2 \xi},$$

$$\xi = \frac{\pi}{2} - \theta,$$

where θ is the angle of incidence and for vertical polarization,[23]

$$a = \frac{\sqrt{2}}{s}[\epsilon\sqrt{s + r} + q\sqrt{s - r}],$$

$$b = \frac{\sqrt{2}}{s}[q\sqrt{s + r} - \epsilon\sqrt{s - r}],$$

$$c = \frac{1}{s}(\epsilon^2 + q^2);$$

while for horizontal polarization,

$$a = \frac{\sqrt{2}}{s}\sqrt{s + r},$$

$$b = -\frac{\sqrt{2}}{s}\sqrt{s - r},$$

$$c = \frac{1}{s},$$

where

$$q = 2\sigma/f,$$

$$r = \epsilon - \cos^2 \xi,$$

$$s = \sqrt{r^2 + q^2},$$

f is the frequency in cycles per second, and ϵ and σ are the dielectric constant and conductivity respectively, both in electrostatic units.[24]

[23] Vertical polarization refers to vertical electric field. Horizontal polarization refers to horizontal electric field. This is different from the concepts of optics.

[24] If σ is expressed in electromagnetic units, $q = 2\sigma V^2/f$, where V is the velocity of light (3×10^{10}).

For angles near grazing incidence, both $(1 - K)$ and ψ are proportional to ξ.

$$1 - K = a\xi, \qquad [\xi \to 0],$$
$$\psi = b\xi, \qquad [\xi \to 0],$$

where a and b are now both independent of ξ. If $K = 1$, the ratio of the resultant of the direct and reflected waves to the direct wave becomes $2 \sin (\gamma/2)$. If in addition γ is small, this ratio becomes simply γ.

For angles near normal incidence, both K and ψ are independent of ξ.

$$K = \sqrt{\frac{1 + c - a}{1 + c + a}}, \qquad [\xi \to \pi/2],$$

$$\psi = \tan^{-1}\left(\frac{b}{1 - c}\right), \qquad [\xi \to \pi/2],$$

where a, b, and c are now independent of ξ.

For good conductivity, $q(= 2\sigma/f) \gg \epsilon > r(= \epsilon - \cos^2 \xi)$; $a = b = \sqrt{2q}$; $c = q$ for vertical polarization. For horizontal polarization $a = -b = \sqrt{2/s}$, $c = 1/q$.

For poor conductivity, $q(= 2\sigma/f) \ll r(= \epsilon - \cos^2 \xi) < \epsilon$; $a = 2\epsilon/\sqrt{r}$, $b = 0$; $c = \epsilon^2/r$; $\psi = 0$ when $\xi < \cot^{-1}\sqrt{\epsilon}$, and $\psi = \pi$ when $\xi > \cot^{-1}\sqrt{\epsilon}$ for vertical polarization. For horizontal polarization $a = 2/\sqrt{r}$, $b = 0$, $c = 1/r$, $\psi = 0$.

Appendix II—Refractive Index and Curvature of Rays

The dielectric constant, ϵ, of dry air is given by the expression

$$\epsilon - 1 = 210 \times 10^{-6} p/K,$$

where p is the pressure in millimeters of mercury and K is the temperature in degrees absolute.

When water is present, however, an appreciable change is produced in the dielectric constant and doubtful points arise. Such, for example, are the effect of association of water molecules with each other or with other molecules, and the effect of adsorption on the surface of the plate of the test condenser. The work of Zahn [25] seems to have clarified

[25] *Phys. Rev.*, 27, 329, March, 1926.

the situation for pure water vapor. He showed that in his own experiments the anomalies which appeared at the lower temperatures were probably due to adsorption and not to association, as Jona [26] had assumed, and he states that his results are consistent with those measured by Jona at higher temperatures.

For pure water vapor, we may use the following formula which has been based on Zahn's data:

$$\epsilon - 1 = 1800 \times 10^{-6} \frac{p}{K}\left(1 + \frac{200}{K}\right).$$

Even though the separate values for water and for air may be considered to be known with sufficient accuracy, it does not follow that a mixture of the two will necessarily follow the usual additivity law for mixtures of gases. According to this law the values of $\epsilon - 1$ for the several components may be added to give the $\epsilon - 1$ for the mixture. Delcelier, Guinchant and Hirsch [27] gave some data for moist air taken as a preliminary to a more thorough study. They interpreted their results as denying this law for a mixture of water and air. Their experiments were carried out at 15° C. and at 25° C. It should be noted that this is the temperature range in which Zahn found anomalous behavior due to adsorption. It is therefore natural to suppose that this same spurious effect may have been present in the work of Delcelier, Guinchant and Hirsch.

It seems, therefore, that the law of additivity has at least not been disproved for this particular mixture and that we can do no better for the present than to assume that it does hold. We shall therefore proceed on this basis.

In obtaining the derivative with respect to height $d\epsilon/dH$, it must be remembered that ϵ is a function of the partial pressures of dry air and water vapor, and of the temperature. All of these vary with H. The values of significance are those occurring in the first kilometer or so above the ground. The conditions actually observed are variable and we have therefore chosen to use average values as given by Humphreys,[28] obtaining the rates of change from the values that he gives for 0.0 and 0.5 km. above sea-level.

The following table summarizes the results obtained:

[26] M. Jona, *Phys. Zeit.*, 20, 14 (1919).
[27] *L'Onde Electrique*, May 1926, p. 211 et seq.
[28] "Physics of the Air," McGraw-Hill, 1929, p. 55 and p. 74.

Condition	Radius of Curvature of Ray = ρ	$\frac{\rho}{r_0}$ [29]	Equiv. Earth Radius Without Refrac., r_e	$\frac{r_e}{r_0}$
Average summer (average moisture)	23,800 km.	3.74	8,650	1.36
Same, without moisture	31,600	4.95	7,950	1.25
Average winter	26,500	4.15	8,420	1.32
Same without moisture	29,300	4.61	8,100	1.27
Annual Average Used in Computations		4.0	8,500	1.33

r_0 = radius of the earth = 6370 km.

Appendix III—Effect of Refraction

In the following it will be shown that the transformation given in the text gives the proper path for the ray and the proper phase relations. The latter are more conveniently treated by determining the "phase time," or the time required for a given phase to traverse the path. As a matter of fact the ray paths and phase times are not exactly the same in the two constructions but it will be shown that for one distribution of refractive index, n, which closely resembles that actually encountered, the error is negligibly small.

As indicated, this analysis is based on the customary ray treatment of refraction through a medium with a continuously varying refractive index. This simple ray theory is known not to be exact but in the present case we shall always be dealing with very small gradients, a condition in which the error becomes very small.

A good summary of the relations which we shall use is given in "The Propagation of Radio Waves," by P. O. Pedersen on pp. 154 and 155. The nomenclature is indicated in Fig. 17.

The length of the element of path, bb', equals

$$\frac{rd\theta}{\sin \varphi} \tag{1}$$

and the time required for the wave to traverse it is

$$dt = \frac{rd\theta}{v \sin \varphi} = \frac{nr}{c} \frac{d\theta}{\sin \varphi} \tag{2}$$

[29] It is inferred from a statement made by Jouaust, *Proc. I. R. E.*, Vol. 19, p. 487, Mar. 1931, that for his experiments between France and Corsica ρ/r_0 would have to be 5 or less in order for the direct ray to be unobstructed. Our figure of 4 therefore would indicate that his is an "optical" path. We do not believe, however, that an optical path is a necessary or sufficient condition for strong signals, although it certainly does help to make them probable.

(c is velocity of light and n the refractive index, which is assumed approximately equal to one at point a). But by Pedersen's equation 9'

$$nr \sin \varphi = r_0 \cos \psi. \tag{3}$$

Hence

$$dt = \frac{n^2 r^2}{r_0 c \cos \psi} d\theta. \tag{4}$$

Now, Eccles [30] has shown that when the dielectric constant varies with r (distance to center of earth) as follows:

$$n = \left(\frac{r_0}{r}\right)^{s+1}, \tag{5}$$

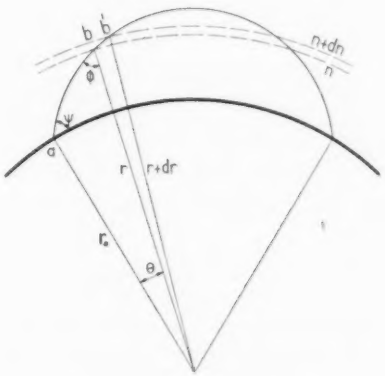

Fig. 17

the solution for the path of the ray is

$$r_0^s \cos (s\theta - \psi) = r^s \cos \psi. \tag{6}$$

Here s is a constant and r_0 is the distance to the center of the earth from a, the arbitrarily fixed point of reference in the path. r_0 is therefore not very different in our case from the radius of the earth.

By combining (5) with (6) we find that

$$nr = \frac{r_0 \cos \psi}{\cos (s\theta - \psi)}, \tag{7}$$

which when substituted in (4) gives

$$dt = \frac{r_0 \cos \psi}{c} \cdot \frac{d\theta}{\cos^2 (s\theta - \psi)}, \tag{8}$$

[30] *Electrician*, 71, 969–970 (1913).

integrating which from $\theta = 0$ to θ we obtain

$$t - t_0 = \frac{r_0 \cos \psi}{cs} [\tan (s\theta - \psi) + \tan \psi]. \tag{9}$$

If s in (5) is made somewhat less than one in absolute value and is negative, we obtain a fairly good approximation of the distribution actually encountered. The exponent $s + 1$ has then a small positive value and from (5)

$$\rho = -\frac{1}{dn/dr} = \frac{r}{n(s+1)} . \tag{10}$$

Since n is very close to unity and since we may assume $\rho/r = 4.0$ (Appendix II), we find that $s = -0.75$. This value will be used later.

Consider now a second series of values in equation (9), t', r_0', s', etc. which represent another situation which we shall define as follows:

$s' = -1$ (*i.e.*, constant index and no bending of the rays)

$\psi' = \psi$ (*i.e.*, no change in the initial direction of the ray)

$$s'\theta' = s\theta \text{ and } r_0' = -\frac{r_0}{s},$$

so that $r_0'\theta' = r_0\theta$, that is, the peripheral distance traveled is the same in the two cases although the radius of the earth has been increased from r_0 to $r_0(-1/s)$.

By substituting these new primed values for the unprimed values in equation (9), we obtain

$$t' - t_0' = \frac{r_0 \cos \psi}{cs} [\tan (s\theta - \psi) + \tan \psi], \tag{11}$$

which is identical with $(t - t_0)$ in (9). Note that the only assumption that has been made, limiting the generality of this equivalence, is the special distribution assumed in (5). The phase time is therefore unaltered by this substitution.

We have yet to prove, however, that in these two cases, rays leaving at the same angle, $(\psi = \psi')$, and describing angles θ and θ' at the real and fictitious centers of the earth, will have the same increase in elevation above sea level. If this can be shown, the equivalence will have been completely established.

The increases in elevation of the ray above that of the starting point

is found with the help of (6) to be as follows for the two cases:

$$r - r_0 = r_0([1 + L]^{1/s} - 1) \qquad \text{(real case)}, \tag{12}$$

$$(r' - r_0') = -\frac{r_0}{s}([1 + L]^{-1} - 1) \quad \text{(fictitious case)}. \tag{13}$$

where L is defined by the equation

$$(1 + L) = \left(\frac{r}{r_0}\right)^s = \frac{\cos(s\theta - \psi)}{\cos\psi}. \tag{14}$$

L is small compared with unity in the cases that we are considering. By expanding each and subtracting, the error caused by assuming that $(r - r_0)$ equals $(r' - r_0')$ is found to be

$$\frac{r_0 L^2}{2s^2}(1 + s) + \text{higher order terms in } L. \tag{15}$$

We have found above that s is approximately equal to -0.75. Taking $r_0 = 6370$ km. and remembering that we are ordinarily not concerned with rays farther above the earth than, say, 5 km., we have from (14)

$$\frac{r}{r_0} = (1 + L)^{1/s} \leq \frac{6375}{6370},$$

whence $L \geq -0.0006$.

Substituting these values in (15) we find that the error in height is less than 50 cm. This is negligible in the altitude of 5 km. which was assumed and we may consider the equivalence to be proved.

Appendix IV—Diffraction Calculations

The method of Huyghens applied to optical diffraction past a straight edge results in the following expression for the received field, E, in terms of Fresnel integrals.

$$\frac{E}{E_0} = a - jb = C\exp(-j\eta),$$

where

$$a = \frac{1}{\sqrt{2}}\int_v^\infty \cos\frac{\pi v^2}{2}\,dv,$$

$$b = \frac{1}{\sqrt{2}}\int_v^\infty \sin\frac{\pi v^2}{2}\,dv,$$

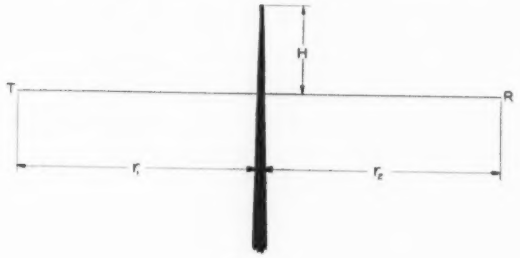

Fig. 18

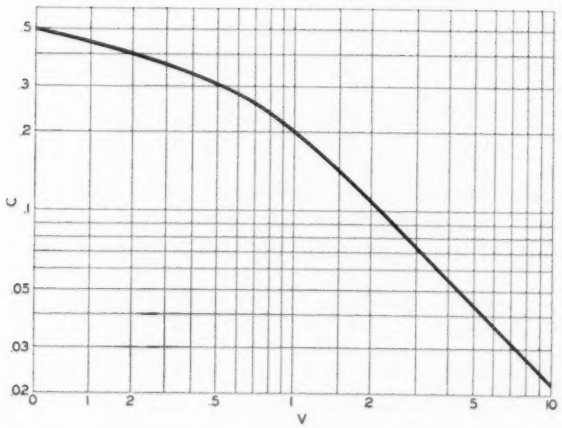

Fig. 19

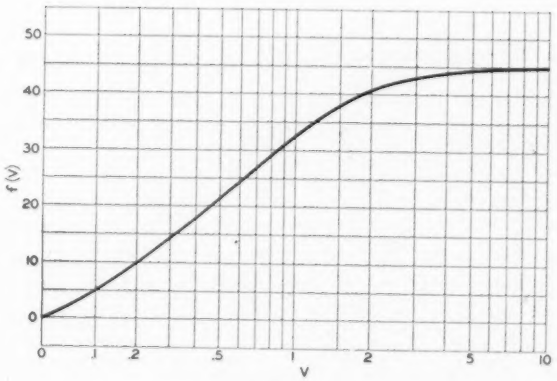

Fig. 20

and

$$v = H\sqrt{\frac{2}{\lambda}\left(\frac{1}{r_1}+\frac{1}{r_2}\right)}.$$

E_0 is the field with straight edge removed, a and b are Fresnel integrals, H is the height of the obstruction above the straight line from transmitter to receiver, r_1 and r_2 are the distances from the obstruction to the transmitter and receiver respectively (Fig. 18).

To facilitate calculation the value of C has been plotted in Fig. 19. η may be expressed as follows,

$$\eta = f(v) + \pi v^2/2,$$

where $f(v)$ is the function plotted in Fig. 20.

Mutual Impedance of Grounded Wires for Horizontally Stratified Two-Layer Earth *

By JOHN RIORDAN and ERLING D. SUNDE

A general formula is derived for the mutual impedance of wires embedded in a conducting medium and lying in one of two parallel planes of discontinuity in the conductivity. The general formula is quite complicated, but simplifies in a number of important cases, and summarizes the published mutual impedance formulas relating to two-layer earth and its special cases. The two most important cases are obtained by making the conductivity of one or the other of the outer regions zero. The special case in which the conductivity of the outer region adjoining the wires is zero gives the mutual impedance of any thin grounded wires lying on the surface of a horizontally stratified earth having conductivities λ_1 and λ_2 at depths less than or greater than b, respectively. When the conductivity of the other outer region is zero, the formula gives the mutual impedance of wires lying in the plane of separation, at the depth b. The formulas in both cases involve integrals which apparently cannot be evaluated in closed form: for practical application the use of curves of the kind given is suggested for approximate numerical results. The formulas for the special cases, of which there are 11, together with some of their limiting forms, are tabulated together for ready reference.

I

THE general formula for the mutual impedance of wires embedded in a conducting medium and lying in one of two parallel planes of discontinuity in the conductivity with displacement currents neglected is of the following form:

$$Z_{Ss} = \int_a^b \int_A^B \left\{ \frac{d^2Q(r)}{dSds} + i\omega P(r) \cos \epsilon \right\} dSds. \qquad \text{(I)}$$

The integrations are extended in the double integral over the two wires S and s extending between points A, B, and a, b, respectively, whose elements dS and ds are separated by distance r and include the angle ϵ between their directions. $Q(r)$ and $P(r)$ are functions of the frequency, the conductivities, and of the separation b between the planes of discontinuity in the conductivities as well as of r.

For wires on the surface of a horizontally stratified earth having conductivities λ_1 and λ_2 at depths less than or greater than b, respectively, $Q(r)$ and $P(r)$ are given by:

* A preliminary report of some of the results of this paper has been given in a letter to the Editor of the *Physical Review*, Vol. 37, No. 10, pp. 1369–1370 (May 15, 1931).

$$Q(r) = \frac{1}{2\pi\lambda_1}\int_0^\infty \left[1 + \frac{4\alpha_1^2(u+\alpha_2)(\lambda_1-\lambda_2)e^{-2b\alpha_1}}{\Delta[\alpha_1\lambda_2 + \alpha_2\lambda_1 + (\alpha_1\lambda_2 - \alpha_2\lambda_1)e^{-2b\alpha_1}]}\right] \times J_0(ru)du,$$

$$P(r) = 2\int_0^\infty \frac{u}{\Delta}[\alpha_1 + \alpha_2 + (\alpha_1 - \alpha_2)e^{-2b\alpha_1}]J_0(ru)du.$$

For wires lying in the plane of separation, at the depth b:

$$Q(r) = \frac{1}{2\pi}\int_0^\infty \frac{u[\alpha_1 + u + (\alpha_1 - u)e^{-2b\alpha_1}] \times [\alpha_1 + \alpha_2 + (\alpha_1 - \alpha_2)e^{-2b\alpha_1}] + 4\alpha_1^2\alpha_2 e^{-2b\alpha_1}}{\Delta[\alpha_1\lambda_2 + \alpha_2\lambda_1 + (\alpha_1\lambda_2 - \alpha_2\lambda_1)e^{-2b\alpha_1}]} J_0(ru)du,$$

$$P(r) = 2\int_0^\infty \frac{u}{\Delta}[\alpha_1 + u + (\alpha_1 - u)e^{-2b\alpha_1}]J_0(ru)du.$$

In these formulas:

$i = \sqrt{-1}$ = imaginary unit,
$\omega = 2\pi f$ = radian frequency,
$\Delta = (\alpha_1 + \alpha_2)(u + \alpha_1) + (\alpha_1 - \alpha_2)(u - \alpha_1)e^{-2b\alpha_1}$,
$\alpha_j^2 = u^2 + i4\pi\omega\lambda_j$. $(j = 1 \text{ and } 2)$,
J_0 = Bessel function of the first kind, zero order.

Expression (I) is identical in general form with the formula for mutual impedances of grounded wires given by R. M. Foster [1] and the $Q(r)$ and $P(r)$ functions for the two cases above reduce to agreement with his formula, with appropriate changes in notation where necessary, in any of the cases resulting in wires on the surface of homogeneous earth, namely, for the first pair of functions, (i) $\lambda_1 = \lambda_2$, (ii) $b = 0$, (iii) $b = \infty$, and for the second, (i) $b = 0$, (ii) $\lambda_1 = 0$, (iii) $b = \infty$, $\lambda_2 = 0$.

It may be noted that the integrations involving the $Q(r)$ function are accomplished by inserting the four limits, which are the four distances between wire terminals, since each of the indicated integrations has a corresponding differentiation. Symbolically the result of carrying out the integrations in (I) may be written as follows:

$$Z_{Sa} = Q_{(A-B)(a-b)} + i\omega N_{Sa}, \qquad \text{(II)}$$

where

$$Q_{(A-B)(a-b)} = \int_a^b \int_A^B \frac{d^2Q(r)}{dSds}\,dSds = Q(Aa) - Q(Ab) + Q(Bb) - Q(Ba)$$

[1] R. M. Foster, "Mutual Impedances of Grounded Wires Lying on the Surface of the Earth," *Bulletin of the American Math. Soc.*, Vol. XXXVI, pages 367–368, May, 1930. *Bell System Technical Journal*, Vol. X, pages 408–419, July, 1931.

and

$$N_{S_s} = \int_a^b \int_A^B P(r) \cos \epsilon \, dSds.$$

Both $Q_{(A-B)(a-b)}$ and N_{S_s} are generally complex-valued and thus do not represent resistance and inductance, as ordinarily defined, as might be inferred from the similarity of expression (II) to the usual impedance expression. At zero frequency $i\omega N_{S_s}$ vanishes and $Q_{(A-B)(a-b)}$ becomes $R_{(A-B)(a-b)}$, a real number, the d.-c. mutual resistance of the circuits. For frequencies sufficiently low, such that terms involving higher powers of the frequency in the expansions of the functions in powers of the frequency are negligible, the mutual impedance can be expressed in the ordinary form; that is, in the formula

$$Z_{S_s} = R_{(A-B)(a-b)} + i\omega[N^\circ_{(A-B)(a-b)} + N^\circ_{S_s}] \qquad \text{(III)}$$

$R_{(A-B)(a-b)}$ is as above the d.-c. mutual resistance; $N^\circ_{(A-B)(a-b)}$ is the coefficient of $i\omega$ in the expansion of $Q_{(A-B)(a-b)}$, a real number, and generally equal to the sum of the Neumann integrals of the earth flows with the wires and with each other, the earth flows being those for direct current; $N^\circ_{S_s}$ is generally the Neumann integral of the wires.[2] The bracketed terms thus give the d.-c. mutual inductance of the wires with earth return.

For infinite distance between all terminal grounds A, B, a, b, taken in pairs, $Q_{(A-B)(a-b)}$ vanishes.

The physical distinction of $Q_{(A-B)(a-b)}$ and N_{S_s} may be illustrated by the following two cases: In the first, one wire is supposed straight and of arbitrary length; the second extends at right angles to it from two grounding points and is closed at infinity (that is, by a segment parallel to the first wire and at such distance that its mutual impedance with the first wire is negligibly small). In this case, in the perpendicular segments $\cos \epsilon = 0$, and in the parallel segment $P(r) = 0$, since $r = \infty$, so that $N_{S_s} = 0$ and the mutual impedance is given entirely by $Q_{(A-B)(a-b)}$; that is, the mutual impedance depends only on the grounding points. In the second case, the two perpendicular segments of the second wire extend away from a parallel segment to grounding points at infinity. Here the mutual impedance is given entirely by N_{S_s}, since $Q(r)$ and, therefore, $Q_{(A-B)(a-b)}$ vanishes for the limit $r = \infty$.

Table I is a summary of mutual impedance formulas obtained as special cases of the general formula. For each case the first column entries consist of the $Q(r)$ and $P(r)$ functions in the mutual impedance

[2] An ambiguity concerning this statement as well as that referring to $N^\circ_{(A-B)(a-b)}$, arising in certain particular cases, is discussed below.

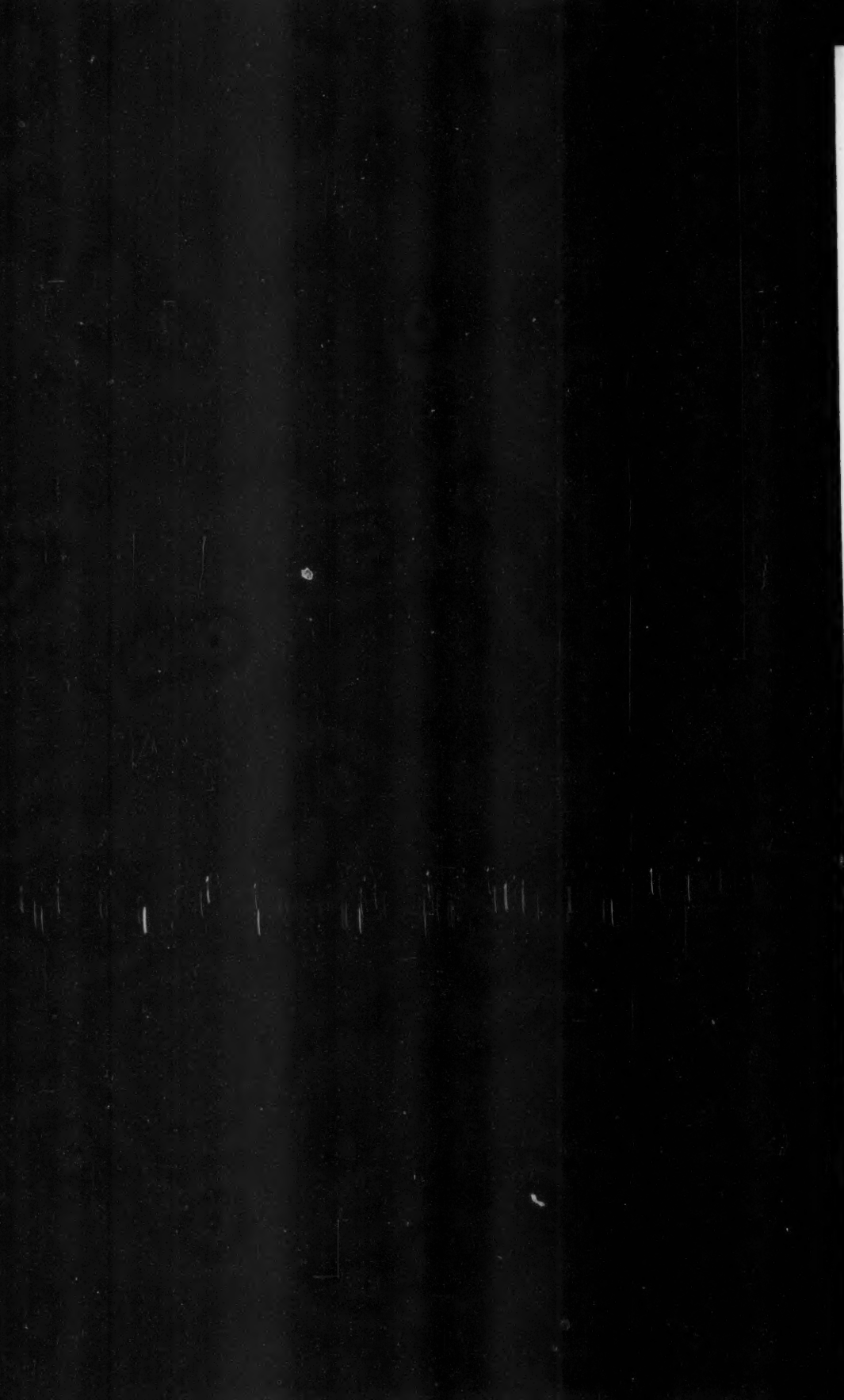

TABLE I—MUTUAL IMPEDANCE FORMULAS

Condition	Mutual Impedance		D-C. Mutual Resistance	
Horizontally Stratified Earth the Conductivities of Which at Depths Less than and Greater than b Are Resp.	$Z_{S_s}=\int_a^b\int_A^B\left\{\frac{d^2Q(r)}{dSds}+i\omega P(r)\cos\epsilon\right\}dSds$		$R_{(A-B)(a-b)}=R(Aa)-R(Ab)+R(Bb)-R(Ba)$	$L^o{}_{S_s}$
	$Q(r)$	$P(r)$	$R(r)$	
	Wires on the Surface of the Ea			
1.1 λ_1 and λ_2	$\frac{1}{2\pi\lambda_1}\int_0^\infty\left\{1+\frac{4\alpha_1^2(u+\alpha_2)(\lambda_1-\lambda_2)e^{-2b\alpha_1}}{\Delta[\alpha_1\lambda_2+\alpha_2\lambda_1+(\alpha_1\lambda_2-\alpha_2\lambda_1)e^{-2b\alpha_1}]}\right\}J_0(ru)du$ $\Delta=(\alpha_1+\alpha_2)(u+\alpha_1)+(\alpha_1-\alpha_2)(u-\alpha_1)e^{-2b\alpha_1}$	$2\int_0^\infty\frac{u}{\Delta}[\alpha_1+\alpha_2+(\alpha_1-\alpha_2)e^{-2b\alpha_1}]J_0(ru)du$	$\frac{1}{2\pi\lambda_1 r}\left\{1+2\int_0^\infty\frac{\beta e^{-ku}}{1-\beta e^{-ku}}J_0(u)du\right\}$ $=\frac{1}{2\pi\lambda_1 r}\left\{1+2\sum_{n=1}^\infty\frac{\beta^n}{(1+n^2k^2)^{1/2}}\right\}$ (1)	
1.2 λ and 0	$\frac{1}{2\pi\lambda}\int_0^\infty\left\{1+\frac{8\alpha^2}{\Delta(e^{2b\alpha}-1)}\right\}J_0(ru)du$ $\Delta=(u+\alpha)^2-(u-\alpha)^2e^{-2b\alpha}$	$2\int_0^\infty\frac{u}{\Delta}[u+\alpha-(u-\alpha)e^{-2bu}]J_0(ru)du$	$\frac{1}{2\pi\lambda}\int_0^\infty\coth(bu)[J_0(ru)-1]du$	
1.3 0 and λ	∞	$\frac{1}{r}-\frac{1}{R}+2\int_0^\infty\frac{ue^{-2bu}}{u+\alpha}J_0(ru)du$	∞	
1.4 λ and ∞	$\frac{1}{2\pi\lambda}\int_0^\infty\frac{u+\alpha+(u-\alpha)e^{-2b\alpha}}{u+\alpha-(u-\alpha)e^{-2b\alpha}}\frac{1-e^{-2b\alpha}}{1+e^{-2b\alpha}}J_0(ru)du$	$2\int_0^\infty\frac{1-e^{-2b\alpha}}{u+\alpha-(u-\alpha)e^{-2b\alpha}}J_0(ru)udu$	$\frac{1}{2\pi\lambda r}\left\{1+2\sum_{n=1}^\infty\frac{(-1)^n}{(1+k^2n^2)^{1/2}}\right\}$	
1.5 $\sigma=\lim_{b\to\infty}b\lambda_1$ and λ	$\frac{1}{2\pi\sigma}\int_0^\infty\frac{(u+\alpha)J_0(ru)du}{(u+\alpha+i4\pi\sigma\omega)(\alpha+\lambda\sigma^{-1})}$	$2\int_0^\infty\frac{J_0(ru)udu}{u+\alpha+i4\pi\sigma\omega}$	$\frac{1}{4\sigma}[\mathbf{H}_0(\lambda\sigma^{-1}r)-Y_0(\lambda\sigma^{-1}r)]$	
1.6 $\sigma=\lim_{b\to\infty}b\lambda_1$ and 0	$\frac{1}{4\sigma}[\mathbf{H}_0(i2\pi\sigma\omega r)-Y_0(i2\pi\sigma\omega r)]$	$\frac{1}{r}\{1-i\pi^2\sigma\omega r[\mathbf{H}_0(i2\pi\sigma\omega r)-Y_0(i2\pi\sigma\omega r)]\}$	$\frac{1}{2\pi\sigma}\log\left(\frac{1}{r}\right)$ (6)	
1.7 λ and λ	$\frac{1}{2\pi\lambda r}$ (9)	$\frac{2}{\gamma^2r^2}[1-(1+\gamma r)e^{-\gamma r}]$ (9)	$\frac{1}{2\pi\lambda r}$ (7)	
	Wires in the Plane of Separation, at the Depth b			
2.1 λ_1 and λ_2	$\frac{1}{2\pi}\int_0^\infty\frac{u[\alpha_1+u+(\alpha_1-u)e^{-2b\alpha_1}][\alpha_1+\alpha_2+(\alpha_1-\alpha_2)e^{-2b\alpha_1}]+4\alpha_1^2\alpha_2e^{-2b\alpha_1}}{\Delta[\alpha_1\lambda_2+\alpha_2\lambda_1+(\alpha_1\lambda_2-\alpha_2\lambda_1)e^{-2b\alpha_1}]}J_0(ru)du$ $\Delta=(\alpha_1+\alpha_2)(u+\alpha_1)+(\alpha_1-\alpha_2)(u-\alpha_1)e^{-2b\alpha_1}$	$2\int_0^\infty\frac{u}{\Delta}[\alpha_1+u+(\alpha_1-u)e^{-2b\alpha_1}]J_0(ru)du$	$\frac{1}{2\pi(\lambda_1+\lambda_2)r}\int_0^\infty\frac{1+e^{-ku}}{1-\beta e^{-ku}}J_0(u)du$ $=\frac{\lambda_1}{\pi(\lambda_1^2-\lambda_2^2)r}\sum_0^\infty\frac{\beta^n}{(1+n^2k^2)^{1/2}}$	$\frac{2\lambda_1}{(\lambda_1+\lambda_2}$
2.11 λ_1 and λ_2 $b\to\infty$	$\frac{1}{2\pi}\int_0^\infty\frac{u}{\alpha_1\lambda_2+\alpha_2\lambda_1}J_0(ru)du$	$\frac{2}{(\gamma_1^2-\gamma_2^2)r^2}[(1+\gamma_2r)e^{-\gamma_2r}-(1+\gamma_1r)e^{-\gamma_1r}]$	$\frac{1}{2\pi(\lambda_1+\lambda_2)r}$	
2.2 λ and λ	$\frac{1}{4\pi\lambda}\left\{\frac{e^{-\gamma r}}{r}+\frac{2}{R}\left[Z_2J_0(Z_1)K_1(Z_2)+Z_1I_1(Z_1)K_0(Z_2)-\frac{e^{-\gamma R}}{2}\right]\right\}$ $Z_1=\frac{1}{2}\gamma(R-2b)\qquad Z_2=\frac{1}{2}\gamma(R+2b)$	$\frac{e^{-\gamma r}}{r}-\frac{e^{-\gamma R}}{R}+2\int_0^\infty\frac{ue^{-2bu}}{u+\alpha}J_0(ru)du$	$\frac{1}{4\pi\lambda}\left[\frac{1}{r}+\frac{1}{R}\right]$	
2.21 λ and λ $b\to\infty$	$\frac{1}{4\pi\lambda}\frac{e^{-\gamma r}}{r}$	$\frac{e^{-\gamma r}}{r}$	$\frac{1}{4\pi\lambda r}$	

Notation

The integrations in the formula for Z_{S_s} are extended over the wires S and s; whose elements dS and ds are separated by distance r, and include the angle ϵ between their directions; the wires extend from A to B and from a to b, respectively. Distances are in cm.; conductivity in abmhos per cm.

$i=\sqrt{-1}$

$\omega=2\pi f$ = Radian frequency

y = Horizontal separation between wires

$\gamma^2=i4\pi\omega\lambda\qquad\alpha^2=u^2+\gamma^2\qquad\gamma_j^2=i4\pi\omega\lambda_j\qquad\alpha_j^2=u^2+\gamma_j^2\qquad j=1$ and 2

$R^2=r^2+4b^2$

$\beta=\frac{\lambda_1-\lambda_2}{\lambda_1+\lambda_2}$

$k=\frac{2b}{r}$

$\mathbf{H}_0$ = Struve's associated Bessel function, zero order.*

$\mathbf{H}_1$ = " " " " " " , first order.*

I_0 = Bessel function of first kind for imaginary argument, zero order.*

I_1 = " " " " " " " , first order.*

J_0 = " " " " " , zero order.*

K_0 = " " " second kind for imaginary argument, zero order.*

K_1 = " " " " " " " " , first order.*

Y_0 = " " " " " , zero order.*

Y_1 = " " " " " , first order.*

Ei = Exponential integral, as defined by Jahnke and Emde, Funktionentafeln.

$N^o{}_{S_s}$ = Mutual Neumann integral of wires S and $s=\int\int\frac{\cos\epsilon}{r}dSds$

$-\psi(1)=.5772$ = Euler's Constant.

* As defined in G. N. Watson's "Theory of Bessel Functions," Cambridge, 1922.

(1) Ollendorff, F.: " Erdströme,"

(2) Evans, H. P.: *Phys. Rev.*, vol.

(3) Pollaczek, F.: Ueber das Feld

(4) Carson, J. R.: Wave Propaga

(5) Haberland, G.: Theorie der L

(6) Breisig, F.: " Theoretische Te

(7) Campbell, G. A.: Mutual Imp

(8) Mayr, O.: Die Erde als Wech

(9) Foster, R. M.: Mutual Impe

(10) Carson, J. R.: Ground Retur

(11) Rudenberg, R.: Die Ausbreit

TABLE I—MUTUAL IMPEDANCE FORMULAS

	D-C. Mutual Resistance	D-C. Mutual Inductance
	$R_{(A-B)(a-b)} = R(Aa) - R(Ab) + R(Bb) - R(Ba)$	$L^\circ_{s_s} = N^\circ_{s_s} + N^\circ(Aa) - N^\circ(Ab) + N^\circ(Bb) -$
$P(r)$	$R(r)$	$N^\circ(r)$
Wires on the Surface of the Earth		
$\frac{u}{\Delta}[\alpha_1+\alpha_3+(\alpha_1-\alpha_3)e^{-2bu_1}]J_0(ru)du$	$\frac{1}{2\pi\lambda_1 r}\left\{1+2\int_0^\infty \frac{\beta e^{-bu}}{1-\beta e^{-bu}} J_0(u)du\right\} = \frac{1}{2\pi\lambda_1 r}\left\{1+2\sum_{n=1}^{\infty}\frac{\beta^n}{(1+n^2k^2)^{1/2}}\right\}$ (1)	$2\beta r\int_0^\infty e^{-ku}\frac{\beta(1-e^{-ku})-ku}{(1-\beta e^{-ku})^2}\frac{J_0(u)-1}{u^2}$
$\int_0^\infty \frac{u}{\Delta_s}[u+\alpha-(u-\alpha)e^{-2ba}]J_0(ru)du$	$\frac{1}{2\pi\lambda}\int_0^\infty \coth(bu)[J_0(ru)-1]du$	$2r\int_0^\infty e^{-ku}\frac{1-e^{-ku}-ku}{(1-e^{-ku})^2}\frac{J_0(u)-1}{u^2}d$
$\frac{1}{r}-\frac{1}{R}+2\int_0^\infty \frac{ue^{-2bu}}{u+\alpha}J_0(ru)du$	∞	$2r\int_0^\infty e^{-ku}\frac{1-e^{-ku}+ku}{(1+e^{-ku})^2}\frac{J_0(u)-1}{u^2}d$
$\int_0^\infty \frac{1-e^{-2ba}}{u+\alpha-(u-\alpha)e^{-2ba}}J_0(ru)udu$	$\frac{1}{2\pi\lambda r}\left\{1+2\sum_{n=1}^{\infty}\frac{(-1)^n}{(1+k^2n^2)^{1/2}}\right\}$	$2r\int_0^\infty e^{-ku}\frac{1-e^{-ku}+ku}{(1+e^{-ku})^2}\frac{J_0(u)-1}{u^2}d$
$2\int_0^\infty \frac{J_0(ru)udu}{u+\alpha+i4\pi\sigma\omega}$	$\frac{1}{4\sigma}[\mathbf{H}_0(\lambda\sigma^{-1}r)-Y_0(\lambda\sigma^{-1}r)]$	$\frac{2\sigma}{\lambda}\left[\log r+\frac{\pi}{2}\mathbf{H}_0(\lambda\sigma^{-1}r)-\frac{\pi}{2}Y_0(\lambda\sigma^{-1}r\right.$ $\left.-r\left[1-\frac{\pi}{2}\mathbf{H}_1(\lambda\sigma^{-1}r)+\frac{\pi}{2}Y_1(\lambda\sigma^{-1}r)\right.\right.$
$-i\pi^2\sigma\omega r[\mathbf{H}_0(i2\pi\sigma\omega r)-Y_0(i2\pi\sigma\omega r)]\}$	$\frac{1}{2\pi\sigma}\log\left(\frac{1}{r}\right)$ (6)	r
$\frac{2}{\gamma^2r^2}[1-(1+\gamma r)e^{-\gamma r}]$ (9)	$\frac{1}{2\pi\lambda r}$ (7)	0
Wires in the Plane of Separation, at the Depth b		
$\frac{u}{\Delta}[\alpha_1+u+(\alpha_1-u)e^{-2bu_1}]J_0(ru)du$	$\frac{1}{2\pi(\lambda_1+\lambda_2)r}\int_0^\infty \frac{1+e^{-bu}}{1-\beta e^{-bu}}J_0(u)du = \frac{\lambda_1}{\pi(\lambda_1^2-\lambda_2^2)r}\sum_0^\infty \frac{\beta^n}{(1+n^2k^2)^{1/2}}$	$\frac{2\lambda_1}{(\lambda_1+\lambda_2)^2}\int_0^\infty \frac{\lambda_1(1-e^{-ku}-ku)e^{-ku}-\lambda_2(1-e^{-2ku})}{(1-\beta e^{-ku})^2}$
$\frac{2}{\gamma_2^2)r^3}[(1+\gamma_2 r)e^{-\gamma_2 r}-(1+\gamma_1 r)e^{-\gamma_1 r}]$	$\frac{1}{2\pi(\lambda_1+\lambda_2)r}$	$\frac{2\lambda_1\lambda_2}{(\lambda_1+\lambda_2)^2}r$
$\frac{e^{-\gamma r}}{r}-\frac{e^{-\gamma R}}{R}+2\int_0^\infty \frac{ue^{-2bu}}{u+\alpha}J_0(ru)du$	$\frac{1}{4\pi\lambda}\left[\frac{1}{r}+\frac{1}{R}\right]$	$\frac{1}{2}(r-R)+2b\log\frac{R+2b}{4b}$
$\frac{e^{-\gamma r}}{r}$	$\frac{1}{4\pi\lambda r}$	$\frac{1}{2}r$

unction, zero order.*
" , first order.*
d for imaginary argument, zero order.*
" " " , first order.*
, zero order.*
kind for imaginary argument, zero order.*
" " " " , first order.*
" , zero order.*
" , first order.*
efined by Jahnke and Emde, Funktionentafeln.
of wires S and $s = \int\int \frac{\cos\epsilon}{r}dSds$

Theory of Bessel Functions," Cambridge, 1922.

(1) Ollendorff, F.: " Erdströme," Julius Springer, Berlin, 1928, pp. 69–71.
(2) Evans, H. P.: *Phys. Rev.*, vol. 36, no. 10, Nov. 15, 1930, pp. 1579–158
(3) Pollaczek, F.: Ueber das Feld einer unendlich langen Wechselstromdu
(4) Carson, J. R.: Wave Propagation in Overhead Wires with Ground Re
(5) Haberland, G.: Theorie der Leitung von Wechselstrom durch die Erd
(6) Breisig, F.: " Theoretische Telegraphie," F. Vieweg u. Sohn, Braunsch
(7) Campbell, G. A.: Mutual Impedances of Grounded Circuits, *Bell Syst*
(8) Mayr, O.: Die Erde als Wechselstrom leiter, *E. T. Z.*, Sept. 1925, pp.
(9) Foster, R. M.: Mutual Impedance of Grounded Circuits, *Bull. Am.*
(10) Carson, J. R.: Ground Return Impedance: Underground Wire with E
(11) Rudenberg, R.: Die Ausbreitung der Erdströme in der Umgebung vo

$)+N°(Bb)-N°(Ba)$	$\frac{dZ_{s_2}}{ds}=i\omega\int_{-\infty}^{\infty}P(r)ds$	
	Exact	Approximate
$\frac{ku}{}\ \frac{J_0(u)-1}{u^3}\,du$	$4i\omega\int_0^\infty\frac{1}{\Delta}[\alpha_1+\alpha_2+(\alpha_1-\alpha_2)e^{-2b\alpha_1}]\cos yudu$ $\Delta=(\alpha_1+\alpha_2)(u+\alpha_1)+(\alpha_1-\alpha_2)(u-\alpha_1)e^{-2b\alpha_1}$ (2)	
$\frac{J_0(u)-1}{u^3}\,du$	$4i\omega\int_0^\infty\frac{1}{\Delta}[u+\alpha-(u-\alpha)e^{-2b\alpha}]\cos yudu$ $\Delta=(u+\alpha)^2-(u-\alpha)^2e^{-2b\alpha}$	
$\frac{J_0(u)-1}{u^3}\,du$	$4i\omega\left[\log\frac{y^2+4b^2}{y^2}+\int_0^\infty\frac{e^{-2bu}\cos yudu}{u+\alpha}\right]$ (3) (4) (5)	$\frac{\pi\omega}{2}+i\omega\log\frac{e^{[1+2\psi(1)]}}{\pi\lambda\omega y^2}$ $\sqrt{y^2+4b^2}\cdot\sqrt{4\pi\lambda\omega}\ll1$
$\frac{J_0(u)-1}{u^3}\,du$	$4i\omega\int_0^\infty\frac{(1-e^{-2b\alpha})}{u+\alpha-(u-\alpha)e^{-2b\alpha}}\cos yudu$	
$-\frac{\pi}{2}Y_0(\lambda\sigma^{-1}r)\Big]$ $\frac{\pi}{2}Y_1(\lambda\sigma^{-1}r)\Big]$	$4i\omega\int_0^\infty\frac{\cos yudu}{u+\alpha+i4\pi\sigma\omega}$ (5)	
(7)	$\omega\pi e^{-u}-i\omega[e^u\mathrm{E}i(-u)+e^{-u}\mathrm{E}i(u)]$ $u=2\pi\sigma\omega y$ (8)	$\omega\pi+i\omega\log\frac{e^{2\psi(1)}}{(2\pi\sigma\omega y)^2}\quad 2\pi\sigma\omega y\ll1$
(7)	$\frac{1}{\pi\lambda y^2}[1-\gamma yK_1(\gamma y)]$ (3) (5)	$\frac{\pi\omega}{2}+i\omega\log\frac{e^{[1+2\psi(1)]}}{\pi\lambda\omega y^2}\quad y\sqrt{4\pi\lambda\omega}\ll1$
$\frac{-\lambda_2(1-e^{-2bu})}{}\ \frac{J_0(u)-1}{u^3}\,du$	$4i\omega\int_0^\infty\frac{1}{\Delta}[\alpha_1+u+(\alpha_1-u)e^{-2b\alpha_1}]\cos yudu$ $\Delta=(\alpha_1+\alpha_2)(u+\alpha_1)+(\alpha_1-\alpha_2)(u-\alpha_1)e^{-2b\alpha_1}$	
	$\frac{1}{\pi(\lambda_1-\lambda_2)y}[\gamma_2K_1(\gamma_2y)-\gamma_1K_1(\gamma_1y)]$	$\frac{\pi\omega}{2}+i\omega\left[\log\frac{e^{[1+2\psi(1)]}}{\pi\omega y^2}-\frac{\lambda_1\log\lambda_1-\lambda_2\log\lambda_2}{\lambda_1-\lambda_2}\right]$ $y\sqrt{4\pi\lambda_1\omega}\ll1\quad y\sqrt{4\pi\lambda_2\omega}\ll1$
$\frac{R+2b}{4b}$	$2i\omega\left[K_0(\gamma y)-K_0(\gamma\sqrt{y^2+4b^2})+2\int_0^\infty e^{-2bu}\frac{\cos yudu}{u+\alpha}\right]$ (10)	
(7)	$2i\omega K_0(\gamma y)$ (11)	$\frac{\pi\omega}{2}+i\omega\log\frac{e^{2\psi(1)}}{\pi\lambda\omega y^2}\quad y\sqrt{4\pi\lambda\omega}\ll1$

REFERENCES

3, pp. 69–71.
pp. 1579–1588.
hselstromdurchflossenen Einfachleitung, *E. N. T.*, **3**, Sept. 1926, pp. 339–359; **4**, Jan. 1927, pp. 18–30.
Ground Return, *Bell System Technical Journal*, **5**, Oct. 1926, pp. 539–554.
rch die Erde, *Z. ang. Math. u. Mech.*, **5**, Oct. 1926.
hn, Braunschweig, 1910, p. 86.
its, *Bell System Technical Journal*, Vol. II, No. 4, Oct. 1923.
ot. 1925, pp. 1352–1355, 1436–1440.
Bull. Am. Math. Soc., Vol. XXXVI, pp. 367–368, May 1930; *Bell System Tech. Journal*, Vol. X, pp. 408–419, July 1931.
Wire with Earth Return, *Bell System Technical Journal*, Vol. VIII, pp. 94–98, Jan. 1929.
mgebung von Wechselstrom Leitungen, *Z. ang. Math. u. Mech.*, **5**, Oct. 1925, pp. 361–389.

formula for arbitrary paths; then follow the d.-c. mutual resistance and inductance, and in the last columns exact and approximate expressions for the mutual impedance gradient parallel to a straight wire of infinite length.

The first entry in each group is the general case of two-layer earth. In the first group, the next three entries are those in which one of the conductivities is given the special value zero or infinity, one of the four possible cases being trivial. The fifth and sixth entries involve finite surface conductivity which is defined by $\sigma = \lim_{b \to 0} b\lambda_1$; in the first of these the surface conductivity differs from the conductivity of the homogeneous earth below it, in the second the earth below is abolished. The latter may serve as a convenient approximation to the case in which the earth consists of a thin upper layer of high conductivity relative to the layer below. The final entry of this group is the case of homogeneous ground. In the second group the second entry is the limiting case for $b = \infty$, which places the wires at the plane of separation of two semi-infinite media of conductivities λ_1 and λ_2; the general formula for this case has been independently obtained by R. M. Foster. With either conductivity zero this case reduces to the case of homogeneous earth; with equal conductivities the case of an infinite medium is obtained, which is the final entry of this group. The third entry is the case of wires at depth b in homogeneous earth; for sufficiently large depths the formulas approach those of an infinite medium.

Further information regarding these special cases may be obtained from the papers referred to in Table I.

In case 1.4 where the conductivity λ_2 approaches an infinite limit, an ambiguity arises concerning the d.-c. mutual inductance, two cases appearing according as the approach of λ_2 to infinity is assumed faster or slower, respectively, than the approach of the frequency to zero, that is, according as the limits are taken $\lambda_2 \to \infty$, $\omega \to 0$ or $\omega \to 0$, $\lambda_2 \to \infty$. The entry in the table corresponds to the latter limit and also to d.-c. distribution of earth current. The alternate limit gives:

$$L^\circ_{Sa} = N^\circ_{Sa} - N^\circ_{Sa'} + N^\circ_{(A-B)(a-b)},$$

where

$N^\circ_{Sa'}$ = Mutual Neumann integral of one wire and the image of the other wire, the image plane being the plane of separation of the media.

$$N^\circ(r) = -r \int_0^\infty e^{-ku} \frac{1 - e^{-2ku} - 2ku}{(1 + e^{-ku})^2} \frac{J_0(u) - 1}{u^2} du$$

$$(0 > N^\circ(r) > -.2r).$$

The ambiguous cases arise only in the limits $\lambda \to \infty$, $\omega \to 0$ and $\lambda \to 0$, $\omega \to \infty$, the product $\lambda\omega$ appearing in the expressions then being strictly indeterminate, until the order of the limits is defined.

II

Different problems are encountered in obtaining numerical results for the two functions $Q_{(A-B)(a-b)}$ and N_{Sa}; $Q_{(A-B)(a-b)}$ is determined in terms of four values, with proper sign, as given in equation (II), of $Q(r)$; while $Q(r)$ apparently is not generally expressible in terms of known functions it may always be evaluated by numerical integration. The case of N_{Sa} is different because of the necessity of double integration over the wires; general numerical results involve carrying out at least one of these integrations in addition to that required in evaluating $P(r)$, involving a considerable amount of labor and complexity of results.

However, without carrying out either of the evaluations completely, the formulas for the limiting cases may be used to obtain results approximating certain practical conditions. The important limiting cases are (i) one wire infinite, and (ii) zero frequency. Curves for these cases for wires on the surface of the ground and for special values of the parameters are given in Figs. 1–6, as described below.

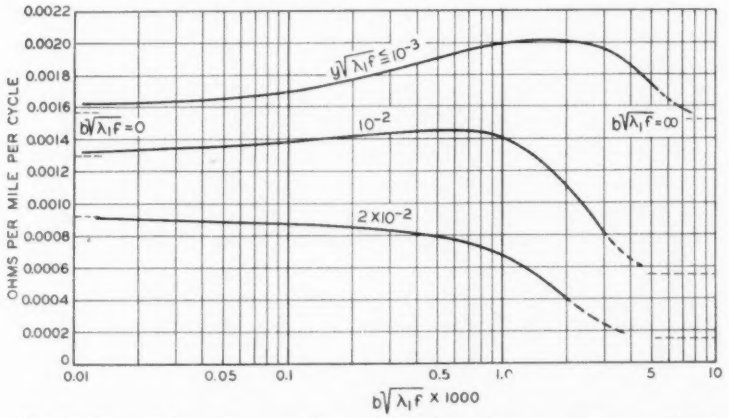

Fig. 1—Mutual impedance gradient at earth's surface parallel to an infinite straight wire on the earth's surface; real component; two-layer earth $\lambda_1 = 10\lambda_2$; b and y in feet, frequency in cycles per second, conductivities in abmhos per cm.

Figures 1 and 2 show, respectively, the real and imaginary parts of the mutual impedance gradient parallel to an infinite straight wire for the conductivity ratio $\lambda_2/\lambda_1 = 0.1$; Figs. 3 and 4 show the same

quantities for $\lambda_2/\lambda_1 = 10$. When the depth b approaches the limits zero and infinity, the ground condition approaches the limits of homogeneous ground of conductivities λ_2 and λ_1, respectively. By reference to Figs. 2 and 4 it will be seen that there is a wide range in which the curves for other values of the depth are parallel to these

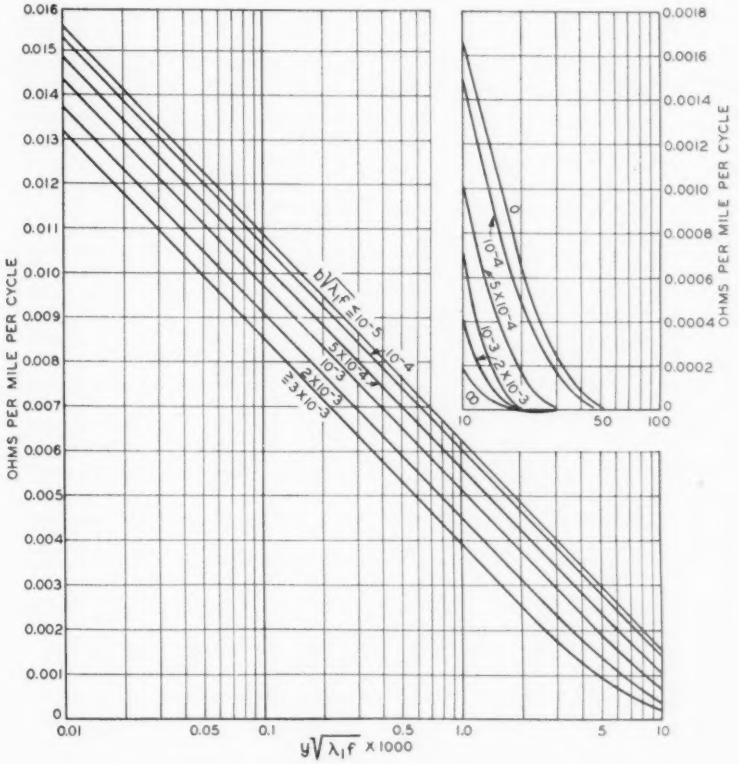

Fig. 2—Imaginary component of mutual impedance gradient for conditions of Fig. 1.

limiting curves so that for a given frequency a properly chosen homogeneous ground conductivity leads to equivalent results. The equivalent conductivity varies with the frequency, increasing or decreasing with increasing frequency according as λ_1 is greater or less than λ_2; this variation of apparent homogeneous conductivity with frequency has been frequently observed in results obtained from mutual im-

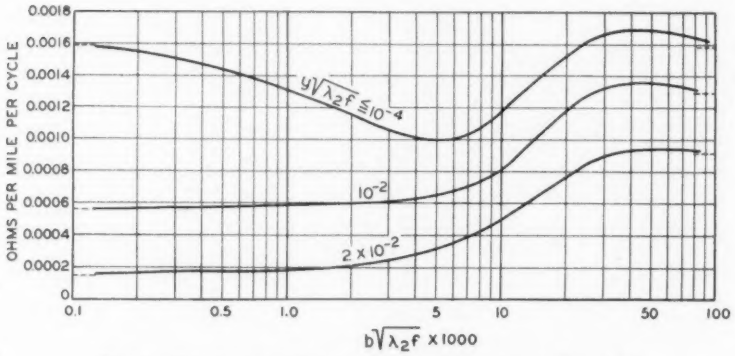

Fig. 3—Two-layer earth $\lambda_2 = 10\lambda_1$; real component of mutual impedance gradient.

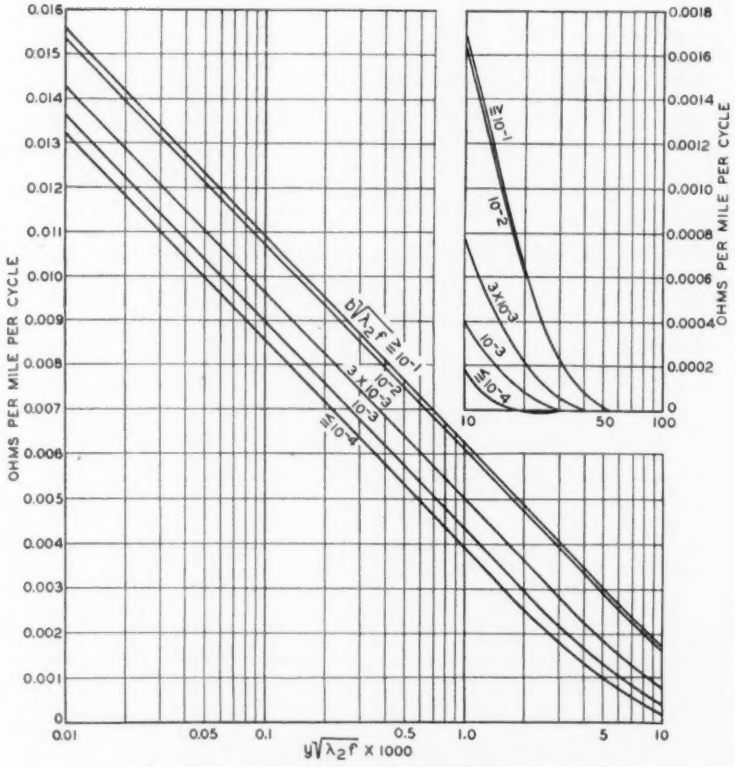

Fig. 4—Imaginary component of mutual impedance gradient for conditions of Fig. 3.

pedance measurements.[3] For a given frequency the complete group of curves of which Figs. 2 and 4 are examples may be put in more convenient form by plotting the equivalent conductivity as dependent on the other parameters of the problem.

The d.-c. mutual inductance of wires S and s, as given at the head of the corresponding column in Table I, is:

$$L^\circ_{Ss} = N^\circ_{Ss} + N^\circ(Aa) - N^\circ(Ab) - N^\circ(Ba) + N^\circ(Bb),$$

where N°_{Ss} is the mutual Neumann integral of the wires and is the main term in the formula.[4] The small contribution arising from the remaining terms is as shown on Fig. 5 always less than $\Delta = -Aa$

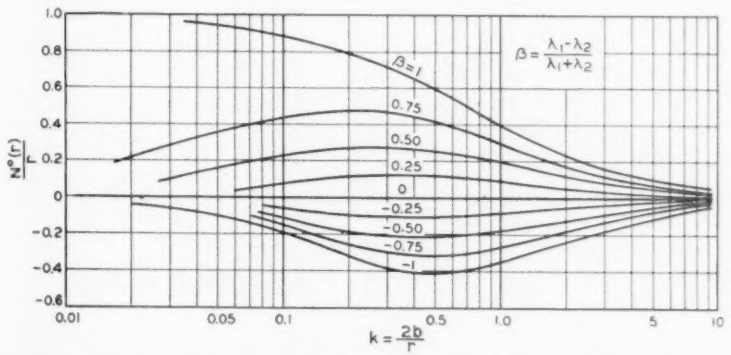

Fig. 5—D.-C. mutual inductance, exclusive of mutual Neumann integral of wire paths, of wires on surface of two-layer earth;

$$N^\circ_{(A-B)(a-b)} = N^\circ(Aa) - N^\circ(Ab) + N^\circ(Bb) - N^\circ(Ba).$$

$+ Ab + Ba - Bb$. Figure 5 shows values of $N^\circ(r)/r$ for values of $k = 2b/r$ from .01 to 10 and for a range of values of $\beta = (\lambda_1 - \lambda_2)/(\lambda_1 + \lambda_2)$ from -1 to $+1$.

The d.-c. mutual resistance, of course, also varies between the

[3] Extensive results of such measurements are published in the following papers:

A. E. Bowen and C. L. Gilkeson: "Mutual Impedances of Ground Return Circuits," *Trans. A.I.E.E.*, *49*, 1370–1383 (Oct. 1930), and *Bell System Technical Journal*, *9*, 628–651, Oct. 1930.

G. Swedenborg: "Investigations Regarding Mutual Induction in Parallel Conductors Earthed at the Ends." The L. M. Ericsson Review, English Ed. No. 7–9, 1931, pages 189–204.

H. Klewe: "Gegeninductivitäts Messungen an Leitungen mit Erdruckleitung," *Elektrische Nachrichten Technik*, 1929, page 467, and 1931, page 533.

J. Collard: "Measurement of Mutual Impedance of Circuits with Earth Return," *The Journal of The Institution of Electrical Engineers*, Vol. 71, No. 430 (Oct. 1932), pages 674–682.

[4] The only formal result in the evaluation of the Neumann integral known to us is that for arbitrary straight paths published by G. A. Campbell, "Mutual Inductances of Circuits Composed of Straight Wires," *Phys. Rev.*, *5*, pp. 452–458 (June 1915); see also his "Mutual Impedance of Grounded Circuits," *Bell System Technical Journal*, *2*, pp. 1–30 (Oct. 1923).

limiting cases of conductivities λ_2 and λ_1 corresponding to the limiting depths zero and infinity. The curves showing the dependence of mutual resistance on the depth and conductivities are put in the simplest form in terms of the two quantities $2b/r$ and the conductivity ratio λ_1/λ_2. Curves of this kind are shown on Fig. 6.[5]

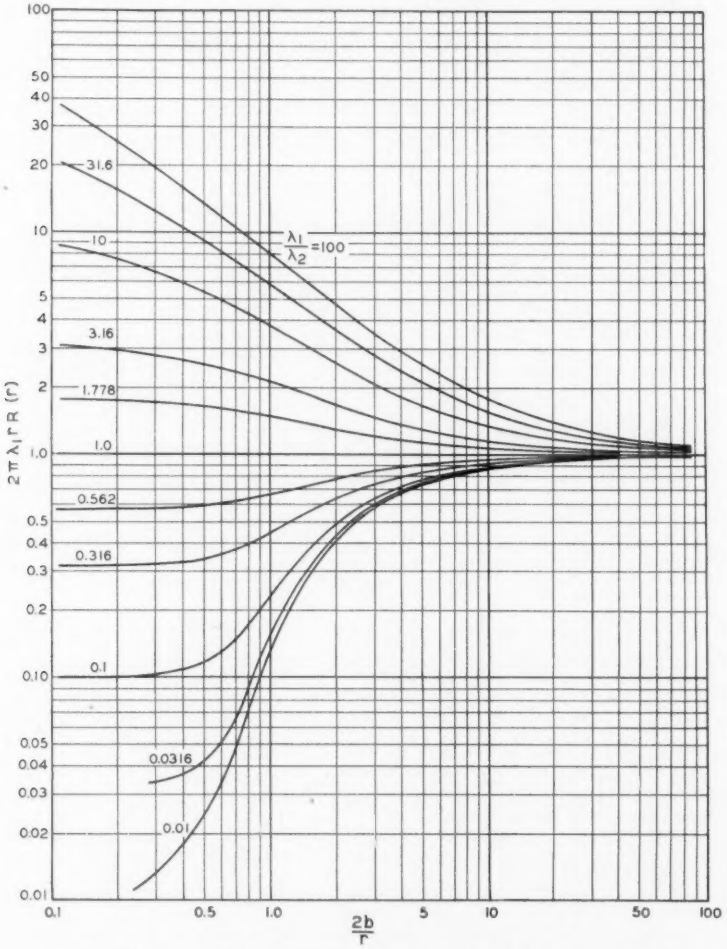

Fig. 6—D.-C. mutual resistance of wires on surface of two-layer earth;
$R_{(A-B)(a-b)} = R(Aa) - R(Ab) + R(Bb) - R(Ba)$.

[5] We are indebted to our colleague Mr. L. L. Lockrow for these curves. Tables from which the function $R(r)$ can be evaluated are published in the Bureau of Mines Technical Paper No. 502.

Thus for low frequencies and short wires the main effect of two-layer earth will consist of the effect on the d.-c. mutual resistance.

III

The mutual impedance of wires in a medium having two parallel planes of discontinuity in the conductivity may be derived by extension of certain results published by A. Sommerfeld,[6] who has obtained the electric and magnetic fields of a horizontal electric doublet in a medium having one plane of discontinuity; the doublet may be regarded as an element dS of a wire of negligible diameter carrying a finite current and the mutual impedance of wires obtained by double integration over their lengths. The general formula may also be derived by extension of the second method of derivation given by R. M. Foster (loc. cit.), but for brevity this derivation is omitted here.

In the following both rectangular coordinates (x, y, z) and cylindrical coordinates (r, ϕ, z) are employed, with the origin in the upper horizontal plane of discontinuity, z in the vertical direction and x in the direction of the doublet. Electromagnetic c.g.s. units are used, and the field variation with time taken as $e^{i\omega t}$, this factor being omitted throughout. The fields are defined through "Hertzian Vectors,"[7] the rectangular components of which must individually satisfy the wave equation:

$$\frac{\partial^2 \Pi}{\partial x^2} + \frac{\partial^2 \Pi}{\partial y^2} + \frac{\partial^2 \Pi}{\partial z^2} - \gamma^2 \Pi = 0, \tag{1}$$

and in terms of which

$$E = c \text{ grad div } \Pi - c\gamma^2 \Pi, \tag{2}$$

$$H = -\frac{ic}{\omega} \gamma^2 \text{ curl } \Pi, \tag{3}$$

where

Π = Hertzian vector = Π_x, Π_y, Π_z,

$\gamma^2 = 4\pi\lambda i\omega - \epsilon\omega^2$,

λ, ϵ = conductivity and dielectric constant,

$\omega = 2\pi f$ = radian frequency,

c = velocity of light.

[6] A. Sommerfeld, "Über die Ausbreitung der Wellen in der drahtlosen Telegraphie," *Annalen der Physik* (4), *81*, 1135–1153, December, 1926.

[7] Abraham and Föppl, "Theorie der Elektrizität," 7th ed., Leipzig and Berlin, 1922, Vol. I, § 79, page 322.

The conductivities and dielectric constants are taken as:

$$\begin{aligned} &\lambda_0, \epsilon_0 \quad \text{for} \qquad z > 0 \\ &\lambda_1, \epsilon_1 \quad \text{for} \; -b < z < 0 \\ &\lambda_2, \epsilon_2 \quad \text{for} \qquad z < -b \end{aligned}$$

where b is the distance between the parallel planes of discontinuity.

The primary field of a doublet in the direction of the x-axis at $z = h$ is given by

$$\Pi_{0x}' = A\frac{e^{-\gamma_0 R}}{R} = A\int_0^\infty \frac{e^{\alpha_0(z-h)}}{\alpha_0} uJ_0(ru)du \qquad 0 > z > h, \tag{4}$$

where

$$\begin{aligned} r^2 &= x^2 + y^2, \\ R^2 &= r^2 + (z-h)^2, \\ \gamma_0^2 &= 4\pi i\omega\lambda_0 - \omega^2\epsilon_0, \\ \alpha_0^2 &= u^2 + \gamma_0^2. \end{aligned}$$

The constant A which is the moment of the doublet is as yet undetermined. From (3):

$$H_0' = -A\frac{ic}{\omega}\gamma_0^2 \operatorname{curl} \Pi_{0x}',$$

and for $\gamma_0 = 0$:

$$H_0' = \left[-A\frac{ic}{\omega}\gamma_0^2\right]_{\gamma_0=0} \operatorname{curl}\frac{1}{R}.$$

For this case the magnetic force due to unit current in an element dS is given by Biot-Savart's law [8] as

$$H = dS \operatorname{curl}\frac{1}{R},$$

so that

$$A = \frac{i\omega dS}{\gamma_0^2}.$$

The secondary fields are derived from Hertzian vectors having components in the direction of the x and z axes. Components in the direction of the y-axis are eliminated due to symmetry with respect to the $x - z$ plane. The resulting fields are then composed as follows:

$$\begin{aligned} &\Pi_{0x} = \Pi_{0x}' + \Pi_{0x}'', \quad \Pi_{0z} = \Pi_{0z}'' && z \geqslant 0, \\ &\Pi_{1x}, \quad \Pi_{1z} && -b \leqslant z \leqslant 0, \\ &\Pi_{2x}, \quad \Pi_{2z} && z \leqslant -b, \end{aligned} \tag{5}$$

[8] Abraham and Föppl, "Theorie der Elektrizität," 7th ed., Vol. I, § 55, page 189.

in the first of which the double primes indicate the components of the secondary field.

The expressions for the field intensities in terms of the Hertzian vector components may now be written out by equations (2) and (3) and are as follows:

$$
\begin{aligned}
H_x &= -\frac{ic}{\omega}\gamma^2\frac{\partial \Pi_x}{\partial y}, \\
H_y &= -\frac{ic}{\omega}\gamma^2\left[\frac{\partial \Pi_x}{\partial z} - \frac{\partial \Pi_z}{\partial x}\right], \\
H_z &= \frac{ic}{\omega}\gamma^2\frac{\partial \Pi_x}{\partial y}, \\
E_x &= -c\gamma^2\Pi_x + c\frac{\partial}{\partial x}\left(\frac{\partial \Pi_x}{\partial x} + \frac{\partial \Pi_z}{\partial z}\right), \\
E_y &= c\frac{\partial}{\partial y}\left(\frac{\partial \Pi_x}{\partial x} + \frac{\partial \Pi_z}{\partial z}\right), \\
E_z &= -c\gamma^2\Pi_z + c\frac{\partial}{\partial z}\left(\frac{\partial \Pi_x}{\partial x} + \frac{\partial \Pi_z}{\partial z}\right).
\end{aligned}
\tag{6}
$$

The proper general solution of (1) for the components of the secondary fields is of the following form:

$$
\Pi = \cos n\phi \int_0^\infty (f(u)e^{\alpha z} + g(u)e^{-\alpha z})J_n(ru)du. \tag{7}
$$

where $\alpha^2 = u^2 + \gamma^2$ and $\cos\phi = \frac{x}{r}$.

The boundary conditions at $z = 0$ and $z = -b$ consist in the continuity of the tangential (x, y) components of H and E. The equations arising from the boundary conditions can be simplified by differentiation or integration with respect to x or y (which is possible by virtue of (7)), and are taken in the following convenient form:
$z = 0$:

$$
\gamma_0^2\Pi_{0z} = \gamma_1^2\Pi_{1z}, \tag{8}
$$

$$
\gamma_0^2\frac{\partial \Pi_{0x}}{\partial z} = \gamma_1^2\frac{\partial \Pi_{1x}}{\partial z}, \tag{9}
$$

$$
\frac{\partial \Pi_{0x}}{\partial x} + \frac{\partial \Pi_{0z}}{\partial z} = \frac{\partial \Pi_{1x}}{\partial x} + \frac{\partial \Pi_{1z}}{\partial z}, \tag{10}
$$

$$
\gamma_0^2\Pi_{0x} = \gamma_0^2\Pi_{1x}; \tag{11}
$$

$z = -b$:

$$\gamma_1^2 \Pi_{1z} = \gamma_2^2 \Pi_{2z}, \tag{12}$$

$$\gamma_1^2 \frac{\partial \Pi_{1x}}{\partial z} = \gamma_2^2 \frac{\partial \Pi_{2x}}{\partial z}, \tag{13}$$

$$\frac{\partial \Pi_{1x}}{\partial x} + \frac{\partial \Pi_{1z}}{\partial z} = \frac{\partial \Pi_{2x}}{\partial x} + \frac{\partial \Pi_{2z}}{\partial z}, \tag{14}$$

$$\gamma_1^2 \Pi_{1x} = \gamma_2^2 \Pi_{2x}. \tag{15}$$

From boundary conditions (9), (11), (13), and (15), the x-components of the Hertzian vectors can be determined separately and then used in finding the z-components.

For the x-components the arbitrary functions $f(\lambda)$ and $g(\lambda)$ can be determined from the boundary conditions if in (7) $n = 0$. These components are therefore taken as follows:

$$\Pi_{0x}'' = \int_0^\infty f_0(u) e^{-\alpha_0 z} J_0(ru) du \qquad z \geqslant 0, \tag{16}$$

$$\Pi_{1x} = \int_0^\infty (f_1(u) e^{\alpha_1 z} + g_1(u) e^{-\alpha_1 z}) J_0(ru) du \qquad -b \leqslant z \leqslant 0, \tag{17}$$

$$\Pi_{2x} = \int_0^\infty f_2(u) e^{\alpha_2 z} J_0(ru) du \qquad z \leqslant -b. \tag{18}$$

The arbitrary functions $f(u)$ and $g(u)$ are then determined by the following equations, obtained from (9), (11), (13), and (15):

$$\begin{aligned}
\gamma_1^2 \alpha_1 (f_1 - g_1) &= A \gamma_0^2 u e^{-\alpha_0 h} - \gamma_0^2 \alpha_0 f_0, \\
\gamma_1^2 \alpha_0 (f_1 + g_1) &= A \gamma_0^2 u e^{-\alpha_0 h} + \gamma_0^2 \alpha_0 f_0, \\
\gamma_1^2 \alpha_1 (f_1 e^{-\alpha_1 b} - g_1 e^{\alpha_1 b}) &= \gamma_2^2 \alpha_2 f_2 e^{-\alpha_2 b}, \\
\gamma_1^2 (f_1 e^{-\alpha_1 b} + g_1 e^{\alpha_1 b}) &= \gamma_2^2 f_2 e^{-\alpha_2 b},
\end{aligned} \tag{19}$$

where for convenience the argument u of the arbitrary functions has been omitted.

The solutions of (19) for f_1 and g_1 are

$$\begin{aligned}
f_1 &= \frac{2Au(\alpha_1 + \alpha_2)}{\Delta} e^{-h\alpha_0}, \\
g_1 &= \frac{2Au(\alpha_1 - \alpha_2)}{\Delta} e^{-h\alpha_0 - 2b\alpha_1},
\end{aligned} \tag{20}$$

where

$$\Delta = {}_0\alpha) + \alpha_1)(\alpha_1 + \alpha_2) + (\alpha_0 - \alpha_1)(\alpha_1 - \alpha_2) e^{-2b\alpha_1}.$$

The boundary conditions for the z-components may be satisfied by taking $n = 1$ in equation (7); the resulting expressions are as follows:

$$\Pi_{0z} = \cos\phi \int_0^\infty p_0(u)e^{-\alpha_0 z}J_1(ru)du \qquad z \geqslant 0, \tag{21}$$

$$\Pi_{1z} = \cos\phi \int_0^\infty (p_1(u)e^{-\alpha_0 z} + q_1(u)e^{-\alpha_0 z})J_1(ru)du \quad -b \leqslant z \leqslant 0, \tag{22}$$

$$\Pi_{2z} = \cos\phi \int_0^\infty p_2(u)e^{\alpha_0 z}J_1(ru)du \qquad z \leqslant -b. \tag{23}$$

From boundary conditions (8), (10), (12), and (14) and the values of the x-components as now determined, Π_{1x} being given by equation (17), Π_{0x} and Π_{2x} being given in terms of it by equations (11) and (15), the following equations are obtained:

$$\begin{aligned}
\gamma_1^2(p_1 + q_1) &= \gamma_0^2 p_0, \\
\alpha_1\gamma_0^2(p_1 - q_1) &= -\alpha_0\gamma_0^2 p_0 + u(\gamma_0^2 - \gamma_1^2)(f_1 - g_1), \\
\gamma_1^2(p_1e^{-\alpha_1 b} + q_1e^{\alpha_1 b}) &= \gamma_2^2 p_2 e^{-\alpha_2 b}, \\
\alpha_1\gamma_1^2(p_1e^{-\alpha_1 b} - q_1e^{\alpha_1 b}) &= \alpha_2\gamma_2^2 p_2 e^{-\alpha_2 b} \\
&\quad + u(\gamma_2^2 - \gamma_1^2)(f_1e^{-\alpha_1 b} + g_1e^{\alpha_1 b}),
\end{aligned} \tag{24}$$

the arguments of the functions being omitted as before.

From (24), p_1 and q_1 are obtained as

$$\begin{aligned}
p_1 &= u\,\frac{(\gamma_0^2 - \gamma_1^2)(\alpha_1\gamma_2^2 + \alpha_2\gamma_1^2)(f_1 + g_1) - (\gamma_1^2 - \gamma_2^2)(\alpha_0\gamma_1^2 - \alpha_1\gamma_0^2)(f_1e^{-\alpha_1 b} + g_1e^{\alpha_1 b})e^{-\alpha_1 b}}{(\alpha_0\gamma_1^2 + \alpha_1\gamma_0^2)(\alpha_1\gamma_2^2 + \alpha_2\gamma_1^2) + (\alpha_0\gamma_1^2 - \alpha_1\gamma_0^2)(\alpha_1\gamma_2^2 - \alpha_2\gamma_1^2)e^{-2b\alpha_1}}, \\
q_1 &= u\,\frac{(\gamma_0^2 - \gamma_1^2)(\alpha_1\gamma_2^2 - \alpha_2\gamma_1^2)(f_1 + g_1)e^{-2b\alpha_1} + (\gamma_1^2 - \gamma_2^2)(\alpha_0\gamma_1^2 + \alpha_1\gamma_0^2)(f_1e^{-\alpha_1 b} + g_1e^{\alpha_1 b})e^{-\alpha_1 b}}{(\alpha_0\gamma_1^2 + \alpha_1\gamma_0^2)(\alpha_1\gamma_2^2 + \alpha_2\gamma_1^2) + (\alpha_0\gamma_1^2 - \alpha_1\gamma_0^2)(\alpha_1\gamma_2^2 - \alpha_2\gamma_1^2)e^{-2b\alpha_1}}.
\end{aligned} \tag{25}$$

The tangential components of the electric force at $z = 0$ are by (6), (17), and (22):

$$\begin{aligned}
E_x = &-c\gamma_1^2 \int_0^\infty (f_1(u) + g_1(u))J_0(ru)du \\
&+ c\frac{\partial}{\partial x}\cos\phi \int_0^\infty [-u(f_1(u) + g_1(u)) \\
&\qquad + \alpha_1(p_1(u) - q_1(u))]J_1(ru)du,
\end{aligned} \tag{26}$$

$$E_y = + c\frac{\partial}{\partial y}\cos\phi \int_0^\infty [- u(f_1(u) + g_1(u)) + \alpha_1(p_1(u) - q_1(u))]J_1(ru)du.$$

Or since $\cos\phi \int_0^\infty J_1(ru)du = -\frac{\partial}{\partial x}\int_0^\infty \frac{J_0(ru)}{u}$,

$$E_x = - c\gamma_1^2 \int_0^\infty (f_1(u) + g_1(u))J_0(ru)du - c\frac{\partial^2}{\partial x^2}\int_0^\infty \left[- (f_1(u) + g_1(u)) + \frac{\alpha_1}{u}(p_1(u) - q_1(u))\right] J_0(ru)du, \quad (26a)$$

$$E_y = - c\frac{\partial^2}{\partial x \partial y}\int_0^\infty \left[- (f_1(u) + g_1(u)) + \frac{\alpha_1}{u}(p_1(u) - q_1(u))\right] J_0(ru)du.$$

Inserting the values of $f_1(u)$, $g_1(u)$, $p_1(u)$, and $q_1(u)$ for $h = 0$ and neglecting all displacement currents ($\epsilon_0 = \epsilon_1 = \epsilon_2 = 0$), the following expression is obtained:

$$E_x, E_y = dS\left[- i\omega P(r) + \frac{\partial^2 Q(r)}{\partial x^2}, \frac{\partial^2 Q(r)}{\partial x \partial y}\right], \quad (27)$$

where

$$P(r) = 2\int_0^\infty \frac{u}{\Delta}[\alpha_1 + \alpha_2 + (\alpha_1 - \alpha_2)e^{-2b\alpha_1}]J_0(ru)du,$$

$$Q(r) = \frac{1}{2\pi}\int_0^\infty \frac{u}{\Delta\Delta_1}\{4(\lambda_1 - \lambda_2)\alpha_0\alpha_1^2 e^{-2b\alpha_1} + [\alpha_1 + \alpha_2 + (\alpha_1 - \alpha_2)e^{-2b\alpha_1}]\Delta_2\}J_0(ru)du,$$

where as before

$$\Delta = (\alpha_0 + \alpha_1)(\alpha_1 + \alpha_2) + (\alpha_0 - \alpha_1)(\alpha_1 - \alpha_2)e^{-2b\alpha_1}$$

and

$$\Delta_1 = (\alpha_0\lambda_1 + \alpha_1\lambda_0)(\alpha_1\lambda_2 + \alpha_2\lambda_1) + (\alpha_0\lambda_1 - \alpha_1\lambda_0)(\alpha_1\lambda_2 - \alpha_2\lambda_1)e^{-2b\alpha_1},$$
$$\Delta_2 = (\alpha_0 + \alpha_1)(\alpha_1\lambda_2 + \alpha_2\lambda_1) + (\alpha_0 - \alpha_1)(\alpha_1\lambda_2 - \alpha_2\lambda_1)e^{-2b\alpha_1}.$$

The mutual impedance of wire elements dS and ds lying in the plane $z = 0$, and including the angle ϵ between their directions, is:

$$dZ_{Ss} = -ds[E_x \cos\epsilon + E_y \sin\epsilon]$$
$$= dSds\left[i\omega P(r)\cos\epsilon - \frac{\partial^2 Q(r)}{\partial x^2}\cos\epsilon - \frac{\partial^2 Q(r)}{\partial x \partial y}\sin\epsilon \right] \quad (28)$$
$$= \left\{ \frac{d^2 Q(r)}{dSds} + i\omega P(r)\cos\epsilon \right\} dSds.$$

Integration over the two wires S and s extending from A to B and from a to b, respectively, gives their mutual impedance:

$$Z_{Ss} = \int_a^b \int_A^B \left\{ \frac{dQ(r)}{dSds} + i\omega P(r)\cos\epsilon \right\} dSds. \quad (29)$$

With $\lambda_0 = 0$, the expressions following (27) for $P(r)$ and $Q(r)$ reduce to those given in Part I for wires on the surface of the earth. The expressions given in Part I for wires in the plane of separation at the depth b below the earth's surface are obtained by putting $\lambda_2 = 0$ and changing λ_0 to λ_2 in the resulting expression.

We are indebted to Mr. R. M. Foster for evaluation of some of the integrals as well as for general suggestions and counsel.

Some Theoretical and Practical Aspects of Gases in Metals *

By J. H. SCAFF and E. E. SCHUMACHER

In this paper there are included a discussion of the theories pertaining to the absorption of gases by metals and descriptions of actual work illustrating them. Apparatus for the analysis and measurement of gases in metals and for melting metals in vacuum are described. Information is included, also, on commercial vacuum melting methods and the results obtained.

Introduction

SINCE Thomas Graham [1] discovered in 1866 that a piece of meteoric iron heated in vacuum yielded 2.8 times its volume of gas,[2] the solubility of gases in metals has been the subject of a large number of investigations. While these studies have not as yet afforded more than a partial understanding of the nature of the processes by which gases are dissolved in metals, they have yielded considerable knowledge of those factors which determine the extent of such solubility, and thus of the methods by which the amount of dissolved gas can be increased or diminished. At the same time they have shown the importance of dissolved gases in determining not merely the behavior of metals in casting processes, but also the magnetic, mechanical, and chemical properties of metallic materials. It is proposed to discuss, in this paper, theories of the absorption of gases by metals and to review important work on this subject.

The Effect of Gases on the Properties of Metals

The importance of producing sound metals should interest every metal founder in the effects of dissolved gases. Any gas whose solubility is greater in the liquid than in the solid metal may cause the formation of blowholes. The formation of these blowholes, however, can be reduced or prevented by cooling the metal slowly enough through its freezing range to permit the escape of liberated gases. Iron saturated with hydrogen, for instance, will yield a sound ingot if cooled very slowly through its freezing point, while chill casting not only will make the metal porous but may cause an evolution of gas violent enough to throw metal from the mold. This phenome-

* *Metals and Alloys*, January, 1933.

[1] Thomas Graham, *Proc. Roy. Soc.*, *15*, 502 (1866).

[2] All gas volumes given in this paper are at N.T.P.

non is known as "spitting" and is a common occurrence when casting iron, copper, cobalt, and platinum saturated with hydrogen, and silver saturated with oxygen.

The magnetic properties of iron and its alloys are known to be greatly affected by gases. Cioffi,[3] of Bell Telephone Laboratories, has shown that the permeability of iron can be increased to 190,000 by heat treating it in hydrogen at 1500° C. This effect is attributed to the removal of carbon, oxygen, nitrogen, and sulphur. In this field, also, Yensen has done interesting work, details of which are contained in his publications.[4] The permeability of iron can be greatly increased, also, by vacuum melting. Here again the gaseous impurities and those which react to form gaseous products are removed by the treatment.

The influence of oxygen on the carburization of steel is not clearly understood, but its importance has been emphasized by many writers. Grossmann [5] believes that steel absorbs oxygen along with carbon during pack carburization and that this favors a solubility of cementite in alpha iron. By this mechanism, he accounts for the phenomenon of split cementite. Guthrie and Wozasek [6] found that the presence of oxygen speeds up the process of gas carburizing, which indicates that oxygen must affect the solubility and rate of solution of carbon in austenite.

The influence of nitrogen on the properties of steel is of commercial importance. It was learned first that nitrogen in steel formed nitrides which were dispersed in the metal and which caused brittleness. Later, nascent nitrogen, obtained from the thermal dissociation of ammonia, was found to react with certain constituents in steel to form an exceedingly hard case. From this discovery, the modern commercial nitriding process has been developed.

Pfeil, Lea, and others have observed that small quantities of hydrogen absorbed by iron during electrolytic pickling appreciably affect its mechanical properties. Pfeil [7] found that the tensile strength of mild steel rods is decreased from 18.34 tons per square inch to 16.69 tons and that the elongation in one inch falls from 62.5 per cent to 10.6 per cent. Normal properties are restored if the steel is allowed to stand for sometime in the air. Lea,[8] also studying mild steel, confirmed Pfeil's elongation data but found only a slight effect on

[3] Cioffi, *Phys. Rev.*, *39*, 363 (1932).
[4] Yensen, *Metal Progress*, June, 1932, p. 28; *A. I. M. M. E. Tech. Pub.* No. 185.
[5] Grossmann, *Trans. A. S. S. T.*, *16*, 1 (1929); *18*, 601 (1930).
[6] Guthrie and Wozasek, *Trans. A. S. S. T.*, *12*, 853 (1927).
[7] Pfeil, *Proc. Roy. Soc.* London, *112*, 182 (1926).
[8] Lea, *Proc. Roy. Soc.* London, *123*, 171 (1929).

tensile strength. Lea claimed, also, that the hydrogen had only a slight effect on the resistance of mild steel to impact and repeated stresses. The fracture produced by repeated stresses, however, was abnormal.

The amount of hydrogen in electrodeposited metals is believed to affect their properties. Schneidewind [9] showed that the hardness of electrodeposited chromium decreases when the metal is heated to approximately 300° C. This decrease could not be caused by recrystallization of the deposit, for its grain size was not appreciably changed by heating even at 850° C.; nor was the decrease caused by the solution of some constituent which had caused precipitation hardening at room temperature, since quenching and aging did not restore the original hardness. Schneidewind believed that the initial hardness was due to the presence of some volatile constituent, probably hydrogen.

In order to obtain sound castings of copper, it is necessary, in the usual fire refining process, to stop the operation before the oxygen is entirely removed. If the operation is continued further the copper would take up gases from the furnace and unsound castings would invariably be the result. Copper in the tough pitch condition, therefore, contains a nominal quantity of oxygen (0.04 per cent). Although for ordinary uses this product is perfectly satisfactory, when exposed to reducing gases at elevated temperatures, the contained oxygen combines with them to form products which cause embrittlement. For use at high temperatures with reducing gases, therefore, copper must be deoxidized. In the past, metallic deoxidizers were added to the copper during the casting operations, but, in order to assure complete deoxidation, an excess had to be added which reduced the electrical conductivity of the finished product.

Recently, a brand of copper [10] has been placed on the market which is said to be kept free from oxygen during melting and therefore needs no deoxidation. This material can be heated in reducing gases without embrittlement, has electrical conductivity comparable to that of electrolytic copper, and is claimed to be tougher and more ductile than fire refined copper and to have better working properties.

The studies of Tullis [11] and Rosenhain [12] on the gas removal and grain refinement of aluminum have yielded results which may have

[9] Schneidewind, *Trans. A. S. S. T.*, *19*, 115 (1931).

[10] Oxygen Free High Conductivity Copper, produced by the United States Metals Refining Co.

[11] Tullis, *Jour. Inst. Metals*, *40*, 55 (1928); *Metal Ind.* (London), *34*, 339 (1929); *Metal Ind.* (London), *34*, 371 (1929).

[12] Rosenhain, *Jour. Inst. Metals*, *44*, 305 (1931), No. 2.

great commercial importance. Tullis has found that the treatment of molten aluminum with gaseous chlorine completely removes the dissolved gases. Subsequent treatment with boron trichloride causes the formation of small grains in the castings. Rosenhain [12] has reported that both gas removal and grain refinement can be effected in one operation by the use of volatile chlorides such as titanium tetrachloride. Both of these methods are being tested on a commercial scale in England. It is claimed that secondary aluminum, treated in this way, gives strong castings as free from pinholes as does virgin metal. If the cost is sufficiently low and if the industrial hazards attending its use can be controlled satisfactorily, this method of gas treatment should have a wide applicability to refining secondary aluminum.

The descriptions, given above, of the effect of gases on the properties of metals should indicate how important these effects are and how small a quantity of gas may suffice to produce them. It seems necessary, therefore, to consider gaseous impurities along with others in metallurgical studies.

THEORY

The Effect of Temperature on the Solubility of Gases in Metals

Metal founders of early times had great difficulty making castings which did not contain blowholes. Knowing that the solubility of gases in aqueous liquids decreased with increasing temperature, they tried to remove the gases from molten metal by heating to a higher temperature before casting. They found, however, that their product was less sound than before. This suggested to later workers a difference between the action of gases in aqueous liquids and in molten metals and several systematic investigations were begun.

Sieverts, one of the first men to study this problem, found that, in general, the solubility of gases in metals increases with increasing temperature.[13] He found, for instance, that one volume of copper absorbs 0.006 volume of hydrogen at 400° C., and 0.19 volume just below its melting point. As the copper melts, the quantity of gas absorbed increases to 0.54 volume, while at 1550° C. 1.25 volumes are absorbed. The amount of hydrogen absorbed by iron increases from 1.05 volumes for the solid to 2.10 volumes for the liquid at the same temperature.

Some known exceptions to the general rule that absorption of gas increases with increasing temperature are the solubility of hydrogen

[12] Loc. cit.

[13] Sieverts published a useful résumé of his work, with references to the original articles in *Zeit. für Metallkunde, 21*, 37 (1929).

in palladium, cerium, thallium, zirconium, titanium, tantulum, and vanadium. The solubility changes of hydrogen in palladium are particularly interesting. One volume of this metal absorbs 670 to 800 volumes of hydrogen at 20° C., 50.6 volumes at 138° C., and in the liquid state at 1600° C. only 4.3 volumes.[13]

Since the solubility of gases in aqueous liquids decreases with increasing temperature, and since these data form the bulk of the total available, some workers have suggested that the increase in solubility of gases in metals with increasing temperature is anomalous. No anomaly appears, however, when the solubility relationship is considered in the light of van't Hoff's law of mobile equilibrium. This law states that when the temperature of a system in equilibrium is raised only that reaction can occur which is accompanied by an absorption of heat, that is, an endothermal reaction. The increasing solubility of gases in metals with increasing temperature, therefore, should be taken as evidence of an endothermic reaction rather than as an anomaly.

Data are available which show that increasing solubility of gases with increasing temperature is not limited to gas-metal systems. Just [14] has shown that the solubility of hydrogen, carbon monoxide, and nitrogen in carbon disulphide, nitrobenzene, acetone, and other organic solvents increases with increasing temperature. Lannung [15] has reported data showing that the solubility of argon, neon, and helium in methyl alcohol, and acetone increases with increasing temperature. In this respect the gas-metal systems seem to be similar to some of the gas-organic liquid systems.

Another fairly well known influence of temperature on the quantity of gas absorbed by a metal is due to an allotropic change in the structure. That the amount of gas absorbed by a metal changes abruptly when the allotropic form changes, is illustrated by the iron-nitrogen system. One hundred grams of iron heated to 878° C. absorbs only 1.6 milligrams of nitrogen, but at 930° C., in the gamma modification, it takes up 21.6 milligrams.[13]

The Effect of Pressure on the Solubility of Gases in Metals

The effect of changes in pressure on the solubility of gases in metals has been studied intensively by Sieverts. He made the discovery that the quantity of gas dissolved in a metal at constant temperature

[13] Loc. cit.
[14] Just, *Zeit. Phys. Chem.*, *37*, 342 (1901).
[15] Lannung, *Jour. Am. Chem., Soc.*, *52*, 73 (1930).

is proportional to the square root of its partial pressure.[13] This square root relationship (which may well be called Sieverts' law) emphasizes the difference between the solution phenomena of gases in metals and gases in aqueous liquids, since, in the latter, solubility is proportional to the partial pressure of the gas (Henry's law). There are, however, some gas-metal systems in which solubility does not follow Sieverts' law. It is well known that the solubility of hydrogen in palladium is not proportional to the square root of the gas pressure and this is true also of hydrogen in cerium, thallium, zirconium, titanium, tantalum, and vanadium. These exceptions are the same as those mentioned in the section above on the effect of temperature. These metals are noteworthy for their comparatively great absorption of hydrogen and for their compound formation with it.

Sieverts' law is usually explained by application of the Nernst distribution law, which states that there is a constant ratio between the concentrations of a given molecular species distributed between two phases of a system in equilibrium. Considering, first, molecular oxygen dissolved in a liquid, let P_{O_2} denote its partial pressure in the gas phase and C_{O_2} its concentration in the liquid. The distribution law is then

$$P_{O_2} = kC_{O_2}. \tag{1}$$

The concentration here is directly proportional to the partial pressure, a fulfillment of Henry's law which is a special case of the distribution law. This adequately describes the solubility of most gases in aqueous liquids.

Considering, now, the solubility of gases in metals, and assuming that molecular gas is dissociated into atoms at the surface of the metal before it is dissolved, let P_{O_2} denote the partial pressure of molecular oxygen, P_O the concentration of atomic gas at the metal surface, and C_O the concentration of atomic gas in the metal. Then, according to the law of mass action,

$$P_{O_2} = k_1(P_O)^2. \tag{2}$$

Applying the distribution law to the equilibrium between atomic oxygen at the metal surface and atomic oxygen dissolved gives

$$P_O = k_2C_O. \tag{3}$$

Combining equations (2) and (3) gives

$$P_{O_2} = k_1(k_2C_O)^2 = KC_O^2. \tag{4}$$

[13] Loc. cit.

This shows that the square root relationship found by Sieverts can be explained by assuming a dissociation of the molecules of gas somewhere in the process of solution.

Donnan and Shaw [16] applied this type of analysis to the solubility of oxygen in silver and have shown that the solubility is proportional to the square root of the gas pressure not only if dissociated gas is dissolved as described above, but also if this dissolved gas reacts with the silver to form a compound containing one atom of gas per molecule, in this instance, Ag_2O. This conclusion can be reached easily by extending the analysis in the preceding paragraph to include an application of the law of mass action to the reaction between the dissolved atomic gas and the metal. If this is done, it is found that the concentration of compound is directly proportional to the concentration of atomic gas, which has been shown to be proportional to the square root of the gas pressure. Hence the concentration of compound is proportional also to the square root of the gas pressure.

It is apparent from this discussion that data showing the effect of pressure on gas solubility do not show whether gases are dissolved in metals as atoms or as compounds. In order to learn the state in which gases exist in metals, Sieverts [13] studied the solubility of sulphur dioxide in copper. He expected that changes in the pressure would affect the solubility of this triatomic gas differently from that of a diatomic gas. He was surprised, therefore, to find that for this system also the solubility was proportional to the square root of the gas pressure. In this instance, adherence to the square root law could not be explained by assuming dissociation of the gas molecules into atoms.

In this field, Stubbs [17] made some interesting contributions after those of Sieverts. He showed that the freezing point of copper saturated with sulphur dioxide was depressed 2.54 times as much from that of pure copper as should be expected from van't Hoff's freezing point formula if the gas remained molecular in solution. If there were complete reaction between the gas in solution and the metal, the freezing point depression should be three times that for the existence of molecules only, and the amount of gas absorbed should vary as the cube root of the pressure. Stubbs took the discrepancy in these figures to indicate that about 70 per cent of the dissolved sulphur dioxide reacted with the copper according to the equation,

$$SO_2 + 6Cu = Cu_2S + 2Cu_2O.$$

[16] Donnan and Shaw, *Jour. Soc. Chem. Ind.*, *29*, 987 (1910).
[13] Loc. cit.
[17] Stubbs, *Jour. Chem. Soc.*, *103*, 1445 (1913).

Stubbs also believed that Sieverts' data showed that the solubility of sulphur dioxide in copper varied as some higher root of the pressure (2.4 root) than the square root and that it supported his theory of partial reaction of the gas with the copper.

Because very little is known of the state in which dissolved gases exist in metals, certain data reported by Franzini [18] are interesting. Franzini believed that, if ionized gas existed in metals, it could be displaced by the action of an electric field. His data on the variation in electrical resistance, caused by application of an electrical field to iron and nickel wires which previously had been saturated with hydrogen, show that the absorbed gas can be displaced toward the negative pole. Thus, evidence of the presence of ionized gas in a metal was obtained.

Illustrative Examples of Gas-Metal Absorption Studies

The Solubility of Oxygen in Silver

Steacie and Johnson's [19] careful experiments on the solubility of oxygen in silver form a good illustration of the problems involved in this type of study. Since their work yielded some of the best data available on any gas-metal system, it is reviewed here in some detail.

The principle of their method of determining solubility is a variation of the method ordinarily used. A known weight of silver, contained in a silica bulb, is heated to a given temperature. All traces of gas are removed by evacuation of the apparatus, and then a known amount of purified oxygen is admitted to the silica bulb. After equilibrium between the oxygen and the silver is reached, the pressure of the gas is measured by a permanently connected manometer. The theoretical pressure of oxygen in the system, assuming none is absorbed by the silver, is calculated from the quantity of gas introduced, its temperature, and the volume of that part of the apparatus it occupies. The difference between calculated and observed pressures is a measure of the amount of gas absorbed by the metal.

In order to determine the solubility of gases in metals accurately, sufficient time must be allowed for equilibrium to be reached. Although equilibrium was reached very quickly at the highest temperature (800° C.) used by Steacie and Johnson, several days were required at the lowest temperature (200° C.). It is obvious that this long time greatly increases the possibility of errors from leakage of gas into the apparatus. Since Steacie and Johnson were especially interested in solubility at low temperatures, to be certain that no errors were

[18] Franzini's work was reviewed in *Nature*, March 12, 1932, p. 404.
[19] Steacie and Johnson, *Proc. Roy. Soc.* London, *112*, 542 (1926).

introduced by leakage, they pumped the gas out of the silica bulb and the silver at the end of each experiment, collected it, and determined its quantity. If the amount of gas collected after an experiment was not substantially the same as the amount introduced originally, the experiment was discarded.

Data relative to the solubility of oxygen in silver are given in Table I. The solubility can be seen to be proportional to the square root of the oxygen pressure, except for pressures below 10 cms. when the temperature is below 600° C. Here a marked divergence from the square root law appears, which might be explained by assuming that these measurements were made before equilibrium was established.

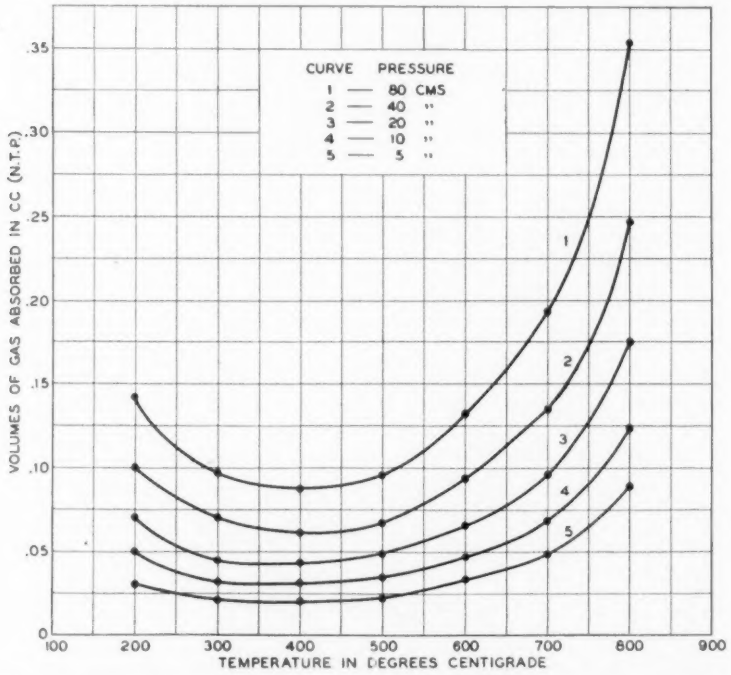

Fig. 1—Solubility of oxygen in silver as a function of temperature with pressure as a parameter (Steacie and Johnson).

These data are plotted, in Fig. 1, to show the variation of solubility with temperature, giving pressure as a parameter.

The curves of Fig. 1 differ from those for other systems in that a minimum point occurs at about 400° C. It would be logical to explain this minimum as an adsorption effect, but Steacie and Johnson

TABLE I

SOLUBILITY OF OXYGEN IN SILVER AT VARIOUS PRESSURES AND TEMPERATURES *

Pressure (cms.)	T_1 = 200° C.		T_2 = 300° C.		T_3 = 400° C.		T_4 = 500° C.		T_5 = 600° C.		T_6 = 700° C.		T_7 = 800° C.	
	Volumes Absorbed (c.c., n.t.p.)	Constant	Volumes Absorbed (c.c., n.t.p.)	Constant	Volumes Absorbed (c.c., n.t.p.)	Constant	Volumes Absorbed (c.c., n.t.p.)	Constant	Volumes Absorbed (c.c., n.t.p.)	Constant	Volumes Absorbed (c.c., n.t.p.)	Constant	Volumes Absorbed (c.c., n.t.p.)	Constant
P	Q	$\sqrt{P}/Q$	Q	$\sqrt{P}/Q$	Q	$\sqrt{P}/Q$	Q	$\sqrt{P}/Q$	Q	$\sqrt{P}/Q$	Q	$\sqrt{P}/Q$	Q	$\sqrt{P}/Q$
5	0.030	74.5	0.021	106.5	0.020	112.0	0.022	102.0	0.033	68.0	0.048	46.7	0.088	25.5
10	0.050	63.4	0.032	90.8	0.031	102.3	0.034	93.2	0.047	67.5	0.068	46.6	0.124	25.6
20	0.071	63.3	0.045	91.0	0.044	102.3	0.048	93.4	0.066	67.9	0.096	46.7	0.175	25.6
40	0.100	63.5	0.070	90.5	0.061	103.9	0.067	94.5	0.093	68.1	0.134	46.3	0.247	25.7
80	0.142	63.2	0.097	91.7	0.087	103.0	0.095	94.3	0.132	67.9	0.193	46.5	0.354	25.3

* Steacie and Johnson.

found that, below 400° C., the solubility of oxygen in two samples of silver with different ratios of surface to volume was the same. If an appreciable part of the gas had been adsorbed on the surface of the metal instead of being in solution, a difference in apparent solubility should have been observed. They suggested, then, that the minimum point might indicate a change in the silver from one allotropic form to another. This explanation was found unsatisfactory later, because experiments showed that the solubility of hydrogen in silver passes through no minimum as does that of oxygen.

Mechanism of Solution of Oxygen in Silver

Following Langmuir's conception of the mechanism of adsorption Steacie and Johnson [20] proposed an explanation of the mechanism of solution of oxygen in silver in which the solubility minimum is attributed to a change in the form of the oxygen in solution. While a detailed criticism of this explanation would require more space than is available here, it seems unsatisfactory to the present authors, who wish to suggest the following alternative explanation.

Suppose that dissolved gas is held within the interior of the metal, and that it is in equilibrium with that adsorbed on the surface. Now the concentration in the interior which will be in equilibrium with a given surface concentration increases with increasing temperature. The surface concentration, however, which is due to adsorption, will itself decrease with increasing temperature. Hence the final equilibrium depends on two factors which vary with temperature in opposite directions. Below 400° C. surface concentration may be the controlling factor. Thus, as the temperature rises towards 400° C., the surface concentration decreases faster than the dissolved gas in equilibrium with it increases. Hence the solubility decreases with increasing temperature. Above 400° C., the amount of dissolved gas in equilibrium with the adsorbed surface gas increases faster with increasing temperature than the surface concentration decreases, and the amount of gas dissolved increases with increasing temperature. Theoretically, this explanation applies equally well to other gas-metal systems and would lead one to expect solubility minima in them. These minima, however, in some systems may be at temperatures below the range subject to investigation.

The Rate of Solution of Oxygen in Silver

In addition to their determination of solubility of oxygen in silver, Steacie and Johnson made very careful measurements of its rate of

[20] Steacie and Johnson, *Proc. Roy. Soc.* London, *117*, 662 (1928).

solution.[20] These data support their assumption that the process of solution consists first of saturation of a surface layer of the silver with oxygen and then diffusion into the metal. If diffusion is the limiting factor in rate of solution, the data obtained should be expressed by the equation:

$$K = \frac{1}{t} \log \frac{s}{s - x}, \tag{5}$$

where K is a constant, t is time, s is the concentration of a saturated solution of gas in the metal, and x is the average concentration of gas dissolved in the metal at time t. Steacie and Johnson found that their data did fit this equation, if the first few points were neglected, and they plotted curves showing the change in rate of solution with temperature.

The Analysis and Measurement of Gases in Metals

Theory

The most obvious method of determining the quantity and composition of gases in metals consists of melting a sample in vacuum and collecting, measuring, and analyzing the liberated gases. The experimental procedure is difficult, however, and the inherent errors are of such magnitude that most results are at best only qualitative.

One of the principal sources of error in these experiments is the evolution of gases from furnace walls and hot refractories. When the metal is heated by induced high frequency electric currents, however, this error can be reduced, and it can be minimized further by maintaining a large metal to refractory ratio. Another source of error, of equal importance, is introduced when metal vapor condenses on the comparatively cool parts of the apparatus and reabsorbs some of the gas previously liberated. Although this effect results usually from heating the metal in a high vacuum to too high a temperature, it is not easy to eliminate, because, when the temperature is reduced, the evolution of gas becomes too slow and the recovery of gas incomplete. Errors also are introduced by gaseous products often formed by reactions between impurities in the metal melted and the refractory oxides of the crucible. This occurs, for instance, when melting steel in a refractory oxide crucible. The carbon reacts with the oxides to form carbon monoxide, carbon dioxide, or both.

Apparatus and Method

Despite difficulties and errors in the determination of gases evolved from metals melted in vacuum, some special vacuum melting pro-

[20] Loc. cit.

cedures have been devised which can be used satisfactorily for certain gases. A method of determining oxygen, nitrogen, and hydrogen in ferrous alloys, developed by Jordan [21] and his co-workers, and by Oberhoffer,[22] is now widely used.

In the method of Jordan, the samples to be analyzed are melted in vacuum in a gas-free Acheson graphite crucible. The liberated gases consist of carbon monoxide, nitrogen, and hydrogen. The carbon monoxide is formed by interaction of oxygen (or oxides) from the metal with carbon from the crucible. The nitrogen, which may originate from dissociation of nitrides, is evolved from the metal without chemical reaction with the crucible. The form in which hydrogen exists in the metal is unknown. These gases are pumped away from the melting compartment and collected for analysis. The carbon monoxide and hydrogen are oxidized to carbon dioxide and water, respectively, by passing them over heated copper oxide, and their quantities are determined by absorption in suitable absorbents. The residual gas, nitrogen, is determined by a volumetric method.

The Jordan apparatus with some modifications,[23] as shown in Figs. 2 and 3 is used at Bell Telephone Laboratories. The most important change is in the method of determining the weights of carbon dioxide and water formed during the analysis. In Jordan's apparatus, the absorbents for carbon dioxide and water are contained in weighing tubes which must be weighed along with the absorbent and the absorbed gas. In most experiments, the weight of gas absorbed is only a few milligrams and an elaborate technique is required, therefore, to weigh this small quantity when contained in a tube whose weight is relatively large. In the new modification, in order to minimize errors in the measurement of weight, and to simplify the technique required, a quartz spring balance has been substituted for the weighing tube. The absorbent for the gas is contained in a light glass basket attached to a quartz spring. The extension of the spring is measured with a cathetometer and the weight of gas absorbed determined from calibrations. Springs are made in various sizes so that one can always be found to fit the range of weights it is necessary to measure.

[21] Jordan and Eckman, U. S. Bureau of Standards *Scientific Paper No.* 514 (1925). Jordan and Vacher, U. S. Bureau of Standards, *Jour. of Research*, 7, 375 (1931).

[22] Oberhoffer, *Archiv für das Eisenhüttenwesen*, p. 583, March, 1928.

[23] These modifications were developed by Mr. E. S. Greiner who will describe them in the near future in a paper giving the complete details, together with a critical study of the method.

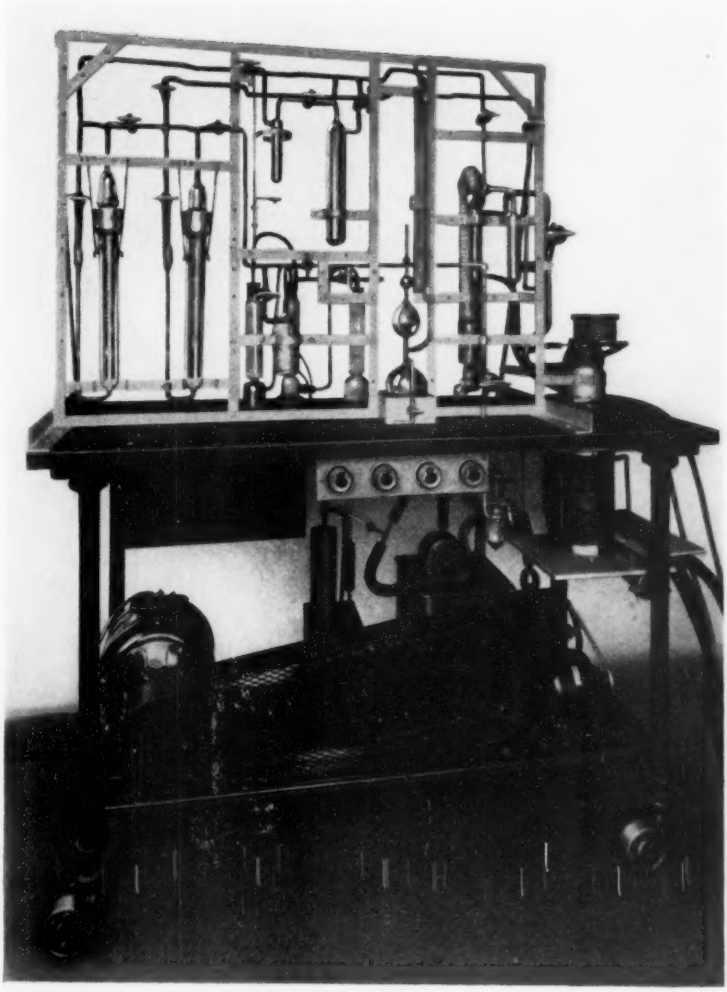

Fig. 2—Modified Jordan apparatus for the determination of oxygen, nitrogen, and hydrogen in ferrous alloys.

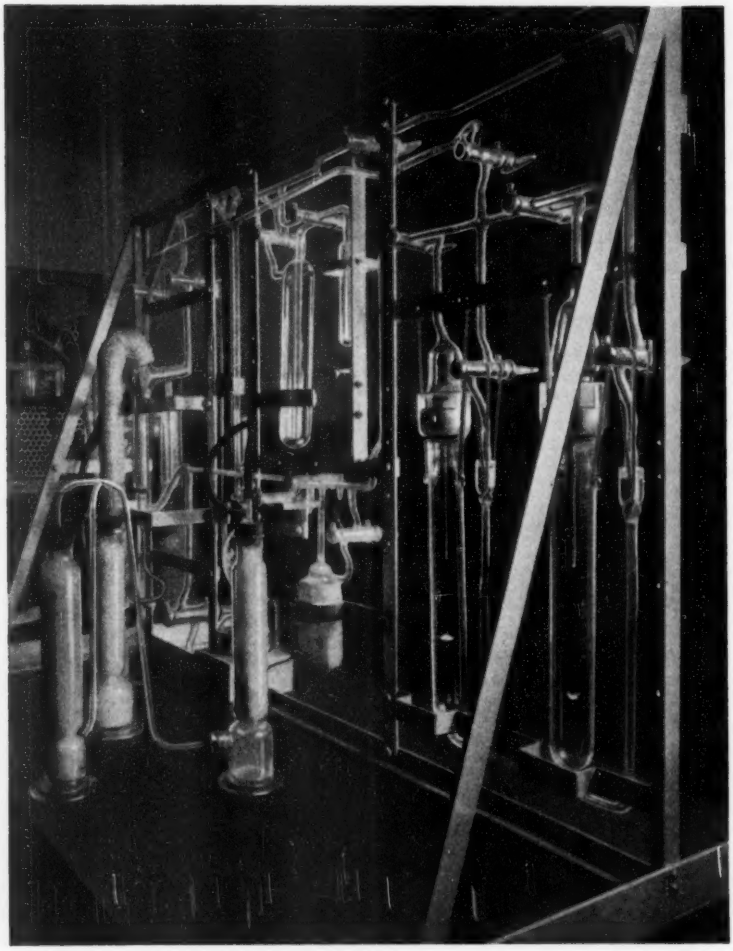

Fig. 3—View of gas analysis apparatus showing quartz spring balances.

Vacuum Melting

Apparatus and Method

In order simply to prepare metals as gas-free as possible, at Bell Telephone Laboratories a special vacuum furnace was devised and constructed which has been extremely satisfactory and helpful in studying the effects of gases on the properties of metals. A schematic diagram of this furnace is shown in Fig. 4. The metal to be melted

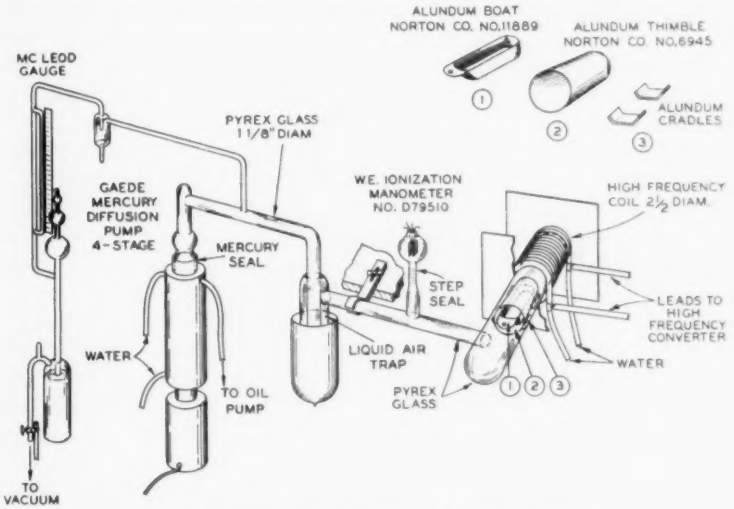

Fig. 4—Furnace for melting metals in high vacuum.

is contained in an alundum boat which is placed horizontally in an alundum thimble. The alundum thimble acts as a radiation shield and is supported concentrically on alundum cradles in a horizontal pyrex glass tube. The metal is heated inductively by high frequency currents supplied by a 35 KVA Ajax Northrup converter.

After the furnace is charged, the pyrex tube is sealed off with an oxygen hand torch, and is baked out at 450° C. by a nichrome wound furnace, the position of which is interchangeable with that of the high frequency induction coil. The pyrex tube is baked out for several hours so that subsequent heating by radiation from the melted metal causes no appreciable evolution of gas.

The gases given up by the liquid metal are pumped out of the system by a four stage Gaede mercury diffusion pump backed by an oil pump. A liquid air trap prevents mercury vapor from entering

the furnace tube and increases the efficiency of the pumping system by removing water vapor and carbon dioxide from the gases to be pumped out. Rough measurements of gas pressure are made with a McLeod gauge on the pump side of the liquid air trap, but measurements of low pressures are made with an ionization manometer on the furnace side.

With this furnace, and using clean alundum parts, metals can be melted with very little contamination of any kind. Copper and iron have been melted under a pressure never rising above 1×10^{-2} mm. Hg and having a final value of 1×10^{-5} to 1×10^{-6} mm. Hg. Even lower pressures can no doubt be obtained by cooling the pyrex furnace tube more effectively, as by use of a water jacket, and by using gas absorbing chemicals such as activated charcoal.

It has been found with this furnace that, even when melting iron, the temperature of the glass furnace tube never rises above 150° C. Since pyrex glass does not soften below 500° C., it should be possible to melt metals with higher melting points than that of iron.

In this furnace, a horizontal boat rather than a crucible is used to hold the sample for two reasons: First, the surface area of metal is greater and the pressure head of metal less so that the melt is degasified more rapidly than it would be in a vertical crucible. Second, very much smaller and less troublesome pipes form in horizontal ingots than in vertical ones.

Commercial Vacuum Melting

Vacuum melting on a commercial scale was developed in Germany during the war because of the need for a method by which the composition of alloys could be accurately controlled. The scarcity of platinum, for instance, necessitated the commercial production of substitute alloys for thermocouples which could be used, without calibration, in direct reading instruments. From the small furnaces used for this work, vacuum furnaces capable of handling up to four tons have been developed.

A brief description of one of these furnaces and of the obstacles encountered in their development has been given by Rohn in his publications.[24] The furnace described by Rohn operates by high frequency induction. It has a horizontal, ring-shaped melting chamber surrounded by the primary induction coils and an iron core. The whole is enclosed in an air-tight casing arranged so that it can be tilted about a horizontal axis. Two molds are fastened on opposite sides of the casing through air-tight connectors. When the charge is

[24] Rohn, *Zeit. für Metallkunde*, *21*, 12 (1929). *Engineering*, Oct. 18, p. 512 (1929).

molten and degassed, the ingots are poured by tilting the entire furnace first to one side and then to the other.

Rohn claims that by dividing the iron core into several parts, a homogeneous field is obtained while there is only a small induction effect in the metal casing. The primary coil, also, is composed of four separate units which can be connected in series or energized separately. Energizing only one unit of the primary, it is claimed, causes vigorous stirring of the molten charge, thus facilitating the degasification. When the units are energized in series, the uniform field obtained causes but little stirring.

One of the chief obstacles it was necessary to overcome during the development of these large furnaces was lack of a satisfactory vacuum casting procedure. Rohn and his co-workers found that, if a normal casting procedure were followed after all the gases were removed from a charge of metal, ingots were obtained with such large shrinkage cavities that working them was impossible. When using iron or sand molds the formation of these cavities could not be prevented. A vertical water-cooled, copper mold was developed, however, that was satisfactory when the melt was poured slowly.

Another obstacle encountered was in obtaining a satisfactory lining for the vacuum furnaces. A moistened material, tamped into place, could not be used because of the difficulty in removing water vapor. The method adopted consisted of packing the regular refractory, as a dry powder, between the outside furnace wall and a template made of the same metal as the charge to be melted. The temperature of the charge was then so controlled that the refractory powder sintered before the template melted.

The Advantages of Vacuum Melting

In addition to freedom from blowholes in castings, one of the main improvements effected by using vacuum furnaces for melting metals is the degree of quality and composition control which can be attained. With this method, no gas can interact with constituents of the melt to cause composition changes, and the melt can therefore be kept liquid for long intervals of time. This allows the suspended particles of slag and oxides to rise to the surface, and results in ingots freer from inclusions. Furthermore, the usual deoxidation methods can be dispensed with. For instance, the iron oxide in molten steel is completely eliminated by reaction with carbon, and therefore, no deoxidation is necessary. Likewise, for non-ferrous metals, no deoxidizers are needed, for during vacuum melting no oxidation of the melt can occur. Thus, inclusions from these sources also are avoided.

In a recent publication [25] Rohn states that iron, nickel, and copper may be freed of oxygen by dissociation of their oxides during vacuum melting. According to our experiments, however, when tough pitch copper is melted under a pressure even as low as 1×10^{-5} mm. approximately, the oxygen is not removed. After this treatment the material is still embrittled by annealing in hydrogen. This failure of the oxide to dissociate may be reasonably ascribed to a reduction in dissociation pressure caused by solution of the oxide in molten copper. This explanation is supported by the thermodynamical calculations of many workers.[26] Furthermore, as the oxide solution in liquid copper becomes less concentrated, its dissociation pressure is lowered so that removal of the last traces of oxygen by dissociation becomes exceedingly difficult.

Rohn [25] has reported that magnetic materials, thermocouple metals, metals for vacuum tube parts, metals for sealing through glass, and nickel-chromium alloys for heating elements are being produced advantageously by vacuum melting. He claims, also, that all of the working properties of the nickel-chromium series of alloys are improved by vacuum melting and that alloys containing up to 33 per cent chromium can be worked satisfactorily.

Concerning the economy of vacuum melting, Rohn points out that production by this method is more costly than production by standard methods. He states that vacuum melting increases the cost of metals ten cents a pound when using a four ton furnace and starting with a cold charge. This can be reduced to one or two cents a pound if the vacuum furnace is used only for the final refining treatment of molten charges. This extra cost should be balanced, in many instances, by the improved quality of metal obtained. Rohn's expectations, which seem to be justified, are that alloys can be made by this process for highly important parts such as turbine blades, tubing for superheaters, and aeroplane parts.

[25] Rohn, *A. I. M. M. E.—Tech. Publication* No. 470.
[26] Ellis, *A. I. M. M. E.—Tech. Publication* No. 478. Allen, Inst. of Metals, Advance Copy No. 604 (1932).

Some Results of a Study of Ultra-Short-Wave Transmission Phenomena *

By C. R. ENGLUND, A. B. CRAWFORD and W. W. MUMFORD

The results of a series of transmission experiments made in the range 3.7 to 4.7 meters and over distances up to 125 miles are reported. These observations were chiefly confined to the region reached by the directly transmitted radiation and are found in good agreement with the assumption that such transmission consists mainly of a directly transmitted radiation plus the reflection components which would be expected from the earth's contour. The residual field not thus explained consists of a more or less pronounced diffraction pattern due to the irregularities of the earth's surface. A hill-to-hill transmission has three demonstrable reflection surfaces.

Quantitative checks on hill-to-hill transmission have been obtained and it has been found that a field intensity of 40 microvolts per meter gives very good transmission. Static is ordinarily entirely absent and no Heaviside layer reflections have been observed.

The almost universal standing wave diffraction patterns have been studied and sample records are given. The methods of measuring field intensity which we have used are described in an appendix. No long range transmissions, such as harmonics of distant (greater than 500 miles) short-wave stations would yield, have been observed.

Introduction

THIS paper details the results of certain studies which have been made on phenomena connected with the transmission of ultra-short waves during the past few years. The work was carried on coincidently with that described in the companion paper by Schelleng, Burrows, and Ferrell.[1] It deals in particular with the establishment of the presence of various ground reflections which must be taken into account in computing ultra-short-wave transmission and with the local disturbances due to both stationary and moving near-by objects.

Apparatus

The transmitting apparatus used by us possessed little novelty; one type of generator has already been described in an earlier paper,[2] a second type consisted of a pair of 75-watt tubes operated "push-pull" and fed by a constant-current modulating system of orthodox type. This latter apparatus served permanently as station W2XM at our Holmdel laboratory, and was ordinarily modulated with the output from a broadcast receiver. We first employed superregenerative re-

* Published in *Proc. I. R. E.*, March, 1933.

[1] Schelleng, Burrows, and Ferrell, "Ultra-short-wave propagation," this issue of *Bell Sys. Tech. Jour.*

[2] *Bell Sys. Tech. Jour.*, vol. 7, p. 404; July (1928).

ceivers and constructed several different types of these. All the quantitative data, however, were obtained with a measuring set employing a double detection receiver.

This receiver is of much the same type as the one described by Friis and Bruce,[3] the modifications in the short-wave circuits necessary to reach the ultra-short-wave range being obvious if not exactly easy to carry out. The intermediate frequency is 1300 kilocycles; there are five amplifier stages preceded by a double tube short-wave detector and followed by a single tube low-frequency detector. The band width (6 decibels down) is approximately 80 kilocycles, and the over-all gain 103 decibels. The amplifier tubes are shielded grid type, and the beating oscillator input is introduced, balanced, in the first detector grid-filament connection. The ultra-short-wave tuning circuits have commercial micrometer heads clamped to the condenser dials. This has proved to be a satisfactory type of vernier adjustment. The shielding extends to the individual tubes and coupling circuits and is complete and thorough. By-pass filters to ground are on all the power input connections. The range is 3.7 to 12 meters using several sets of coils. Two photographs of this receiver are given in Figs. 1a and 1b. For some of this work a manually operated gain recorder was fastened on the set base, with operating pen belted to the set attenuator handle. This recorder is a remodeled sample of the type 289 General Radio fading recorder.

Experimental, Preliminary

The first ultra-short-wave receptions, made in September, 1930, with the superregenerative receiver, showed that a cross-country transit was accompanied by marked variations in field intensity over even rather short distances (one meter for example). Locations were readily found where the reception was very weak, usually areas, as gullies, below the average land level. Hilltop reception was uniformly good and a range of 50 miles (80.5 kilometers) was attained on the third trip. At this site (Musconetcong Mountain, N. J.) the reception, weak at the ground level, was greatly improved by carrying the receiver to the top of an airplane beacon tower. A 75-mile (120.8-kilometer) reception at the Pocono Mountains in Pennsylvania failed, the path being unfavorable for the amount of power available at the transmitter. There was ample indication that straight-line or "optical" transmission was not the only possibility, and there were indications that both earth-reflected and earth-diffracted radiations were present. No fading and no static were noticed. Later trips added little of sig-

[3] *Proc. I. R. E.*, vol. 14, p. 507 (1926).

nificance to these observations as the superregenerative receiver is fundamentally incapable of quantitative field strength indications.

Further work was therefore undertaken using the double detection field strength measuring set. The transmitter site was at first the same

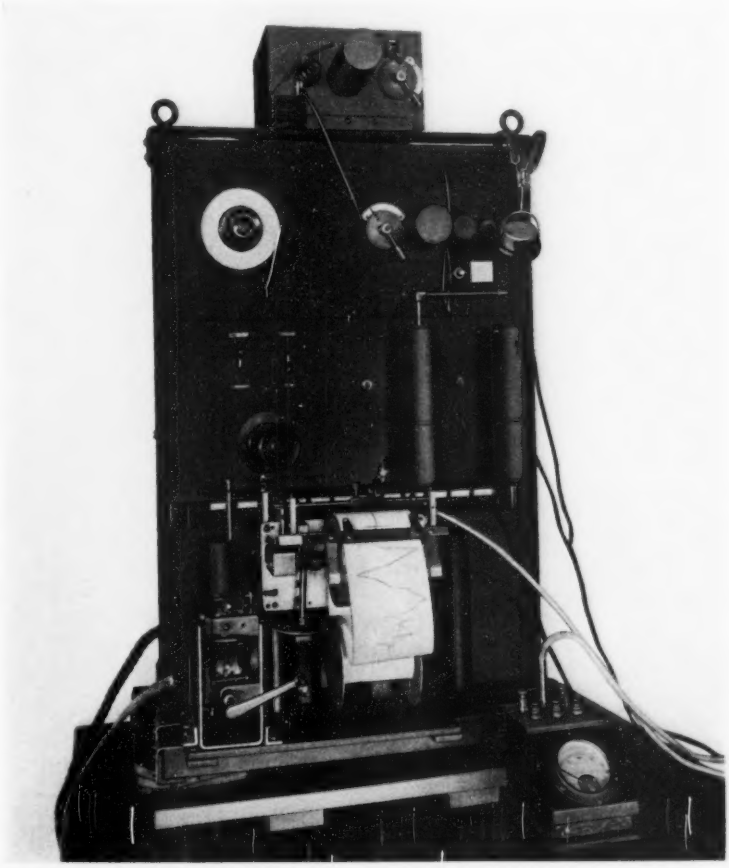

Fig. 1a—Front view of measuring set.

as for the preceding autumn, viz., the Holmdel Laboratory where a half-wave center-tapped antenna on a 65-foot (20-meter) pole was fed with a simple parallel wire transmission line of No. 14 B & S gauge tinned copper wire, 1/4-inch (0.635-centimeter) spacing, with 246 ohms characteristic impedance. With the antenna impedance equal

to approximately 73 ohms the mismatch did not exceed 4 to 1 which gave less than one decibel added loss over impedance matching.[4] As a considerable wave-length range had to be covered, a single wave-length match was of no utility. An open-wire line of less than 250

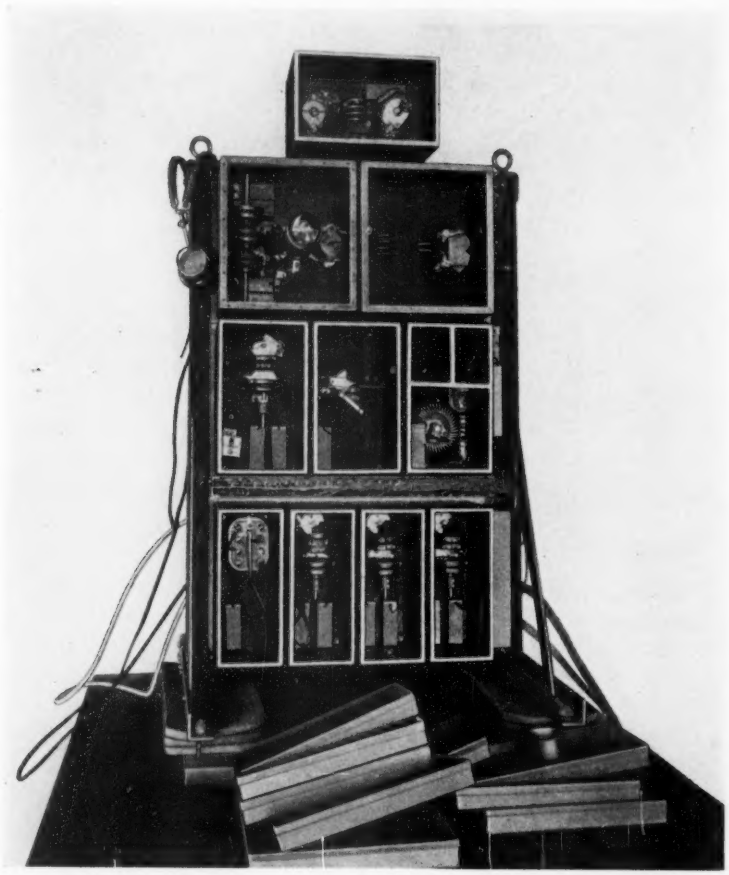

Fig. 1b—Rear view of measuring set with shielding covers removed.

ohms impedance is not easy to construct. A thermocouple was located at the antenna connection, and the resulting direct current was fed down the transmission line and filtered out by a choke coil—con-

[4] Sterba and Feldman, *Proc. I. R. E.*, vol. 20, p. 1163, Fig. 12; July (1932). *Bell Sys. Tech. Jour.*, July, 1932.

denser unit to operate the antenna meter. The antenna current was of the order of 0.6–0.8 ampere ordinarily.

For the entire northwestern half of the horizon the nearby Mt. Pleasant hills screened the country beyond from direct radiation components. The reception in these directions was thus entirely a diffraction phenomenon. Fig. 2 gives the result of a cross-country transit

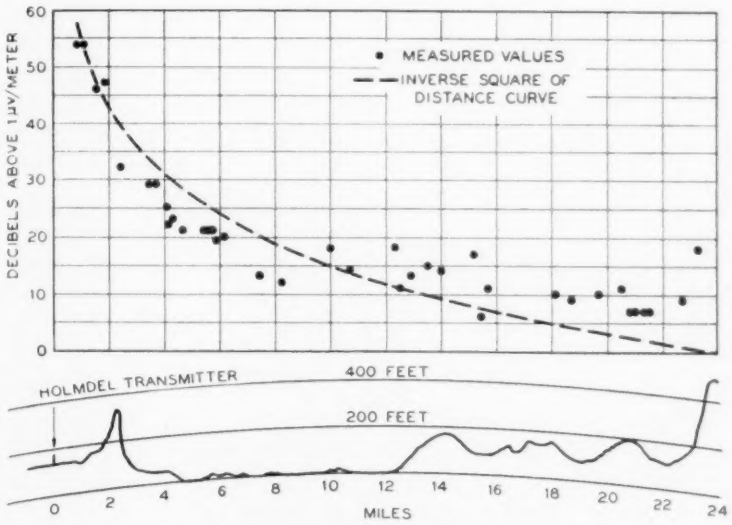

Fig. 2—Transmission along radial line from Holmdel laboratory to Watchtung Mountains.

out beyond these hills. The wave-length was 4.6 meters and at each point the field intensity was obtained by averaging over several maxima and minima. As closely as possible a fixed direction was maintained. The field strengths were first observed as decibels left in the set attenuator and were afterwards corrected as described in a later paragraph. An inverse square of distance curve is drawn in for comparison purposes. Up to the hills a direct plus a reflected radiation component constitutes the transmission; back of the hill a diffraction phenomenon occurs. The transmitting antenna was vertical and the radiation was received by a short rod antenna projecting through the top of the light truck carrying the receiving set.

The observed values are rather erratic, and later experience has shown that this irregularity may be expected for measurements taken on or at the ground level and that it is due to an almost universal and highly irregular standing wave pattern.

Standing Wave Patterns

This standing wave pattern has not yet been sufficiently studied. It is easy, by driving the receiver car sufficiently slowly, to show that some of the "fringes" are due to reradiation from individual trees along the roadside. Vertical metallic guy wires and other metallic structures are equally good reradiators. The type of interference pattern which would be expected from a reradiating tree is shown in Fig. 3, and this is

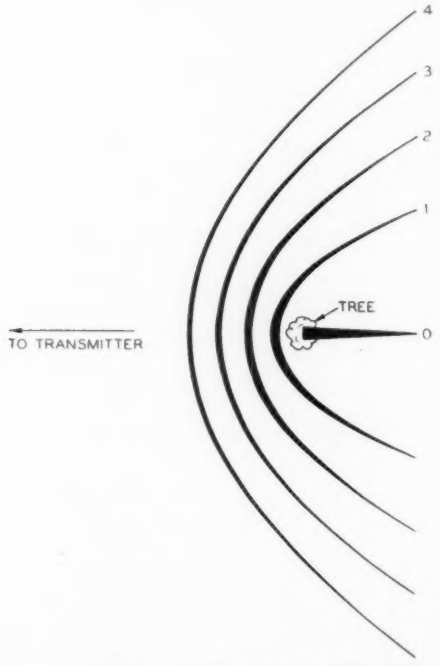

Fig. 3—Standing wave system surrounding a tree. Phase shift on reflection 180 degrees. Curves show first five lines of minimum field.

substantially what was found by driving the receiver car around isolated trees. But in general the pattern is not as simple as this and, what is of more importance, the maximum/minimum ratio may run as high as fifty to one. A road bordered with trees gives a very rough pattern.

An open field of some 20 acres extent was available about a mile (1.6 kilometers) from the transmitter. This field lay on a "bench" about 90 feet (27.5 meters) above the Holmdel laboratory ground

level; the bench slope, and a strip of woods lay immediately in front of the field and on the transmitter side. Covering the entire field was an irregular "fringe" system, the fringe spacing varying something like one to four times the wave-length (4.6 meters). By driving the receiver car back and forth across the field a particularly high field intensity line was located and marked for perhaps a hundred yards (91.5 meters). The car was then placed exactly on the line and the receiving set meter carefully watched for any change in the location of this line. No noticeable shift occurred, and the line was checked on the following day and again several days later. A car movement of one foot (30.5 centimeters) was immediately detected by the receiving set meter. It was necessary each time to drive the car in straight

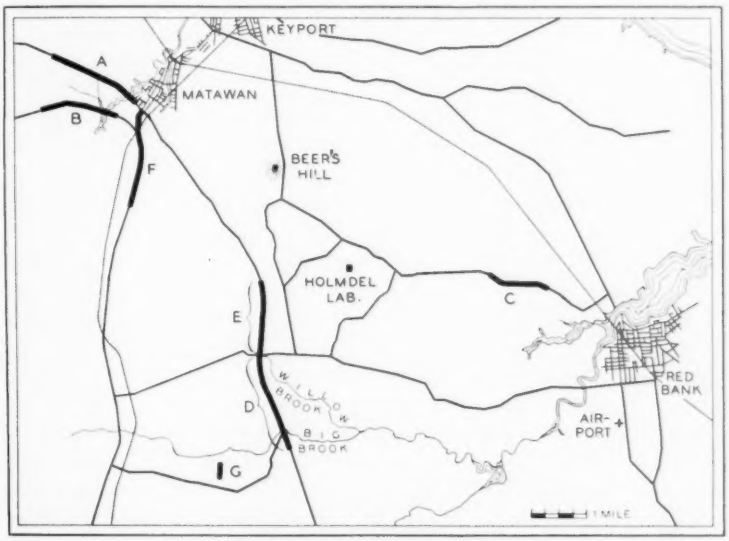

Fig. 4—Map of Holmdel region.

parallel lines since the polar receiving characteristic of the combination of metal car body and radio receiver was not a circle. Opening a car door immediately altered this characteristic. This high field intensity line was not a straight line, being a bit "snaky," and it suffered a shift varying from 2 to 15 feet (0.6 to 4.6 meters) when the transmitting wave-length was changed from 4.6 to 3.7 meters.

These standing wave patterns subside on cleared hilltops and need not therefore seriously affect actual ultra-short-wave channels. They have not been studied by us at distances much exceeding 10 miles (16

kilometers) from the transmitter but they no doubt exist at all ranges. It is certain that both reradiating trees and ground irregularities produce them. By mounting the receiving set with manual recorder in a light truck equipped with superballoon tires we have been able to obtain continuous records of field strength as the truck is slowly (2 to 5 miles per hour) driven along the roads in the neighborhood of the transmitter. Seven of these records and a map of the country are given in Figs. 4 to 6. The records are made by recording the variation in set gain necessary to hold the set output constant versus the distance traversed. They have all been reduced to decibels above one microvolt per meter. The transmitter site was the Beer's hill one, later described, and the records were obtained this year. They are all for a vertical transmitting antenna; the corresponding results for a horizontal antenna are complicated by the almost universal presence of horizontal conductors along the roads. These wires scarcely affect vertical transmission.

As the map indicates, the seven records were taken at distances from two to six miles (air line) from the transmitter. Six were taken along public highways, the seventh was taken in a private field. Of the six, five were taken along roads substantially radial to the transmitter, the sixth along a tangential road.

Record "*A*" was taken along a new road running northwestward from Matawan, N. J. The direction of feed of these records is from left to right, and the arrow indicates that the car was driving northwestward, away from the transmitter. This is a radial road and, being new, is not bordered by straggling trees. It covers 1.7 miles of gently rolling country without steep cuts.

A correspondence of field intensity with topography is to be expected, the favorable addition of direct and reflected radiations being facilitated on slopes facing towards the transmitter and being militated against on slopes facing away from the transmitter. Since the slopes are often short this will put the field maxima near their tops and this is what is found. This record shows this effect perhaps better than any of the others; a profile of the land is included. Profiles are not drawn in on the remaining curves as the country is mostly so irregular that profiles are misleading. Where this topographical coincidence occurs it is noted on the curve.

As the set is carried past them, trees, wired houses, and the like make their presence known on the record. Extended areas of trees, as woods and orchards, usually involve a marked absorption of signal intensity which, however, does not extend much beyond their boundaries.

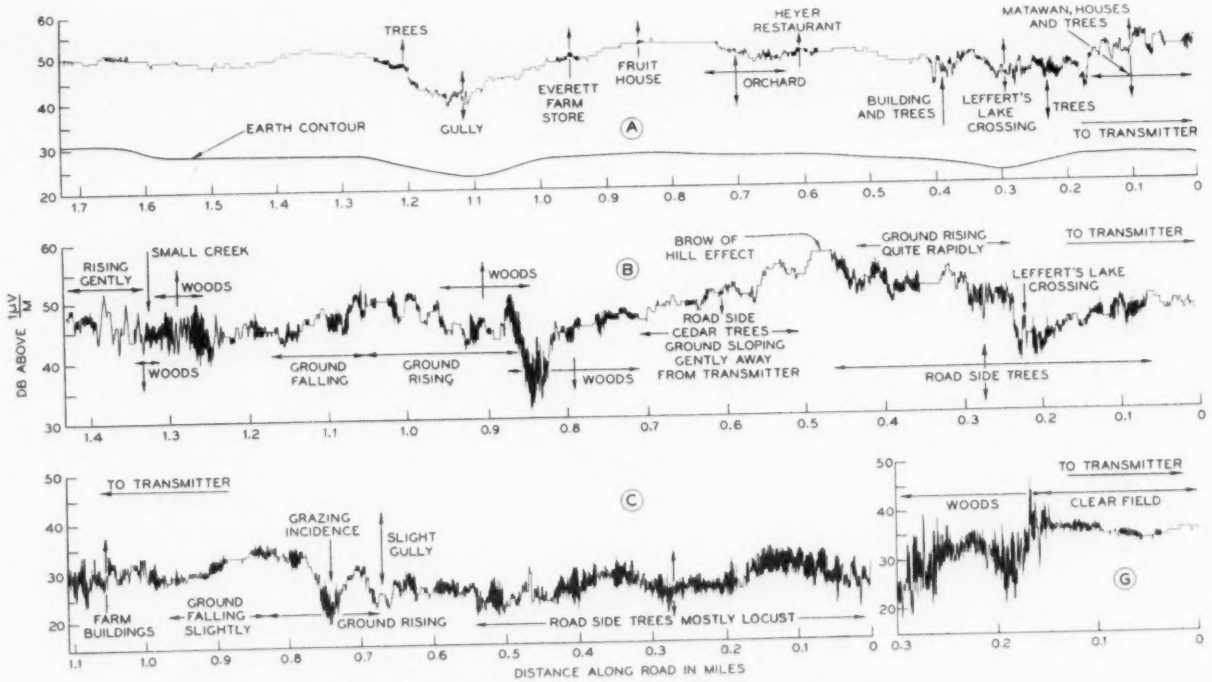

Fig. 5—Four diffraction patterns taken along lines radial to transmitter.

"A" radial 2.54–4.25 miles from transmitter 8–25–'32.
"B" radial 2.94–4.29 miles from transmitter 6–23–'32.
"C" radial 4.25–5.3 miles from transmitter 6–16–'32.
"G" radial 6–23–'32.

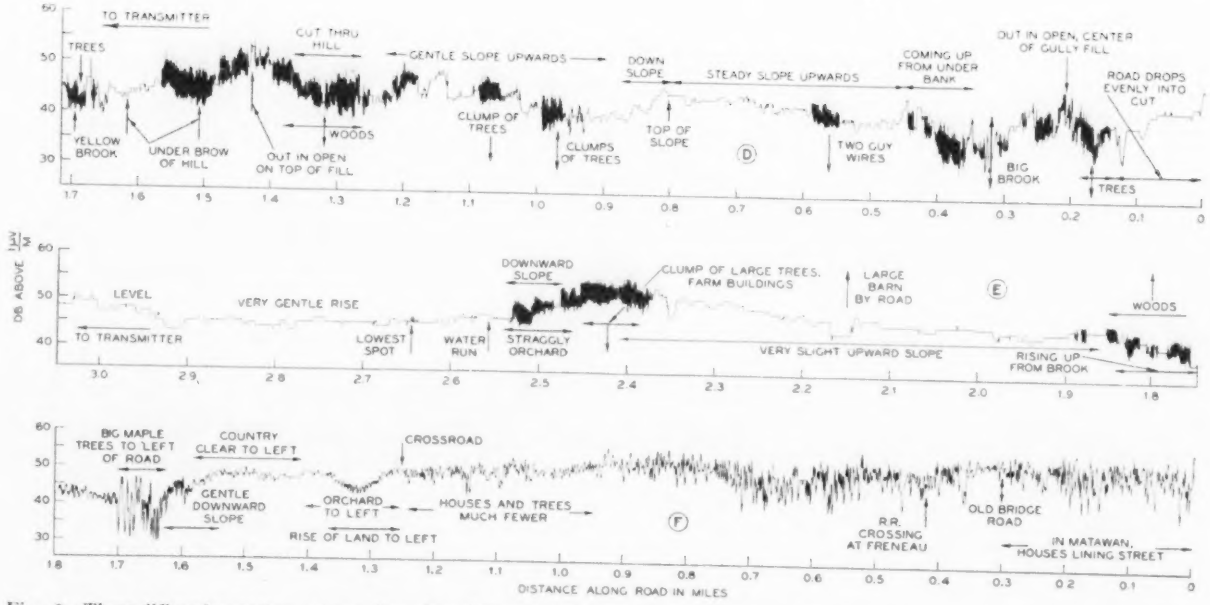

Fig. 6—Three diffraction patterns, two taken along lines radial to transmitter, one along a line perpendicular to transmitter direction.

"D" radial 3.28–4.95 miles from transmitter 6–15–'32.
"E" radial 2.0 –3.28 miles from transmitter 6– 8–'32.
"F" tangential 2.6–2.7 miles from transmitter 8–25–'32.

Record "*B*" was taken along another radial road not far distant and roughly parallel to that of "*A*." This is an old road and has the usual string of nondescript trees along the road edges. These trees roughen up the pattern always, sometimes badly, but the ground slope changes can usually be identified (compare with the previous record). The marked maximum at 0.47 mile, where direct and reflected radiations add favorably, is the equivalent of the "brow-of-hill effect" found for short waves.[5] The very marked undulation at 0.85 mile is apparently due to the overlapping of two extensive patches of woods which here, for a short distance, blanket both sides of the road. In the written comment on the records the direction of the arrows indicates the side of the road on which the objects mentioned lie.

Record "*C*" is that for a radial road southeast of the transmitter. This is an old tree-bordered road and has several turns in it. The trees are mostly locust and there are quite a few vertical guy wires on the power and telephone poles. In the pattern these guy wires are usually indistinguishable from trees. The correspondence with topography appears in several places, but there is an unexpected and deep minimum at 0.74 mile. There are no trees or other objects to explain this, and our feeling is that it is due to a topographical peculiarity whereby the direct and reflected radiations nearly cancel. The road is rising here, in a cut about four feet deep, and in the direction of the transmitter the ground billows up so that one can visualize the explanation given.

Records "*D*" and "*E*" were taken along a new radial road (an extension of "*A*," in fact New Jersey highway No. 34). At the right of "*D*" the road starts downward towards the transmitter at the same time entering a cut. There are no trees and the resulting record is a fast dropping smooth one. Farther on the marked effects of a pair of guy wires and some clumps of trees can be seen; the absence of other trees giving an undisturbed background to work against. A favorable slope, or "brow-of-hill" effect, is seen at 1.43 miles. The latter part of the record is through a succession of cuts and fills, with trees about, and the record is correspondingly rough.

Record "*E*" continues the previous record. There is an initial rise at the start, due to rising ground, and woods to the right roughen up the pattern. From here on to the end there is a slow ground rise, a slight fall, and a final rise. At the center of the stretch is an isolated clump of trees with farm buildings and a straggly orchard below. The contrast between the treeless stretch and that with trees is very marked. The effect of the trees begins suddenly, at about 150 feet in from the edge of the grove.

[5] Potter and Friis, *Proc. I. R. E.*, vol. 20, p. 699; April (1932).

Record "*F*" is that of a tangential run along the old Matawan-Morganville road. Starting in the town of Matawan, with houses and trees about, the pattern irregularities subside slowly, as these objects decrease in number, up to 0.95 mile. At 1.26 miles a rise of ground to the left (transmitter side) is covered with an orchard. Apparently the unfavorable slope is more potent than the trees in reducing field intensity, as the field falls and rises more in accord with this land rise than with the orchard. At the end of the record some large old maples on the transmitter side of the road roughen up the pattern very markedly.

Record "*G*" is a short run taken on a private road where the car was run in from a cleared field into woods.

Field Fluctuations from Moving Bodies

It is well known that the motion of conducting bodies, such as human beings, in the neighborhood of ultra-short-wave receivers produces readily observable variations in the radio field. This phenomenon extends to unsuspected distances at times. Thus, while surveying the field pattern in the field described above, we observed that an airplane flying about 1500 feet (458 meters) overhead and roughly along the line joining us with the transmitter, produced a very noticeable flutter, of about four cycles per second, in the low-frequency detector meter. We then made a trip to the nearby Red Bank, N. J., airport, distant about $5\frac{1}{2}$ miles (8.8 kilometers) and observed even more

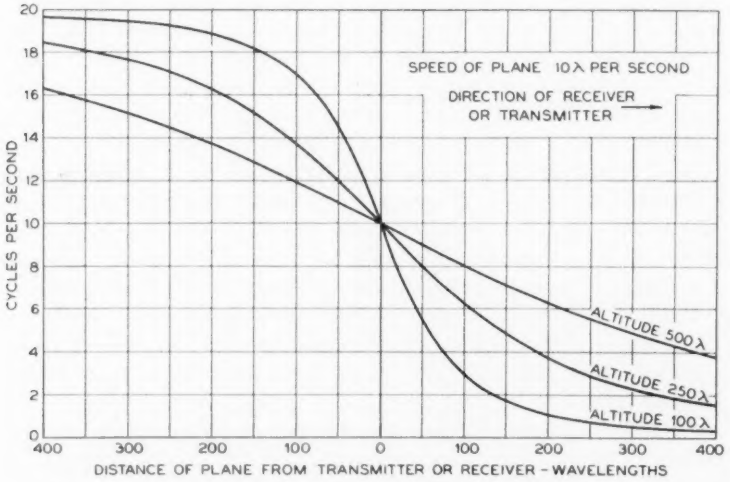

Fig. 7—Beat frequencies produced by reflection from a moving airplane.

striking reradiation phenomena. Nearby planes gave field variations up to two decibels in amplitude, and an airplane flying over the Holmdel laboratory and towards this landing field was detected just as the Holmdel operator announced "airplane overhead." These were all fabric wing planes. If the reradiation field to which such an airplane is exposed is of inverse distance amplitude type while the directly received ground fields are of more nearly inverse distance square type, as in Fig. 2, it is easy to see that at five miles an overhead airplane is exposed to a field intensity about ten times (20 decibels) that existing at the ground, and for ordinary airplane heights a high energy transformation loss in the reradiation process can occur and still give marked indications in the receiver meter. This airplane reradiation was noticed at various subsequent times, sometimes when the airplane itself was invisible. A set of theoretical beat frequency versus distance curves are given in Fig. 7.

Air-Line Transmission

While ordinary ultra-short-wave transmission is complicated by local reradiations and diffraction phenomena these should become relatively innocuous for favored locations such as hilltop-to-hilltop transmissions with the air-line path between them clearing all intervening obstacles. Here the presence of fading, day-to-night changes in transmission, amount of static interference, and the rôle of the earth-reflected radiations should be determinable. After some days of rough surveying such a pair of hilltops was found 39 miles (63 kilometers) apart. We would have preferred a greater distance but none such could be located with certainty, with one of the hills necessarily local.

The transmitter was mounted on this local hilltop, Beer's Hill, two miles (3.2 kilometers) air line to the north northwest of the laboratory. The apparatus consisted of a 40-foot (12.2-meter) lattice mast with nonmetallic guys, mounting a half-wave linear antenna which could be rotated between a vertical and a horizontal position. A low impedance (246-ohm) transmission line, similar to the one earlier described, carried the ultra-short-wave current from the generator shack at the foot of the mast to the antenna itself. The termination and method of antenna current indication were as described for the Holmdel laboratory transmitter. The hilltop altitude (U. S. Bench Mark) was 343 feet (104.6 meters) and the antenna was thus 383 feet (116.8 meters) above sea level.

The receiver site was located on a hill spur on the P. K. McCatharn farm 2½ miles north of Lebanon, N. J., and at an altitude of 750 feet (228.5 meters). Taking the altitudes from the New Jersey geological

survey maps and correcting for earth curvature gives the profile map of Fig. 8, where it is seen that the air line clears the intervening country everywhere by 200 or more feet (61 meters). We were unable to check this by direct optical observations as no sufficiently clear day occurred during our tenure of the Lebanon site but we were able to identify a neighboring hill of about the same altitude (Mt. Cushetunk) and we have no doubt that an air-line path existed.

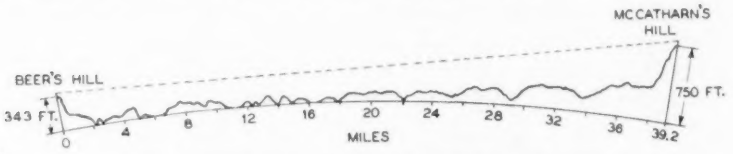

Fig. 8—Profile map. Beer's Hill to McCatharn's Hill.

If we imagine a transmitting and receiving antenna pair located above the earth's surface it is easy to see that the received radiation will consist of a direct plus a reflected component. If now we complicate matters by adding a pair of hills to support the antennas we shall add a pair of reflections from the slopes of the two hills to the initial two radiation components. A final random corrugation of the earth and we have the actual Holmdel-Lebanon situation. The conditions under which the first reflection occurs, practically grazing incidence, with the earth irregularities very small compared with the optical path length, make it very certain that this reflection will substantially survive the corrugation; the proximity of the hills to the antennas themselves ensures the presence of the second pair of reflections. The actual transmission should thus consist of a direct component plus a three-surface set of major reflection components, together with a background of scattered and diffracted radiation arising from the corrugations of the earth's surface. For an extreme path length the lens effect of the earth's atmosphere, decreasing in density upwards and thus refracting the entire radiation ensemble downwards, will produce a path deviation which cannot be neglected.[6]

A verification of this radiation picture should be possible. The hillside reflection components can be demonstrated by separately raising and lowering the two antennas. Inasmuch as the reflections occur nearby, only a small movement of an antenna is required to vary the path difference between the direct and reflected rays by half a wavelength and thus vary the received signal intensity through a maximum-to-minimum, or reversed, cycle. The earth reflection occurs sub-

[6] Pedersen, "Propagation of Radio Waves," chap. X, p. 150. The importance of this refraction effect has most recently been pointed out by Schelleng, Burrows, and Ferrell, companion paper in this issue of *Bell Sys. Tech. Jour.*

stantially halfway between the antenna sites, and very great altitude changes become necessary to exhibit a maximum-to-minimum cycle. This reflection component cannot thus be demonstrated from two hill locations such as we had; but one of the hills together with a receiver carried by an airplane will suffice. We were able thus to demonstrate all the three main reflections.

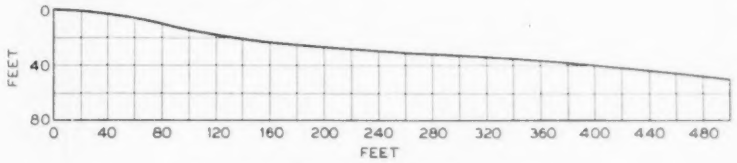

Fig. 9—Profile map of McCatharn's Hill.

Fig. 9 gives a profile of the McCatharn Hill along the radio transmission line and Figs. 10 and 11 show the received field strength

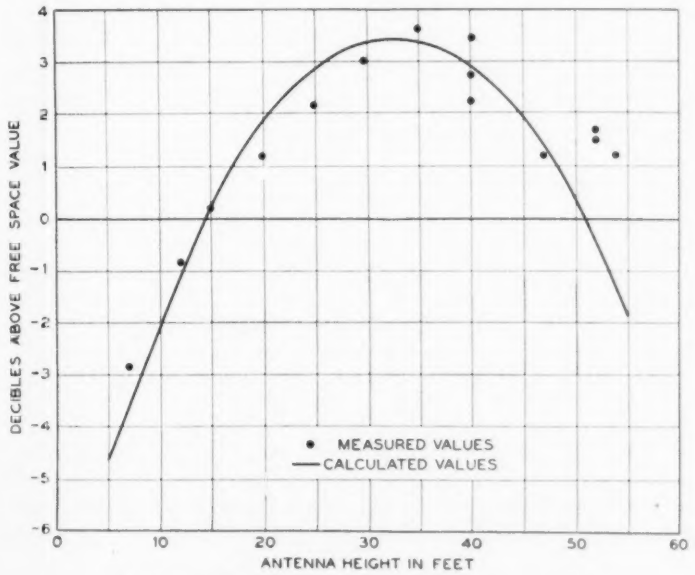

Fig. 10—Local reflection at McCatharn Hill. Vertical polarization $\lambda = 4.08$ meters.

variation as the antenna was raised and lowered [7] for both horizontally and vertically polarized radiations. Assuming this hill to be a medium

[7] The receiving set, in the truck, was located on the hilltop after making sure that stationary diffraction fringes were of negligible amplitude. By permission of

of dielectric constant 10 and resistivity 10,000 ohms per cm. cube, and to have a plane reflecting surface inclined to the horizontal at an angle of 5.9 degrees, reception curves for an antenna raised and lowered over

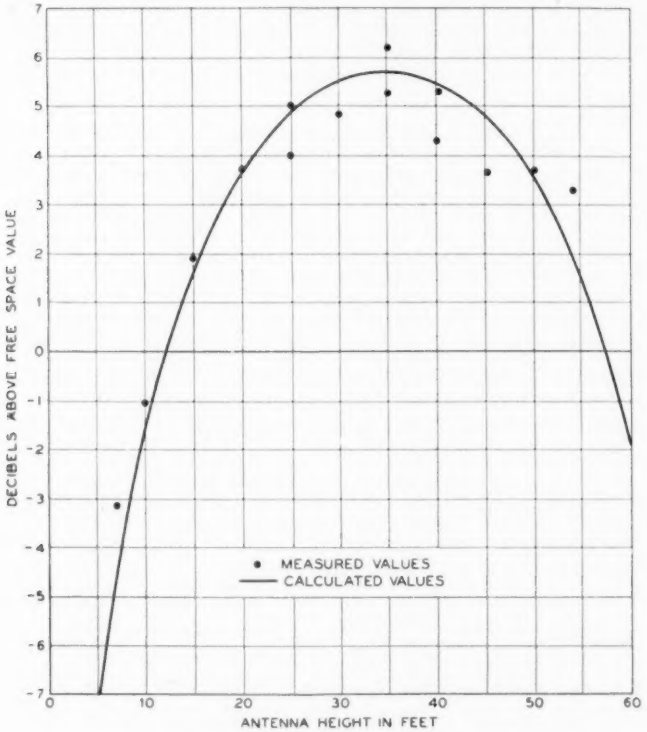

Fig. 11—Local reflection at McCatharn Hill. Horizontal polarization $\lambda = 4.39$ meters.

it have been calculated and are compared with the experimental results. These measurements, being relative only, have been adjusted to best coincidence by adding the necessary decibels. The resulting fit is fairly good. A quantitative comparison between theory and experiment is later given.

---

the owner, some trees below the hill were cut down to clear the radiation path. The antenna structure was a 40-foot lattice mast with a boom carrying the antenna itself and extending fifteen feet above the mast top. The transmission line was incandescent lamp cord (a twisted pair of rubber and cotton insulated conductors) and was tied to boom and mast so as not to swing. It had a measured loss (erected and measured at Holmdel) of 0.1 decibel per foot. The boom swung in an arc in a plane perpendicular to the line of transmission. No evidence of a rotation of the plane of polarization was observed.

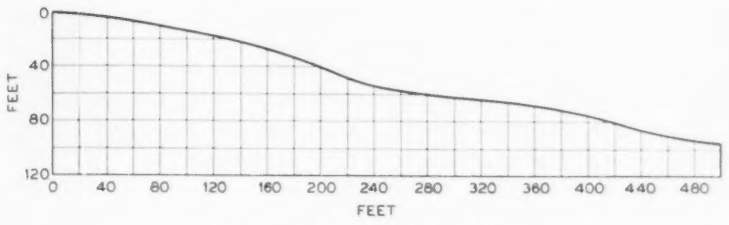

Fig. 12—Profile map of Beer's Hill.

With a sufficiently plane slope a maximum-to-minimum field comparison should yield a dependable value of the amplitude of the reflection coefficient since the other two reflection components (transmitter hill and intermediate earth surface) are not rapidly varied by such a limited change in receiving antenna height. Unfortunately the antenna could not be elevated above 55 feet (16.8 meters), and with the moderate hill slope existing, this was insufficient to reach the first above-ground field minimum.

The intermediate earth surface reflection component, at this near-grazing incidence, acts to reduce the total received field, and it is important to obtain an idea of how great this effect is likely to be. It is necessary to rely on the accuracy of the topographical maps as issued

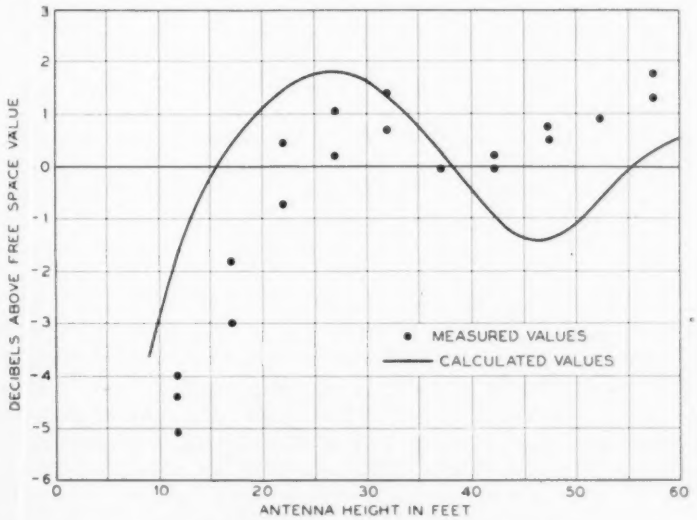

Fig. 13—Local reflection at Beer's Hill. Vertical polarization $\lambda = 4.45$ meters.

by the state of New Jersey but a conservative use of them indicates that at a wave-length of 4.45 meters a phase difference of about 198 degrees exists between the direct and reflected components and the resultant field should be about 31 per cent of that of a simple inverse distance transmission. (The effect of air refraction is included.) This is adequate for good reception at the McCatharn Hill.

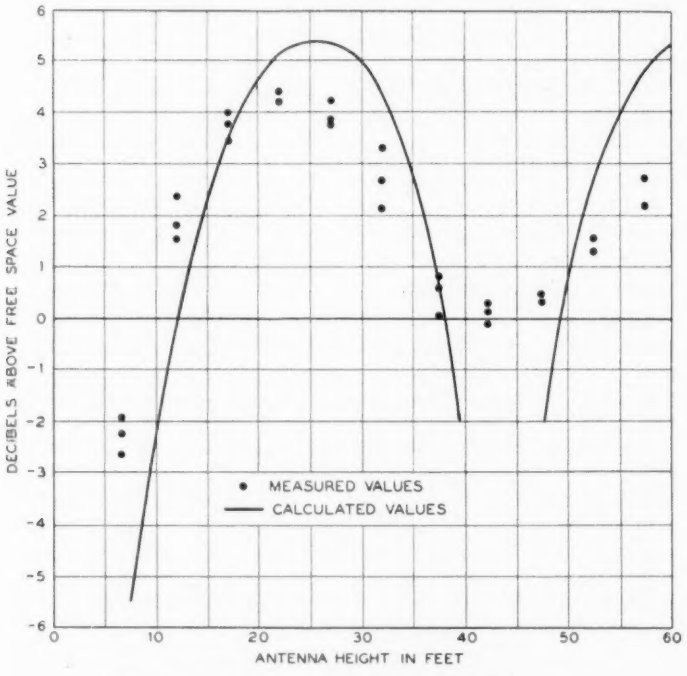

Fig. 14—Local reflection at Beer's Hill. Horizontal polarization $\lambda = 4.45$ meters.

Fig. 12 gives a profile of Beer's Hill along the line of transmission, and Figs. 13 and 14 the McCatharn Hill reception as the transmitting antenna was elevated. The hill slope is steeper here (Beer's Hill) and the curves obtained for the original 40-foot (12.2-meter) structure having indicated that the first off-ground field minimum could be reached with a little more height, an additional 20-foot section was added to the lattice mast making it 60 feet (18.3 meters) high. The difficulty of handling a low-loss bare wire transmission line, as the height was varied, caused us to substitute a twisted pair incandescent

lamp cord for it. In raising and lowering the antenna this transmission line was simply permitted to pile up on the ground. The antenna ammeter showed only small current variations as this coil was handled or pushed about. We originally had some doubts as to whether this hill would give a clean-cut reflection since the surface in the receiver direction was somewhat undulating and had a gully with trees beginning some 200 feet down the hillside. However, as the results indicate, a fairly definite reflection component is produced.

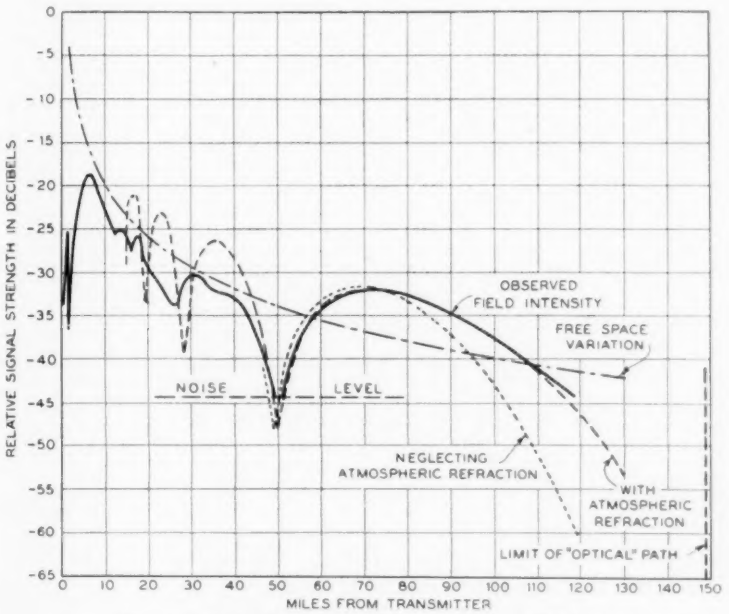

Fig. 15—Flight from transmitter. Altitude—8000 feet; wave-length—4.3 meters, June 24, 1931.

The dots in Figs. 13 and 14 are observed values, the full lines are theoretical curves. These latter were obtained by taking the hill constants the same as for the McCatharn Hill, but the hill itself was not assumed to be a plane. Instead, by graphical plotting from the hill contour, the tangent plane for each antenna height was located and used for the calculation for that height only. The resulting curve is a somewhat better fit than is obtained by averaging the hill to a common plane.

This hill surface, as stated earlier, is a rather poor fit to a plane (the profile cross section shows the hill up too favorably) and has quite a

few trees located on or about the reflection area corresponding to the higher antenna positions. The result is particularly noticeable for the vertically polarized transmission where the fit between observation and experiment is poor. This experiment was later repeated with the same results. The conclusion follows that while the oscillatory character of the field intensity curves indicates a definite local reflection component, it is not as simple as the one arising from a smooth surface by plane optical reflection.

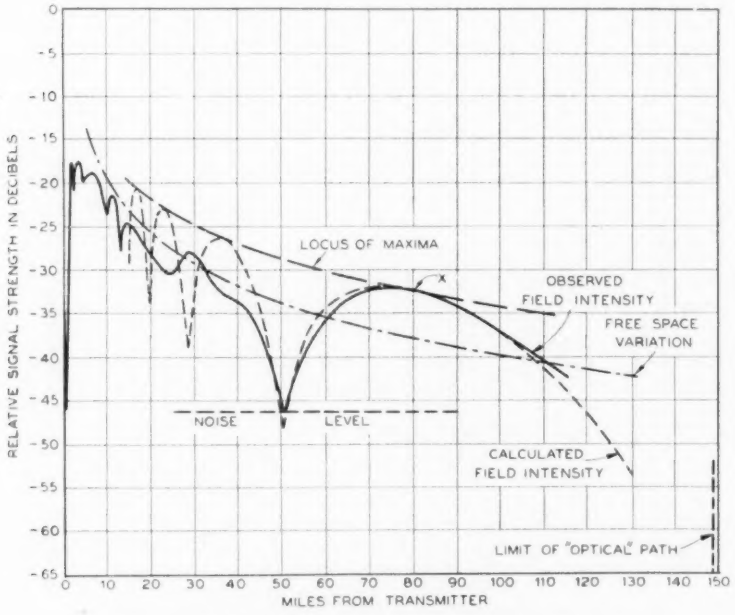

Fig. 16—Flight toward transmitter. Altitude—8000 feet; wave-length—4.3 meters, June 24, 1931.

The middle distance reflection was clearly established by airplane observations. For these only vertically polarized radiation was used, and a simple vertical rod antenna was thrust out of the airplane cabin ceiling. This limited the maximum range which was attained, but antennas of greater effective height were difficult to construct. This plane was the Laboratories' Ford trimotor, and we are indebted to Mr. F. M. Ryan and his staff for their cooperation in this work. The manual recorder already mentioned was used throughout the runs, which were made by flying directly from Beer's Hill to Easton, Pa., and

then veering slightly to the left to follow the main New York-to-Chicago airplane route. Flights were made at 8000, 5000, 2500, and 1000 feet (2440, 1525, 763, and 305 meters) above sea level, and the results are given in Figs. 15 to 20 inclusive. Fig. 21 gives a map of the country.

In these figures the experimental curves are supplemented by theoretical ones, these latter being calculated by assuming the earth at the reflection point to be equivalent to a plane surface medium of a dielec-

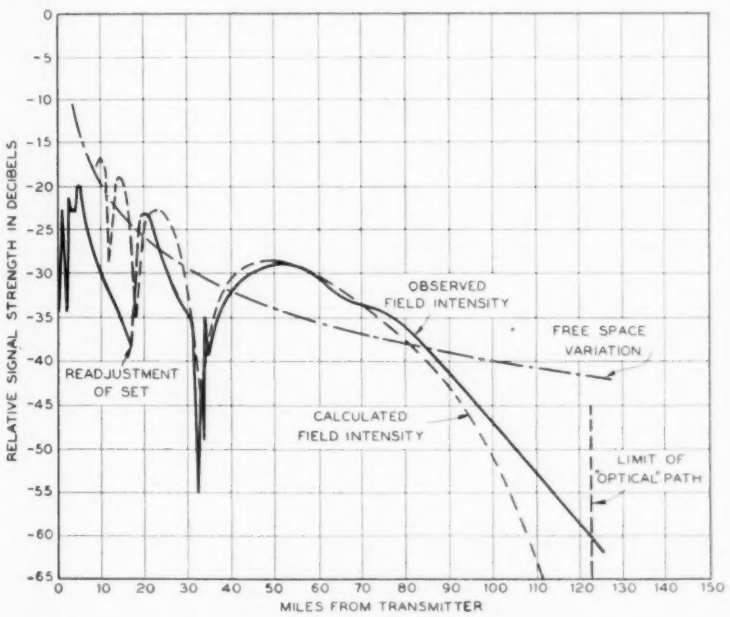

Fig. 17—Flight from transmitter. Altitude—5000 feet; wave-length—4.3 meters, June 29, 1931.

tric constant 10 and a resistivity of 10,000 ohms per cm. cube and 100 feet (30 meters) above sea level. This point, for the outermost deep minimum, varied in location from 1.5 miles out, for the 1000-foot flight, to 2 miles out, for the 8000-foot flight, with corresponding angles of incidence of 88 and 88.5 degrees. The area involved is fairly level and open. The earth's curvature is taken into account and refraction corrections are applied using the Schelleng, Burrows, and Ferrell formula. As shown in Fig. 15 the fit at the extreme distances is considerably improved by this latter correction, thus indicating its validity. The deep

and outermost minimum is due to the middle distance reflection with a 540-degree phase difference. It is unmistakable and definite. The minima corresponding to phase differences of odd numbers of 180-degree angles greater than three are not so clear cut. It is here that the ground corrugations will have the greater destructive effect.

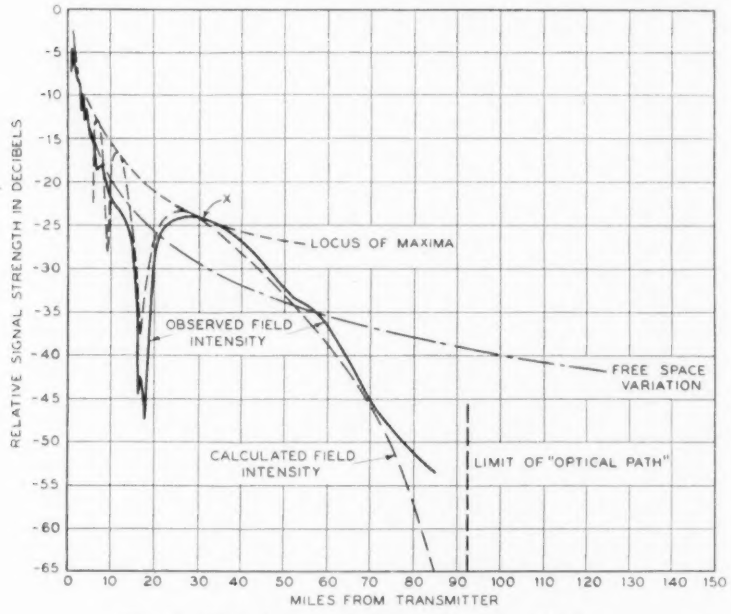

Fig. 18—Flight from transmitter. Altitude—2500 feet; wave-length—4.3 meters, June 26, 1931.

The method of calculation is more fully explained in Appendix I, and the effect of a possible diffraction by Mt. Cushetunk in Appendix II. In the 8000-foot curves ignition noise masked the deep outermost minimum, and in the 1000-foot curve it is poorly defined, but it appears well marked in the 5000- and 2500-foot curves, and is roughly 10 decibels below the theoretical value. This minimal depth corresponds to a reflection coefficient of about 0.92 for this angle of incidence (88.4 degrees); the theoretical reflection coefficient is 0.8.

General Observations

During these experiments no static was observed. It has since been found by Mr. Jansky of the Laboratories that local summer thunderstorms produce noticeable static interference and that such storms may

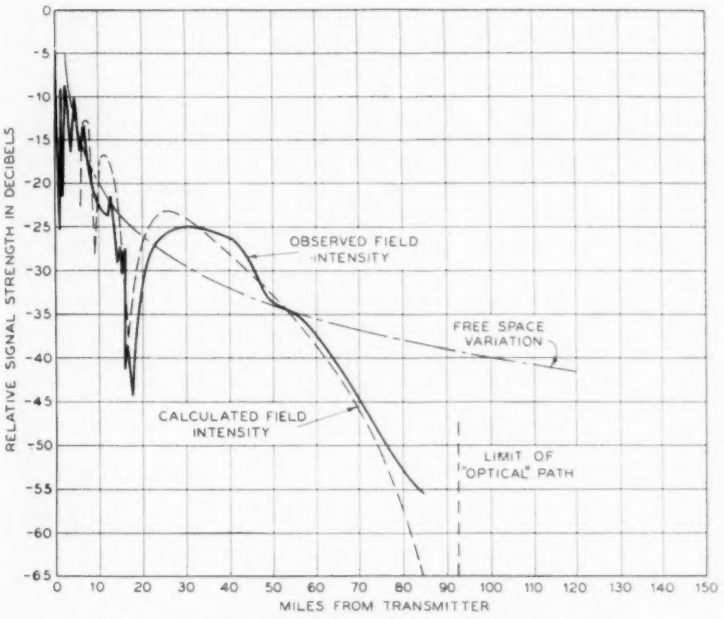

Fig. 19—Flight toward transmitter. Altitude—2500 feet; wave-length—4.3 meters, June 26, 1931.

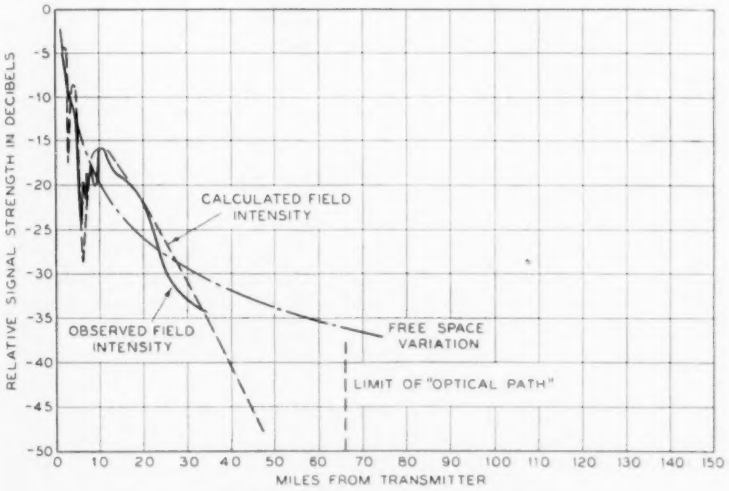

Fig. 20—Flight toward transmitter. Altitude—1000 feet; wave-length—4.3 meters, June 29, 1931.

sometimes be detected up to a distance of 50 miles (81 kilometers). This interference is, however, very much less than on short-wave reception.

One continuous transmission test from Holmdel and Beer's Hill to Lebanon was made April 24 and 25, 1931, extending through the night and over both the sunset and sunrise periods. The Beer's Hill transmission was horizontally polarized, the Holmdel transmission vertically polarized. The wave-lengths were 4.17 and 4.5 meters, respectively. Quarter-hourly observations were taken during the night, and observations were made every five minutes through the sunrise and sunset periods. No signal variations or abnormalities were observed, and harmonics of short-wave stations, though looked for, could not be

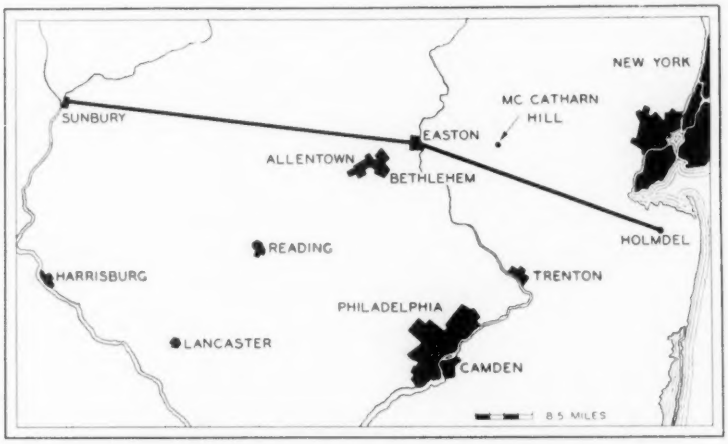

Fig. 21—Map of line covered by airplane flights.

heard. We have since observed these harmonics, for high power stations, but not from any great distance.

The Beer's Hill transmitter power during all our tests never exceeded 6 watts, and gave an ample signal intensity at Lebanon, in spite of the 198 degree phase difference of the middle distance reflection component. Telephone transmission was uniformly good.

Appendix I

Calculation of Airplane Reception Curves

The resultant field strength at a point in the line of flight (Fig. 22) is

$$E_r = \frac{E_0}{D}\left(1 + Ke^{i[\theta+(2\pi/\lambda)(r_2-r_1)]}\right) \qquad (1)$$

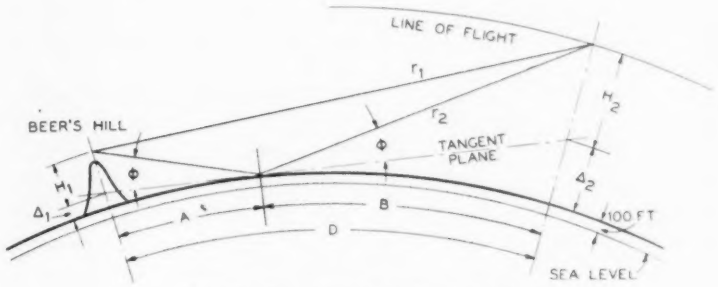

Fig. 22—Geometry of airplane reception.

where,

E_0 = the free space field at distance of 1 mile

K = amplitude change at reflection

θ = phase change at reflection

(K and θ are functions of the angle of incidence and the ground constants)

$(r_2 - r_1)$ = the path length difference between direct and reflected rays.

$$(r_2 - r_1) = \frac{2H_1H_2}{D} = \frac{2AB \tan^2 \Phi}{D} \tag{2}$$

provided H_1 and H_2 are small in comparison with D.

H_1 and H_2 are the heights of transmitter and receiver above the plane tangent to the earth at the point of reflection.

The height of the tangent plane above the earth's surface is

$$\Delta_1 = R\left(-1 + \sqrt{1 + \frac{A^2}{R^2}}\right) = \frac{A^2}{2R} \text{ (app.)} \tag{3}$$

and,

$$\Delta_2 = \frac{B^2}{2R}.$$

R is the radius of the earth, which, due to atmospheric refraction, is taken to be 5260 miles,[8] an increase of 33 per cent over the actual radius. $(H_1 + \Delta_1)$ is always 280 feet, the height of the transmitting antenna above the reflecting surface, which, in the case at hand, is about 100 feet above sea level.

$(H_2 + \Delta_2)$ is constant for any flight at constant altitude.

For any value of A, H, and hence tan Φ may be calculated and plotted as in Fig. 23. In this figure B is also plotted, for a flight at 8000 feet, against tan Φ. The total distance D is obtained by adding

[8] Schelleng, Burrows, and Ferrell paper, this issue of *Bell Sys. Tech. Jour.*

A and B at constant tan Φ. Thus, for any distance of the plane, we can read from the curves the values of A, B, and tan Φ, and can calculate the path difference $(r_2 - r_1)$ by equation (2).

In this manner, the theoretical reception curves, which are given in Figs. 15 to 20 (dotted curves), were calculated for flights at 8000, 5000, 2500, and 1000 feet. The ordinate "Relative Signal Strength—Decibels," is 20 $\log_{10} E_0/E_r$, and gives the received signal strength in decibels below the field strength in free space at a distance of one mile from the transmitter.

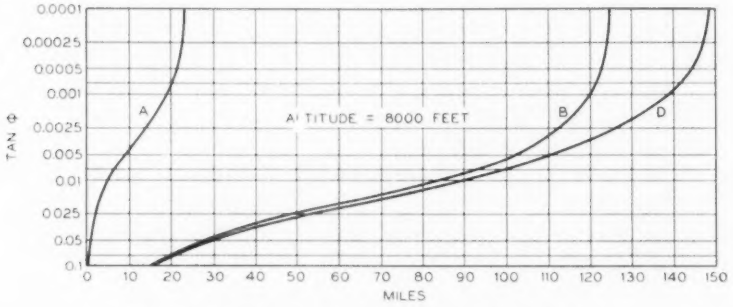

Fig. 23—Sample curve for calculating airplane results.

Since the scale of the observed reception curves is unknown, they are superimposed upon the calculated ones by causing the maxima of the observed curves to coincide at some point with the theoretical loci of maxima (see for example, the points marked "x" in Figs. 16 and 18).

In the limit, as grazing incidence is approached, the theoretical reception approaches zero. In equation (1), K becomes unity and θ becomes 180 degrees and the path length difference $(r_2 - r_1)$ becomes zero. The observed field at distances greater than those required for grazing incidence is a diffraction one.

Appendix II

Diffraction Calculations

In Fig. 25 the data of Fig. 17 for the 5000-foot airplane flight are compared with a theoretical curve which has been corrected from that of Fig. 17 by considering a possible diffraction around Mt. Cushetunk. This hill, 650 feet high, is 36 miles from Beer's Hill along the line of flight, and is the first major obstruction to an optical path at the greater airplane distances. For this calculation the points of reflection, angles of incidence, and path length differences are determined in the manner described in Appendix I, just as if the hill were absent. The

hill is then introduced in the picture and, considering it as a straight edge, its effect on both direct and reflected rays is calculated. (See Fig. 24.)

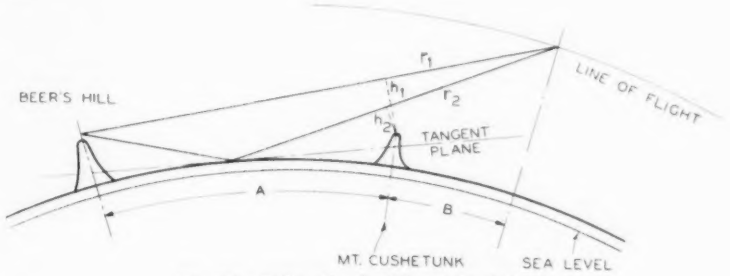

Fig. 24—Diffraction by Mount Cushetunk.

The resultant field at the receiver is then,

$$E_r = \frac{E_0}{(a+b)}\left[F_1 + KF_2 e^{i[2\pi/\lambda(r_2-r_1)+\theta+\beta_2-\beta_1]}\right] \tag{4}$$

where,

F_1 = amplitude change in the direct ray due to diffraction
F_2 = amplitude change in the reflected ray due to diffraction
β_1 = phase change of the direct ray produced by diffraction
β_2 = phase change of the reflected ray produced by diffraction
K = amplitude change due to reflection at the ground
θ = phase change at reflection
E_0 = free space field strength at distance of one mile.

The amplitude factors F_1 and F_2 and the phase changes β_1 and β_2 may be calculated from the Fresnel integrals to the parameter "v" (see note at end), where

$$v_1 = h_1\sqrt{\frac{2}{\lambda}\left(\frac{1}{a}+\frac{1}{b}\right)}$$
$$v_2 = h_2\sqrt{\frac{2}{\lambda}\left(\frac{1}{a}+\frac{1}{b}\right)} \tag{5}$$

"h_1" and "h_2" are the heights of the direct and reflected rays above the straight edge.

"a" and "b" are distances from the straight edge to transmitter and receiver.

A comparison of Figs. 17 and 25 shows that by taking account of diffraction around Mt. Cushetunk better agreement of calculated and observed curves is obtained. However, at grazing incidence this simple theory is inadequate; in this case $F_1 = F_2$, $\beta_1 = \beta_2$, $K = 1$,

$\theta = 180$, and the resultant field strength is zero as in the reflection case treated above.

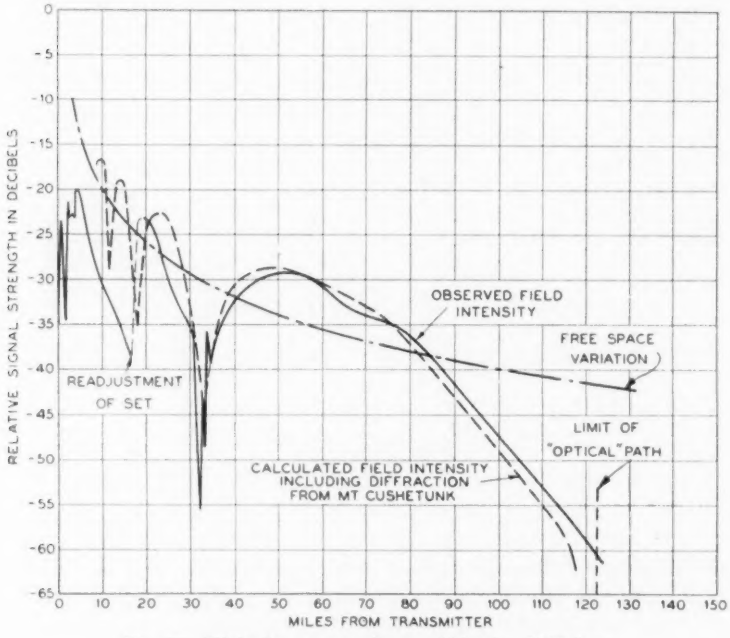

Fig. 25—Flight from transmitter. Altitude—5000 feet; wave-length—4.3 meters, June 29, 1931.

For large values of v_1 and v_2, that is for h_1 and h_2 large, F_1 and F_2 approach unity, and β_1 and β_2 approach zero. Equation (4) then reduces to the ordinary reflection case of equation (1).

Note: The ratio of the diffracted field strength to the field with edge removed is

$$Fe^{i\beta} = \frac{1}{\sqrt{2}}(C + iS)$$

where,

$$C = \int_{-\infty}^{v} \cos\frac{\pi v^2}{2}\,dv = \frac{1}{2} + \int_{0}^{v} \cos\frac{\pi v^2}{2}\,dv$$

$$S = \int_{-\infty}^{v} \sin\frac{\pi v^2}{2}\,dv = \frac{1}{2} + \int_{0}^{v} \sin\frac{\pi v^2}{2}\,dv$$

and,

$$F = \frac{1}{\sqrt{2}}\sqrt{C^2 + S^2}.$$

Appendix III

Quantitative Check on the Beer's Hill-McCatharn Hill Transmission

The Beer's Hill antenna was set at the height of 22 feet, and the receiver taken to the McCatharn Hill where it was operated out of a portable antenna 18 feet high. The optimum height here was 35 feet, and to reach it a more elaborate antenna would have had to be erected. The height used was just as good for a quantitative check as the optimum height. The effective radius of curvature of the earth's surface, corrected for air refraction, is taken as 5260 miles.

Intermediate Reflection Component

Beer's Hill antenna	365 feet above sea level
Intermediate reflection surface	67 feet above sea level
McCatharn Hill antenna	768 feet above sea level.

Referring to the equations of Appendix I, we have

$$\begin{cases} D = 39.2 \text{ miles} \\ A = 13.7 \quad " \qquad \tan \Phi = 0.00278 \\ B = 25.5 \quad " \end{cases}$$

and path difference between direct and reflected rays

$$= \frac{2AB \tan^2 \theta}{D} = 0.727 \text{ feet, or at } 4.45$$

meters wave-length an equivalent phase difference of 17.9 degrees results.

The angle of incidence is $90 - \Phi = 89.84$ degrees and hence

$K = 0.977$ for vertical polarization
$= 1.0$ for horizontal polarization
$\theta = 180$ degrees for both polarizations.

Adding the middle distance reflected component to the free space field "E_0", we obtain

$$E = E_0(1 + Ke^{i197.9^\circ})$$

and,

$$\begin{cases} \dfrac{E_v}{E_0} = 0.308 = -10.24 \text{ db} \\ \dfrac{E_H}{E_0} = 0.311 = -10.14 \text{ db.} \end{cases}$$

Local Hill Reflection Components

By the same process as for the above, and taking the geometry of Figs. 9 and 12 we obtain the site gains,

Beer's Hill reflection, vertical polarization + 1.5 decibels
Beer's Hill reflection, horizontal polarization + 5.1 decibels
McCatharn Hill reflection, vertical polarization + 0.68 decibel
McCatharn Hill reflection, horizontal polarization + 2.76 decibels

giving finally:

Vertical polarization transmission 8.1 decibels below free space transmission.

Horizontal polarization transmission 2.3 decibels below free space transmission.

Measured Field Values

The actual field intensity measurements were made using a split half-wave antenna with a transmission line which gave a total loss of about one decibel. Knowing the radiation resistance of antenna and grid circuit input impedance, the transfer voltage ratio could be calculated, and from the grid-to-grid over-all amplification of the receiver the voltage step-up for a given set output determined. The field intensity in microvolts per meter was thus obtained. The measured values were

Vertical polarization 21.6 microvolts per meter
Horizontal polarization 38.5 microvolts per meter.

The transmitter antenna current was 0.05 ampere, and the free space field to be expected at 39.2 miles equal to 47.5 microvolts per meter.

Summarizing the results we have:

Predicted vertical polarization + 8.1 db below free space field.
Measured vertical polarization + 6.8 db below free space field.
Predicted horizontal polarization + 2.3 db below free space field.
Measured vertical polarization + 1.8 db below free space field.

The measured values are thus within 16 and 6 per cent, respectively, of the calculated values, a satisfactory agreement.

Appendix IV

We have given three methods of field intensity measurement a trial. These are:

1. Comparison of field intensity with the mean first circuit noise voltage of the receiver. As shown by Johnson [9] the latter can be calculated, and by knowing the transfer voltage factor of the antenna-transmission line-input circuit combination and the difference in receiver set amplification for the two voltages the field intensity can be calculated.

2. Local oscillator comparison.[10] Here a local oscillator, with a

[9] Johnson, *Phys. Rev.*, vol. 32, p. 97 (1928).

[10] Described in the Schelleng, Burrows, and Ferrell paper.

small loop antenna is mounted in the neighborhood of the set, precautions being taken to keep ground reflected fields down in intensity. From loop current and physical dimensions and the oscillator-receiver spacing the resultant field is calculated and compared with the field to be measured.

3. Modified short-wave method. This is the method we have chiefly used and which appears at the moment to be most promising. From a knowledge of the impedances of antenna and receiver input circuits, the voltage transfer ratio from effective antenna input to resultant grid input can be calculated for optimum power transfer conditions, and to a good degree of accuracy. This factor, together with the antenna effective height and overall set gain, permits a measurement of the field intensity. In effect this is a variation of the Friis and Bruce method.

New Results in the Calculation of Modulation Products

By W. R. BENNETT

A new method of computing modulation products by means of multiple Fourier series is described. The method is used to obtain for the problem of modulation of a two-frequency wave by a rectifier a solution which is considerably simpler than any hitherto known.

THE problem of computing modulation products has long been recognized as being of fundamental importance in communication engineering. Heretofore certain quite fundamental modulation problems have been attacked by methods which are difficult to justify from the standpoint of mathematical rigor and some of the solutions obtained have been in the form of complicated infinite series that are not easy to use in practical computations. In this paper these problems are solved by means of a new method which is mathematically sound and which yields results in a form well suited for purposes of computation.

The analysis here given applies specifically to the case of two frequencies applied to a modulator of the "cut off" type; i.e., a modulator which operates by virtue of its being insensitive to input changes throughout a particular range of values. A simple rectifying characteristic forms a convenient basis of approximation for study of such modulators, and hence we consider in detail methods of calculating modulation in rectifiers when two frequencies are applied. Applications to certain other types of modulation problems and to the case of more than two applied frequencies are discussed briefly at the close.

Half Wave Linear Rectifier—Two Applied Frequencies

We shall define a half wave linear rectifier as a device which delivers no output when the applied voltage is negative and delivers an output wave proportional to the applied voltage when the applied voltage is positive. We may take the constant of proportionality as unity since its only effect is to multiply the entire solution by a constant. Assume the input voltage $e(t)$ to be specified by

$$e(t) = P \cos (pt + \theta_p) + Q \cos (qt + \theta_q). \tag{1}$$

The output wave will then consist of the positive lobes of the above function with the negative lobes replaced by zero intervals. It is

convenient to represent the amplitude ratio Q/P by k, and without loss of generality to take

$$P > 0 \text{ and } 0 \leq k \leq 1. \tag{2}$$

The problem we now consider is the resolution of the output wave into sinusoidal waves, a complete solution requiring the determination of the frequencies present, their amplitudes, and their phase relations.

The method of solution used employs the auxiliary function of two independent variables $f(x, y)$ defined by

$$\left.\begin{aligned} f(x, y) &= P(\cos x + k \cos y), && \cos x + k \cos y \geq 0, \\ &= 0, && \cos x + k \cos y < 0. \end{aligned}\right\} \tag{3}$$

It is clear that the function $f(x, y)$ may be represented by a surface which does not pass below the xy-plane and which coincides with the xy-plane throughout certain regions which are bounded by the multi-branched curve,

$$\cos x + k \cos y = 0. \tag{4}$$

If either x or y is increased or decreased by any multiple of 2π, the value of $f(x, y)$ is unchanged. Hence $f(x, y)$ is a periodic function of x and y, and if its value is known for every point in the rectangle bounded by $y = \pm \pi$, $x = \pm \pi$ say, the value of the function may be determined for any point in the entire xy-plane.

From the above considerations we are led to investigate the expansion of $f(x, y)$ in a double Fourier series in x and y. We may readily verify that the function satisfies any one of several sets of sufficient conditions [1] to make such an expansion valid. We may write the expansion thus:

$$f(x, y) = \sum_{m=0}^{\infty} \sum_{n=0}^{\infty} [A_{\pm mn} \cos (mx \pm ny) + B_{\pm mn} \sin (mx \pm ny)], \tag{5}$$

with the summation to be extended over both the upper and lower of the ambiguous signs except when m or n is zero, in which case one value only is taken (it is immaterial which one); when m and n are both zero, we divide the coefficient A_{00} by two in order that all the A-coefficients may be expressed by the same formula. Determining the coefficients by the usual method of multiplying both sides of (5) by the factor the coefficient of which is to be found and integrating both sides throughout the rectangle bounded by $x = \pm\pi$, $y = \pm\pi$, we obtain:

[1] Hobson, "Theory of Functions of a Real Variable," Vol. 2, p. 710.

$$\left.\begin{aligned} A_{\pm mn} &= \frac{1}{2\pi^2}\int_{-\pi}^{\pi}\int_{-\pi}^{\pi} f(x, y)\cos(mx \pm ny)dydx, \\ B_{\pm mn} &= \frac{1}{2\pi^2}\int_{-\pi}^{\pi}\int_{-\pi}^{\pi} f(x, y)\sin(mx \pm ny)dydx. \end{aligned}\right\} \tag{6}$$

We now return to our original problem of representing the positive lobes of a two-frequency wave as a sum of sinusoidal components. We may apply the double Fourier series expansion of $f(x, y)$, which must hold for all values of x and y, to the special case in which x and y are linear functions of the time. If we let

$$\left.\begin{aligned} x &= pt + \theta_p, \\ y &= qt + \theta_q, \end{aligned}\right\} \tag{7}$$

the function $f(x, y)$ represents the rectified two-frequency wave as a function of time. The values of x and y which are used lie on the straight line,

$$y = \frac{q}{p}x + \theta_q - \frac{q}{p}\theta_p, \tag{8}$$

which is obtained by eliminating t from (7). A representation of $f(x, y)$ valid for the entire xy-plane must of course hold for values of x and y on this straight line. Hence we may substitute the values of x and y given by (7) directly into the double Fourier series (5), and the result will evidently be an expression for the rectifier output in terms of discrete frequencies of the type $(mp \pm nq)/2\pi$. The phase angle of the typical component is $m\theta_p \pm n\theta_q$ and the amplitude is expressed by (6).

The solution is thereby reduced to the evaluation of the definite double integrals of (6). Three different methods of reducing these integrals have been investigated, and it appears that each has certain peculiar advantages and points of interest. We shall consider them separately.

I. Straightforward Geometric Method

In this method, which yields remarkably simple results in a direct manner, we determine the boundaries of the region throughout which $f(x, y)$ vanishes and substitute appropriate limits in the integrals to exclude this region from the area of integration. When this exclusion has been accomplished, $f(x, y)$ may be replaced in the integral by $\cos x + k \cos y$. The boundary between zero and non-zero values of $f(x, y)$ is the curve (4), which has two branches crossing the rectangle

over which the integration is performed. The non-zero values of $f(x, y)$ lie in the shaded region of Fig. 1. From the symmetry of the region about the x and y axes we deduce at once that the sine coefficients, $B_{\pm mn}$, must vanish and that the cosine coefficients, $A_{\pm mn}$, may be obtained by integrating throughout one quadrant only and multi-

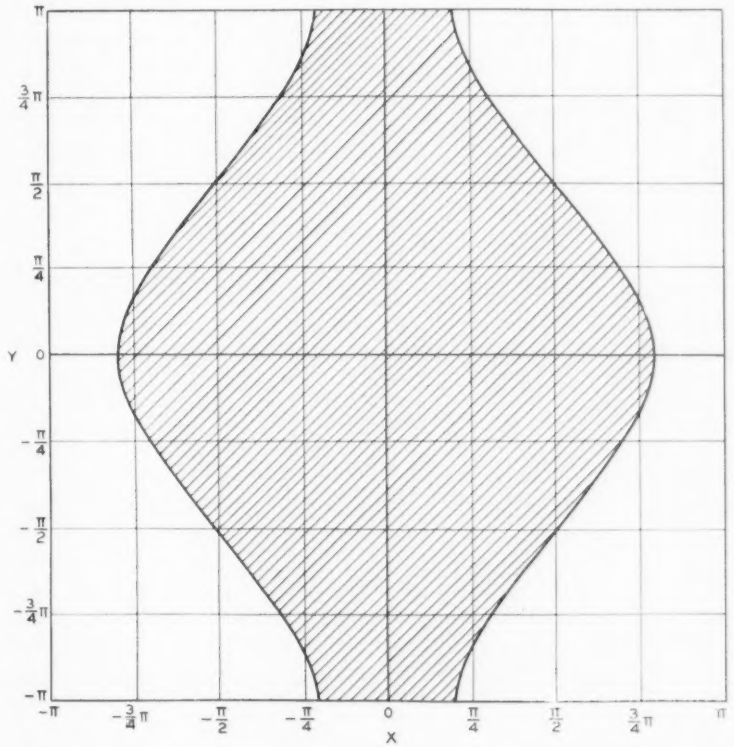

Fig. 1—Region of integration for the determination of the coefficients in the double Fourier series expansion of $f(x, y)$.

plying by four. We therefore obtain, on substitution of the proper limits,

$$A_{mn} = A_{\pm mn} = \frac{2P}{\pi^2} \int_0^{\pi} \cos nydy \times \int_0^{\arccos(-k\cos y)} (\cos x + k \cos y) \cos mxdx \quad (9)$$

This expression gives the amplitude of the typical component of frequency $(mp \pm nq)/2\pi$. The remaining steps are concerned merely with the calculation of the integral (9) for particular values of m and n.

It will suffice to work through one example in detail and give the results in tabular form for the other products up to the fourth order. The second order side frequencies, $(p \pm q)/2\pi$, will be taken as a typical case.

By direct substitution

$$A_{11} = \frac{2P}{\pi^2} \int_0^{\pi} \cos y dy \int_0^{\text{arc cos } (-k \cos y)} (\cos x + k \cos y) \cos x dx. \quad (10)$$

Performing the inner integration and substituting the limits for x, we obtain:

$$A_{11} = \frac{P}{\pi^2} \int_0^{\pi} \cos y [\text{arc cos } (-k \cos y) + k \cos y \sqrt{1 - k^2 \cos^2 y}] dy. \quad (11)$$

Considering separately the integral,

$$\int_0^{\pi} \cos y \text{ arc cos } (-k \cos y) dy,$$

integrate once by parts, letting

$$u = \text{arc cos } (-k \cos y),$$
$$dv = \cos y dy.$$

The result is, after combining with the remainder of the integral for A_{11},

$$A_{11} = \frac{kP}{\pi^2} \int_0^{\pi} \frac{\sin^2 y + \cos^2 y(1 - k^2 \cos^2 y)}{\sqrt{1 - k^2 \cos^2 y}} dy. \quad (12)$$

Now substituting

$$\cos y = z,$$

we obtain

$$A_{11} = \frac{2kP}{\pi^2} \int_0^1 \frac{1 - k^2 z^4}{\sqrt{(1 - z^2)(1 - k^2 z^2)}} dz. \quad (13)$$

This is a standard elliptic form.[2] It is convenient here to let

[2] It may be remarked that a large number of the integrals required in the evaluation of the coefficients are listed by D. Bierens de Haan, "Nouvelles Tables d'Integrales Definies." See in particular Tables 8 and 12, pages 34 and 39.

$$Z_m = \int_0^1 \frac{z^m}{\sqrt{(1 - z^2)(1 - k^2z^2)}}\, dz. \tag{14}$$

By differentiating the expression $z^{m-2}\sqrt{(1 - z^2)(1 - k^2z^2)}$, we may easily derive the useful recurrence formula:

$$Z_m = \frac{(m - 2)(1 + k^2)Z_{m-2} - (m - 3)Z_{m-4}}{(m - 1)k^2}. \tag{15}$$

We may now calculate the value of Z_m for even values of m in terms of Z_0 and Z_2. Z_0 is a complete elliptic integral of the first kind which we shall designate as usual by K; i.e.,

$$Z_0 = K = \int_0^1 \frac{dz}{\sqrt{(1 - z^2)(1 - k^2z^2)}} = \int_0^{\frac{\pi}{2}} \sqrt{1 - k^2 \sin^2 \theta}\, d\theta. \tag{16}$$

Furthermore from the identity:

$$\frac{z^2}{\sqrt{(1 - z^2)(1 - k^2z^2)}} = \frac{1}{k^2}\left[\frac{1}{\sqrt{(1 - z^2)(1 - k^2z^2)}} - \sqrt{\frac{1 - k^2z^2}{1 - z^2}}\right], \tag{17}$$

we have

$$Z_2 = \frac{1}{k^2}(K - E), \tag{18}$$

where E is a complete elliptic integral of the second kind defined by

$$E = \int_0^1 \sqrt{\frac{1 - k^2z^2}{1 - z^2}}\, dz = \int_0^{\frac{\pi}{2}} \sqrt{1 - k^2 \sin^2 \theta}\, d\theta. \tag{19}$$

Now making use of (15), we calculate Z_4 in terms of Z_2 and Z_0 and get finally:

$$Z_4 = \frac{(2 + k^2)K - 2(1 + k^2)E}{3k^4}. \tag{20}$$

We can then evaluate (13) in terms of K and E. The result is

$$A_{11} = \frac{4P}{3\pi^2 k}[(1 + k^2)E - (1 - k^2)K]. \tag{21}$$

The process of evaluating the other coefficients is quite similar. Results are listed in Table I.

Convenient tables of K and E may be found in Peirce's Short Table of Integrals (page 121), Byerly's Integral Calculus, and the Jahnke und Emde tables. For a very extensive set of tables, see Legendre's

TABLE I

TWO FREQUENCY MODULATION PRODUCTS

Applied Wave = $P[\cos(pt + \theta p) + k\cos(qt + \theta q)]$

Order of Product	Symbol for Coefficient	$2\pi \times$ Frequency of Product	Amplitude of Product	
			Half Wave Linear Rectifier	Half Wave Square Law Rectifier
0	$\frac{1}{2}A_{00}$	0	$\frac{2P}{\pi^2}[2E - (1-k^2)K]$	$\frac{1+k^2}{4}P^2$
1	A_{10}	p	$\frac{P}{2}$	$\frac{8P^2}{9\pi^2}[(7+k^2)E - 4(1-k^2)K]$
	A_{01}	q	$\frac{kP}{2}$	$\frac{8P^2}{9\pi^2 k}[(1+7k^2)E - (1+3k^2)(1-k^2)K]$
2	A_{20}	$2p$	$\frac{4P}{\pi^2}[2(2-k^2)E - (1-k^2)K]$	$\frac{P^2}{4}$
	A_{11}	$p \pm q$	$\frac{4P}{3\pi^2 k}[(1+k^2)E - (1-k^2)K]$	$\frac{k}{2}P^2$
	A_{02}	$2q$	$\frac{4P}{9\pi^2 k^2}[2(2k^2-1)E + (2-3k^2)(1-k^2)K]$	$\frac{k^2}{4}P^2$
3	A_{30}	$3p$	0	$\frac{8P^2}{225\pi^2}[(23 - 23k^2 + 8k^4)E - 4(2-k^2)(1-k^2)K]$
	A_{21}	$2p \pm q$	0	$\frac{8P^2}{45\pi^2 k}[(3 + 7k^2 - 2k^4)E - (3+k^2)(1-k^2)K]$
	A_{12}	$p \pm 2q$	0	$\frac{8P^2}{45\pi^2 k^2}[(3k^4 + 7k^2 - 2)E + 2(1-3k^2)(1-k^2)K]$
	A_{03}	$3q$	0	$\frac{8P^2}{225\pi^2 k^3}[(8 - 23k^2 + 23k^4)E - (8 - 19k^2 + 15k^4)(1-k^2)K]$

Phase Angle of Product $(mp \pm nq) = m\theta p \pm n\theta q$

$$K = \int_0^{\frac{\pi}{2}} \frac{d\theta}{\sqrt{1 - k^2\sin^2\theta}} = \int_0^1 \frac{dz}{\sqrt{(1-z^2)(1-k^2z^2)}}; \qquad E = \int_0^{\frac{\pi}{2}} \sqrt{1 - k^2\sin^2\theta}\, d\theta = \int_0^1 \sqrt{\frac{1-k^2z^2}{1-z^2}}\, dz$$

Traité des Fonctions Elliptiques. Numerical calculation of the coefficients making use of these tables and the formulae listed in Table I is a quite simple process. Curves of the coefficients as functions of k have been calculated in this way and are plotted in Fig. 2.

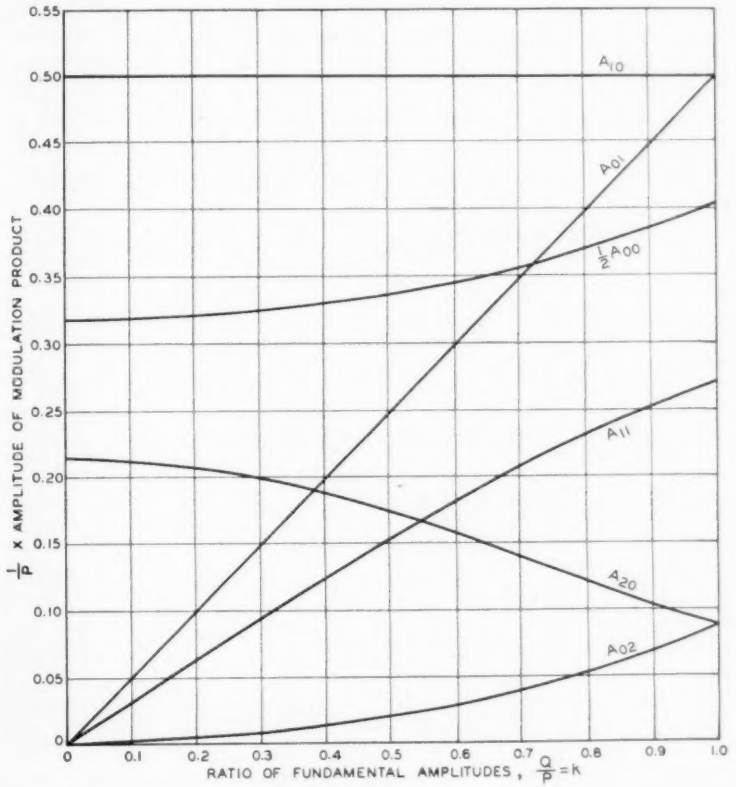

Fig. 2—Curves showing amplitudes of modulation products in output of half wave linear rectifier when input wave consists of two frequencies.

It is perhaps worth noting that the special case of equal fundamental amplitudes ($P = Q$ or $k = 1$) yields the simple result,

$$A_{mn} = \frac{8(-)^m P}{[(m+n)^2 - 1][(m-n)^2 - 1]\pi^2}, \tag{22}$$

where $m + n$ is even. When $m + n$ is odd and greater than one, A_{mn} is zero.

II. Fourier Series Method

The second method is of interest because it obtains the same results as the only previously known solution,[3] which is in terms of infinite series involving Bessel functions. The fact that the results agree is a check on the validity of certain doubtful rearrangements of multiple series necessary in the process by which these results were originally obtained. Furthermore by comparison with the corresponding results of the first method we can sum the infinite series in terms of complete elliptic integrals; a number of interesting mathematical theorems are thus proved, which have been made the basis of a paper by the author in the December, 1932 issue of the *Bulletin of the American Mathematical Society*.

By expanding the function:

$$\left.\begin{aligned} \phi(u) &= -\frac{u}{2}, \qquad -c \leq u \leq 0 \\ &= \frac{u}{2}, \qquad 0 \leq u \leq c \end{aligned}\right\} \tag{23}$$

in a Fourier series in u, we may verify that:

$$\left.\begin{aligned} \frac{c}{4} + \frac{u}{2} - \frac{2c}{\pi^2}\sum_{r=1}^{\infty}\frac{1}{(2r-1)^2}\cos\frac{(2r-1)\pi u}{c} &= 0, \quad -c \leq u \leq 0 \\ &= u, \quad 0 \leq u \leq c. \end{aligned}\right\} \tag{24}$$

If we let $u = P\cos x + Q\cos y$, the left hand member of (24) is equal to $f(x, y)$ provided $|P| + |Q| < c$. With this restriction on c, we may substitute the resulting expression for $f(x, y)$ in the integrand of (6), and no change in the limits of integration are required. Term by term integration of the series may be justified without difficulty, and making use of well known definite integrals, we obtain finally:

$$A_{mn} = \frac{4c}{\pi^2}(-)^{\frac{m+n+2}{2}}\sum_{r=1}^{\infty}\frac{J_m\left(\frac{2r-1}{c}\pi P\right)J_n\left(\frac{2r-1}{c}\pi Q\right)}{(2r-1)^2}, \tag{25}$$

where $m + n$ is an even integer. When $m + n = 0$, the extra term $c/4$ must be added. When $m + n$ is odd and greater than one, the value of A_{mn} is zero; when $m + n = 1$, the values are $A_{10} = P/2$, $A_{01} = Q/2$.

Peterson and Keith obtained the above result [3] by substituting

[3] Peterson and Keith, "Grid Current Modulation," *Bell System Technical Journal*, Vol. 7, pp. 138–9, January, 1928.

$u = P \cos x + Q \cos y$ in the left hand member of (24), applying Jacobi's expansions in series of Bessel coefficients, and rearranging the resulting triple series. It appears that it is much more difficult to justify the series rearrangement than term by term integration. From the results obtained by the first method it follows that the series in (25), which might be termed a generalized Schlömilch series,[4] is summable in terms of elliptic integrals.

III. Trigonometric Integral Method

Following a suggestion of Mr. S. O. Rice, we may make use of the following relation:

$$\left.\begin{aligned} \frac{u}{2} + \frac{u}{\pi}\int_0^\infty \frac{\sin u\lambda}{\lambda}\,d\lambda &= u, \qquad u \geq 0 \\ &= 0, \qquad u \leq 0. \end{aligned}\right\} \tag{26}$$

Evidently if we substitute $u = P\cos x + Q\cos y$, the left hand member of (26) represents the function $f(x, y)$ and may be substituted in the integrand of (6) without change in the limits. Interchange of the order of integration may then be justified without difficulty and the following result is obtained in terms of a special case of the integral of Weber and Schafheitlin:

$$A_{mn} = \frac{2}{\pi}(-)^{\frac{m+n+2}{2}}\int_0^\infty \frac{J_m(P\lambda)J_n(Q\lambda)}{\lambda^2}\,d\lambda, \tag{27}$$

where $m + n$ is even and greater than zero. When $m + n = 0$, the above integral should be replaced by an infinite contour integral taken along the real axis except for an indentation to avoid the origin and with all other quantities remaining the same except for a division by two. For all even order modulation products it may now be deduced [5] that:

$$A_{mn} = \frac{(-)^{\frac{m+n}{2}+1}\Gamma\left(\frac{m+n-1}{2}\right)k^n P}{2\pi\Gamma(n+1)\Gamma\left(\frac{m-n+3}{2}\right)} \times F\left(\frac{m+n-1}{2}, \quad \frac{n-m-1}{2}; \quad n+1; \quad k^2\right). \tag{28}$$

The case of $m + n = 0$ requires a special investigation, which shows that (28) holds for this case also.

[4] Cf. Watson, "Theory of Bessel Functions," Chapter XIX.
[5] Watson, "Theory of Bessel Functions," p. 401.

The hypergeometric function in (28) may always be expressed in terms of K and E by successive applications of recurrence formulae and use of the known relations:

$$\left.\begin{aligned} K &= \frac{\pi}{2} F\left(\frac{1}{2}, \quad \frac{1}{2}; \quad 1; \quad k^2\right), \\ E &= \frac{\pi}{2} F\left(-\frac{1}{2}, \quad \frac{1}{2}; \quad 1; \quad k^2\right). \end{aligned}\right\} \tag{29}$$

By means of the hypergeometric recurrence formulæ we may also show that

$$A_{mn} = -\frac{2[(m-1)k^2 + n - 1]A_{m-1,\,n-1} + (m+n-5)kA_{m-2,\,n-2}}{(m+n+1)k} \tag{30}$$

when $m + n$ is even. A discussion of the hypergeometric function and a derivation of (30) are given in the appendix.

From (30), we can compute successively all even order modulation products starting with say A_{00} and A_{11} known. If negative subscripts occur in applying the formula, they may be replaced by positive subscripts without changing the validity of the results; this is proved in the appendix.

Half Wave Square Law Rectifier—Two Applied Frequencies

The solution for two frequencies applied to a square law rectifier, or in fact to any rectifier operating on an integer power law, can be obtained in a manner quite similar to that used in solving the linear rectifier. In the case of a square law rectifier, we have to represent the function

$$\left.\begin{aligned} f(x, y) &= P^2 (\cos x + k \cos y)^2, && \cos x + k \cos y \geq 0 \\ &= 0, && \cos x + k \cos y < 0. \end{aligned}\right\} \tag{31}$$

Going through the same steps with this function that we did with that of (3), we find that the amplitudes of the modulation products can be expressed in terms of K and E as in the case of the linear rectifier; the results are listed in Table I. A set of curves is plotted in Fig. 3.

We may also show that

$$A_{mn} = (-)^{\frac{m+n+1}{2}} \frac{8c^2}{\pi^3} \sum_{r=1}^{\infty} \frac{J_m\left(\frac{2r-1}{c}\pi P\right) J_n\left(\frac{2r-1}{c}\pi Q\right)}{(2r-1)^3} \tag{32}$$

when $m + n$ is odd and greater than one and $c \geq |P| + |Q|$. For

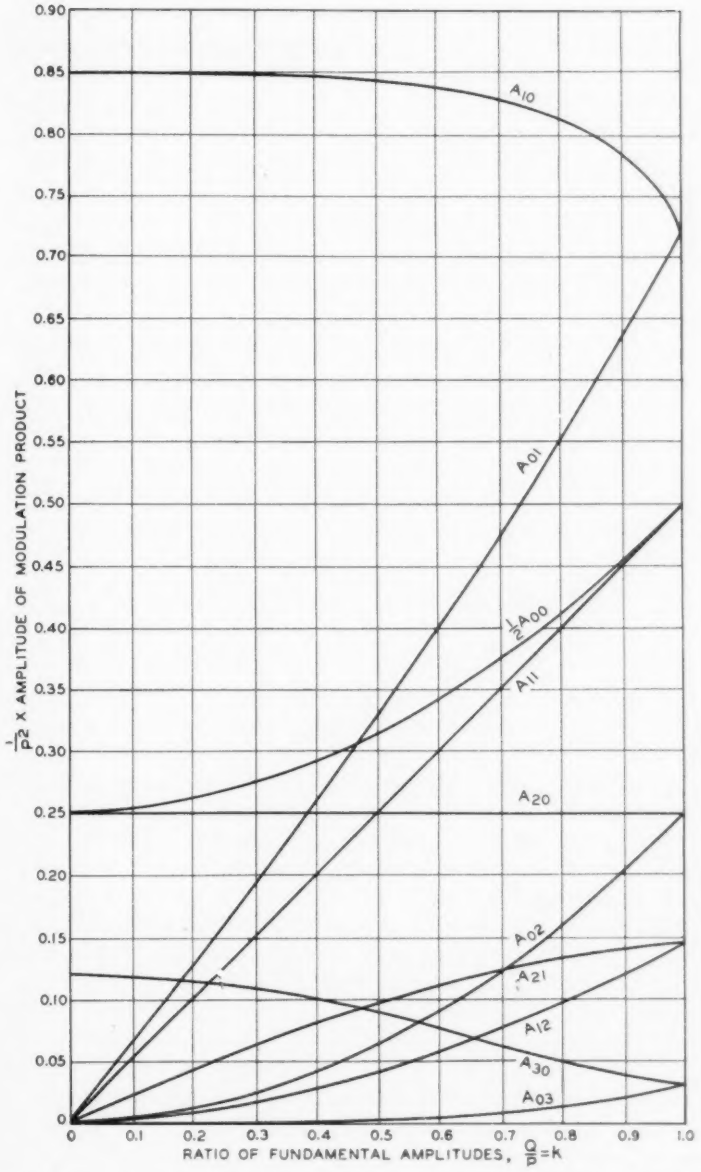

Fig. 3—Curves showing amplitudes of modulation products in output of half wave square law rectifier when input wave consists of two frequencies.

A_{10} and A_{01} we must add $cP/2$ and $cQ/2$ respectively. The value of A_{mn} is zero for $m + n$ even and greater than two; the other even order products are listed in Table I. Another form of the result for odd order products is

$$A_{mn} = \frac{4}{\pi}(-)^{\frac{m+n+1}{2}} \int_0^\infty \frac{J_m(P\lambda)J_n(Q\lambda)}{\lambda^3}\, d\lambda \tag{33}$$

or

$$A_{mn} = (-)^{\frac{m+n+1}{2}} \frac{k^n P^2 \Gamma\left(\frac{m+n-2}{2}\right)}{2\pi\Gamma(n+1)\Gamma\left(\frac{m-n+4}{2}\right)} \times F\left(\frac{m+n-2}{2}, \quad \frac{n-m-2}{2}; \quad n+1; \quad k^2\right). \tag{34}$$

A three term recurrence formula for odd order products is:

$$A_{mn} = -\frac{2[(m-1)k+n-1]A_{m-1,\,n-1}+(m+n-6)kA_{m-2,\,n-2}}{(m+n+2)k}. \tag{35}$$

When $P = Q$, and $m + n$ is odd,

$$A_{mn} = \frac{64\,(-)^{\frac{m+1}{2}}P^2}{(m^2-n^2)[(m+n)^2-4][(m-n)^2-4]\pi^2}. \tag{36}$$

Other Applications and Results

The solution for any full wave rectifier can be obtained from the solution for the corresponding half wave rectifier. Thus we may easily show that the output of a full wave linear rectifier contains neither of the fundamentals and that the amplitudes of all other modulation products are twice as large as the corresponding amplitudes in the output of a half wave linear rectifier. It is also evident that by superposing the solutions for the linear and square law rectifiers we can obtain the solution for a quadratic law rectifier having an output equal to $a_1e(t) + a_2[e(t)]^2$ when $e(t)$ is positive and no output when $e(t)$ is negative. Biased rectifiers, peak choppers, and saturating devices can be solved by the same methods used above, the solution of course becoming more complicated for the more complicated kinds of characteristics. Nor is the method restricted to " cut off " type modulation. Curvature type modulators can be treated in the same way and in many cases solution by the above method is simpler than by the usual power series expansion. The method also appears to have promise in the solution of magnetic modulation problems, where the effect of hysteresis must be considered.

When three frequencies are applied, a triple Fourier series is required, and in the general case of n frequencies, a Fourier series in n variables would be used. The work becomes more complicated as the number of frequencies increases, but there is no theoretical limitation.

In conclusion the writer wishes to express his appreciation of the valuable advice of Messrs. T. C. Fry and L. A. MacColl on the technical features of the paper.

Appendix

The hypergeometric function $F(\alpha, \beta; \gamma; z)$ may be defined by the power series:

$$F(\alpha, \beta; \gamma; z) = 1 + \frac{\alpha\beta}{1!\gamma} z + \frac{\alpha(\alpha+1)\beta(\beta+1)}{2!\gamma(\gamma+1)} z^2 + \cdots .$$

When any one of the three quantities α, β, γ is increased or decreased by unity a new hypergeometric function is formed which is said to be contiguous to the first. Gauss listed fifteen linear relations which connect $F(\alpha, \beta; \gamma; z)$ with pairs of its contiguous functions. In deriving the recurrence formula for A_{mn} we require difference relations between functions which are not contiguous, but the required relations may be obtained from those listed by Gauss by a process of substitution and elimination.

We shall find it convenient to designate $F(\alpha, \beta; \gamma; z)$ by F, $F(\alpha + 1, \beta; \gamma; z)$ by $F_{\alpha+}$, $F(\alpha + 1, \beta; \gamma - 1; z)$ by $F_{\alpha+\gamma-}$, etc., and to let

$$\alpha = \frac{m+n-3}{2}; \qquad \beta = \frac{n-m-1}{2}; \qquad \gamma = n, \qquad z = k^2.$$

In this notation, Equation (27) becomes:

$$A_{mn} = \frac{(-)^{\frac{m+n}{2}+1}\Gamma\left(\frac{m+n-1}{2}\right) k^n P}{2\pi\Gamma(n+1)\Gamma\left(\frac{m-n+3}{2}\right)} F_{\alpha+\gamma+}.$$

The corresponding expressions for $A_{m-1,\,n-1}$ and $A_{m-2,\,n-2}$ are by direct substitution:

$$A_{m-1,\,n-1} = \frac{(-)^{\frac{m+n}{2}}\Gamma\left(\frac{m+n-3}{2}\right) k^{n-1} P}{2\pi\Gamma(n)\Gamma\left(\frac{m-n+3}{2}\right)} F,$$

$$A_{m-2,\,n-2} = \frac{(-)^{\frac{m+n}{2}-1}\Gamma\left(\frac{m+n-5}{2}\right) k^{n-2} P}{2\pi\Gamma(n-1)\Gamma\left(\frac{m-n+3}{2}\right)} F_{\alpha-\gamma-}.$$

Thus a recurrence relation expressing A_{mn} in terms of $A_{m-1,\,n-1}$ and $A_{m-2,\,n-2}$ evidently requires a relation between $F_{\alpha+\gamma+}$, F, and $F_{\alpha-\gamma-}$.

Referring to Gauss' tables,[6] we find

$$(\gamma - \alpha - 1)F + \alpha F_{\alpha+} - (\gamma - 1)F_{\gamma-} = 0,$$
$$\gamma(1 - z)F - \gamma F_{\alpha-} + (\gamma - \beta)zF_{\alpha+} = 0.$$

From the second of these two equations we form two more equations by substituting $\alpha + 1$ for α in one case and $\gamma - 1$ for γ in the other, giving

$$\gamma(1 - z)F_{\alpha+} - \gamma F + (\gamma - \beta)zF_{\alpha+\gamma+} = 0$$
$$(\gamma - 1)(1 - z)F_{\gamma-} - (\gamma - 1)F_{\alpha-\gamma-} + (\gamma - 1 - \beta)zF = 0.$$

Now eliminating $F_{\alpha+}$ and $F_{\gamma-}$ from the first, third, and fourth of the equations, we obtain

$$\alpha(\beta - \gamma)zF_{\alpha+\gamma+} + \gamma[\gamma - 1 + (\alpha - \beta)z]F - \gamma(\gamma - 1)F_{\alpha-\gamma-} = 0,$$

which is the relation desired. Substituting the value of $F_{\alpha+\gamma+}$ in terms of A_{mn}, F in terms of $A_{m-1,\,n-1}$, and $F_{\alpha-\gamma-}$ in terms of $A_{m-2,\,n-2}$ gives the recurrence formula of Equation (30).

In using (30) we may find, as for instance in calculating A_{m0}, A_{m1}, A_{0n}, A_{1n}, that the right hand member involves coefficients with negative subscripts. A simple rule for treating such cases may be demonstrated as follows. We first note that if we replace m by $-m$ in (28) the value of the right hand member is unchanged.[7] Hence since (30) is derivable directly from (28), we conclude that correct results are obtained from (30) if we adopt the convention,

$$A_{-m,\,n} = A_{mn}.$$

The case of n negative is a little more difficult because if n is a negative integer in (28), an indeterminate form results. However, making use of the result just obtained on the interchangeability of sign of the subscripts, m, $m - 1$, $m - 2$ in (30), we can demonstrate a

[6] Gauss, Werke, Bd. III, page 130. The equations used here are numbered (5) and (8) by Gauss.

[7] If we express $(-)^{m/2}\Gamma\left(\frac{m+n-1}{2}\right)\Big/\Gamma\left(\frac{m-n+3}{2}\right)$ in terms of $(-)^{-m/2}\Gamma\left(\frac{-m+n-1}{2}\right)\Big/\Gamma\left(\frac{-m-n+3}{2}\right)$ by successive applications of the recurrence formula for the gamma function, we find the two quantities are equivalent. Changing the sign of m in the hypergeometric function merely interchanges α and β, and hence does not change the value of the function.

similar rule for the subscripts n, $n-1$, $n-2$, valid when (30) is used. For example, by direct application of (30), we deduce that

$$A_{2-m,\,n+2} = -\frac{2[(1-m)k^2+n+1]A_{1-m,\,n+1}+(n-m-1)kA_{-m,\,n}}{(n-m+5)k}.$$

Now since it is known that we may replace the subscripts $2-m$, $1-m$, and $-m$ by $m-2$, $m-1$, and m respectively, we may show that

$$A_{mn} = -\frac{2[(m-1)k^2-n-1]A_{m-1,\,n+1}+(m-n+5)kA_{m-2,\,n+2}}{(m-n+1)k},$$

which is exactly equivalent to the relation we get if we replace n by $-n$ throughout in (30) and then substitute $A_{m,\,-n}=A_{mn}$, $A_{m,\,-n-1}=A_{m,\,n+1}$, $A_{m,\,-n-2}=A_{m,\,n+2}$.

It may be remarked that it would be incorrect to base a proof of interchangeability of sign of subscripts on (27) because the equivalence of (27) and (28) has not been demonstrated for a sufficient range of values of m and n.

Abstracts of Technical Articles from Bell System Sources

North Atlantic Ship-Shore Radio Telephone Transmission During 1930 and 1931.[1] CLIFFORD N. ANDERSON. Considerable data on radio transmission were collected during the years 1930 and 1931 incidental to the operation of a ship-shore radio telephone service with several passenger ships operating in the North Atlantic. This paper discusses briefly the results of an analysis of these data. Contour diagrams are given which show the variation of signal fields with distance and time of day for the various seasons on approximate frequencies of 4, 9, 13, and 18 megacycles. Similar diagrams show the distributions of commercial circuits. Curves are also shown which enable the data to be applied more generally for other conditions of noise and radiated power.

Short-Wave Transmission to South America.[2] C. R. BURROWS and E. J. HOWARD. The results of a year's survey of transmission conditions between New York and Buenos Aires in the short-wave radio spectrum are presented in this article. Surfaces showing the received field strength as a function of time of day and frequency are given. These show that frequencies between 19 and 23 megacycles were best for daytime transmission, and those between 8 and 10 megacycles for nighttime transmission. A transition frequency was required in the early morning, but the useful periods of the day and night frequencies overlapped in the evening.

No variations that could definitely be traced to a seasonal effect were found. This path is much less affected by solar disturbances than the transatlantic.

Frequencies above 30 megacycles appear to have but little commercial value over this path. Frequencies a few megacycles higher could not be received.

The International Telegraph and Radio Conferences of Madrid.[3] L. ESPENSCHIED and L. E. WHITTEMORE. A combined meeting of the International Telegraph and Radio Conferences at Madrid in the fall of 1932 was attended by delegates of government communication administrations and representatives of communication companies from

[1] *Proc. I. R. E.*, January, 1933.
[2] *Proc. I. R. E.*, January, 1933.
[3] *Bell Telephone Quarterly*, January, 1933.

practically the entire world. The conference formulated a treaty, known as the International Telecommunication Convention, to which are attached Regulations relating to (1) the allocation of frequency bands for radio services, the reduction of radio interference and the operation of marine radio service, (2) the transmission of telegrams over international telegraph and cable circuits, and (3) the handling of telephone calls over the European telephone system.

Directional Studies of Atmospherics at High Frequencies.[4] KARL G. JANSKY. A system for recording the direction of arrival and intensity of static on short waves is described. The system consists of a rotating directional antenna array, a double detection receiver and an energy operated automatic recorder. The operation of the system is such that the output of the receiver is kept constant regardless of the intensity of the static.

Data obtained with this system show the presence of three separate groups of static: Group 1, static from local thunderstorms; Group 2, static from distant thunderstorms, and Group 3, a steady hiss type static of unknown origin.

Curves are given showing the direction of arrival and intensity of static of the first group plotted against time of day and for several different thunderstorms.

Static of the second group was found to correspond to that on long waves in the direction of arrival and is heard only when the long wave static is very strong. The static of this group comes most of the time from directions lying between southeast and southwest as does the long wave static.

Curves are given showing the direction of arrival of static of group three plotted against time of day. The direction varies gradually throughout the day going almost completely around the compass in 24 hours. The evidence indicates that the source of this static is somehow associated with the sun.

A Note on an Automatic Field Strength and Static Recorder. W. W. MUTCH.[5] Many types of instruments have been used to record field intensities, both of signals and static, and the varying requirements have produced many widely different pieces of apparatus. One may desire to study the changes taking place over a period as short as one millisecond, or as long as an eleven-year sun-spot period. Obviously the same instrument would not do for both studies. The development work on the recorder described here was started some years ago with

[4] *Proc. I. R. E.*, December, 1932.

[5] *Proc. I. R. E.*, December, 1932.

the aim of producing an instrument capable of recording the energy received from a fading signal during periods of the order of ten seconds. A device for making a continuous record of the energy received from a signal or from static is described. Simple modifications are suggested by means of which peak or average voltage may be recorded.

Short-Wave Transoceanic Telephone Receiving Equipment.[6] F. A. POLKINGHORN. The commercial importance of a single radio channel used for transoceanic telephone communication is such as to permit considerable effort being placed upon obtaining the most efficient and satisfactory operation from each unit of equipment. In this paper there are discussed, in a general manner, the receiving equipment used on the short-wave transatlantic telephone channels to England and some of the methods of analysis used in attacking problems encountered in the design of the receiving equipment.

Observations of Kennelly-Heaviside Layer Heights During the Leonid Meteor Shower of November, 1931.[7] J. P. SCHAFER and W. M. GOODALL. This paper describes the results of radio measurements of the virtual heights of the Kennelly-Heaviside layer during the Leonid meteor shower of November, 1931. While the results are not conclusive, due to the fact that a moderate magnetic disturbance occurred during this same period, there is some reason to believe that the presence of meteors in unusual numbers causes increased ionization of an intermittent nature in the region of the lower layer.

The Ionizing Effect of Meteors in Relation to Radio Propagation.[8] A. M. SKELLETT. From a study of available meteor data it is concluded: (1) that meteors expend the larger part of their energy in the Kennelly-Heaviside regions, that is, in the regions of the upper atmosphere which control the propagation of all long-distance radio waves; (2) that the major portion of a meteor's energy goes into ionization of the gases around its path; (3) that this ionization extends to a considerable distance from the actual path,—in some cases several kilometers or more—and lasts for some minutes after the meteor has passed; (4) meteor trains are produced only in the lower Kennelly-Heaviside layer.

A table of the various sources of ionization of the upper atmosphere is given with values for each in ergs cm^{-2} sec^{-1}. These include sunlight, moonlight, starlight, cosmic rays, and meteors. During meteoric

[6] *Radio Engineering*, February, 1933.
[7] *Proc. I. R. E.*, December, 1932.
[8] *Proc. I. R. E.*, December, 1932.

showers the ionizing effect does not appear to be negligible compared with that due to other ionizing agencies occurring at night.

A meteor of one-gram mass or greater will produce, on the above assumptions, sufficient ionization to affect propagation. One explanation of the general turbulent condition of the ionized layers may be provided by the continuous bombardment of meteors.

Contributors to this Issue

W. R. BENNETT, B.S., Oregon State College, 1925; A.M., Columbia University, 1928. Bell Telephone Laboratories, 1925–. Mr. Bennett has been engaged in the study of the electrical transmission problems of communication.

C. R. BURROWS, B.S. in Electrical Engineering, University of Michigan, 1924; A.M., Columbia University, 1927. Western Electric Company, Engineering Department, 1924–25; Bell Telephone Laboratories, Research Department, 1925–. Mr. Burrows has been associated continuously with radio research and chiefly in studies of the propagation of radio waves.

ARTHUR B. CRAWFORD, B.S. in Electrical Engineering, Ohio State University, 1928. Member of Technical Staff, Bell Telephone Laboratories, 1928–. Mr. Crawford has been engaged chiefly in work relative to radio communication by ultra-short waves.

CARL R. ENGLUND, B.S. in Chemical Engineering, University of South Dakota, 1909; University of Chicago, 1910–12; Professor of Physics and Geology, Western Maryland College, 1912–13; Laboratory Assistant, University of Michigan, 1913–14. Western Electric Company, 1914–25; Bell Telephone Laboratories, 1925–. As Radio Research Engineer Mr. Englund is engaged largely in experimental work in radio communication.

E. B. FERRELL, B.A., 1920; B.S. in Electrical Engineering, 1921; M.A., 1924; Instructor in Mathematics, University of Oklahoma, 1921–24. Bell Telephone Laboratories, 1925–. Mr. Ferrell has been engaged in research in connection with short wave and ultra-short wave transmitters.

WILLIAM W. MUMFORD, B.A., Willamette University, 1930. Bell Telephone Laboratories, 1930–. Mr. Mumford has been engaged in radio receiving work, chiefly on the problem of propagation and measurement in the ultra-short wave region.

JOHN RIORDAN, B.S., Sheffield Scientific School, Yale University, 1923. American Telephone and Telegraph Company, Department of Development and Research, 1926–. Mr. Riordan's work has been mainly on problems associated with inductive effects of electrified railways.

J. H. SCAFF, B.S.E., University of Michigan, 1929; Bell Telephone Laboratories, 1929–. As a member of the Chemical Laboratories, Mr. Scaff has been concerned chiefly with problems relating to the effect of gases on the properties of metals.

J. C. SCHELLENG, A.B., 1915; Instructor in Physics, Cornell University, 1915–18. Engineering Department, Western Electric Company, 1919–25; Bell Telephone Laboratories, 1925–. Mr. Schelleng has been engaged in research in radio communication and is now Radio Research Engineer.

E. E. SCHUMACHER, B.S., University of Michigan; Research Assistant in Chemistry, 1916–18. Engineering Department, Western Electric Company, 1918–25; Bell Telephone Laboratories, 1925–. Mr. Schumacher's work since coming with the Bell System has related largely to research studies on metals and alloys.

ERLING D. SUNDE, E.E., Technische Hochschule Darmstadt, 1926. American Telephone and Telegraph Company, Department of Development and Research, 1927–. Mr. Sunde's work has been mainly concerned with inductive effects of electric railways.